N 62 59820 Copy No. 164

RESTRICTED

RM No. L8H20

FILE COPY
NO 8

NACA RM No. L8H20

NACA

RESEARCH MEMORANDUM

CLASSIFICATION CHANGED TO
UNCLASSIFIED
AUTHORITY CROWLEY CHANGE #2002
DATE 12-14-53 T.C.F.

AN INVESTIGATION AT LOW SPEED OF A 51.3° SWEPTBACK SEMISPAN WING EQUIPPED WITH 16.7-PERCENT-CHORD PLAIN FLAPS AND AILERONS HAVING VARIOUS SPANS AND THREE TRAILING-EDGE ANGLES

By

Jack Fischel and Leslie E. Schneiter

Langley Aeronautical Laboratory
Langley Field, Va.

THIS DOCUMENT ON LOAN FROM THE FILES OF
NATIONAL ADVISORY COMMITTEE FOR AERONAUTICS
LANGLEY AERONAUTICAL LABORATORY
LANGLEY FIELD, HAMPTON, VIRGINIA

CLASSIFIED DOCUMENT

This document contains classified information affecting the National Defense of the United States within the meaning of the Espionage Act, USC 50:31 and 32. Its transmission or the revelation of its contents in any manner to an unauthorized person is prohibited by law. Information so classified may be imparted only to persons in the military and naval services of the United States, appropriate civilian officers and employees of the Federal Government who have a legitimate interest therein, and to United States citizens of known loyalty and discretion who of necessity must be informed thereof.

RETURN TO THE ABOVE ADDRESS.

REQUESTS FOR PUBLICATIONS SHOULD BE ADDRESSED AS FOLLOWS:

NATIONAL ADVISORY COMMITTEE FOR AERONAUTICS
1512 H STREET, N. W.
WASHINGTON 25, D.C.

NATIONAL ADVISORY COMMITTEE FOR AERONAUTICS

WASHINGTON

November 12, 1948

RESTRICTED

NATIONAL ADVISORY COMMITTEE FOR AERONAUTICS

RESEARCH MEMORANDUM

AN INVESTIGATION AT LOW SPEED OF A 51.3° SWEPTBACK SEMISPAN WING EQUIPPED WITH 16.7-PERCENT-CHORD PLAIN FLAPS AND AILERONS HAVING VARIOUS SPANS AND THREE TRAILING-EDGE ANGLES

By Jack Fischel and Leslie E. Schneiter

SUMMARY

A wind-tunnel investigation was performed at low speed to determine the aerodynamic characteristics of a 51.3° sweptback semispan wing equipped with 16.7-percent-chord plain flaps and ailerons having various spans and spanwise locations, and with one span of aileron having trailing-edge angles of 6°, 14°, and 25°. Lift, drag, pitching-moment, and flap hinge-moment data were obtained for the wing equipped with several spans of sealed and unsealed flaps deflected up to 60°, and rolling-moment, yawing-moment, hinge-moment, and aileron-seal-pressure data were obtained for the various combinations of aileron span and trailing-edge angles. In addition, the wing aerodynamic characteristics were determined for a spoiler-type aileron configuration having a span of 60 percent of the wing semispan and a projection of 5-percent wing chord in conjunction with a 92.5-percent-span flap deflected 0°, 30°, and 60°.

The results indicate, in general, that changes in the wing angle of attack, flap deflection, flap span, or flap spanwise location produced trends in the wing lift, drag, pitching-moment, and flap hinge-moment characteristics that were similar to, but of different magnitude from, the trends produced on unswept wings, except possibly at large angles of attack near the wing stall. Also, changes in the wing angle of attack, aileron deflection, aileron span, or aileron spanwise location generally produced effects on the swept-wing lateral-control characteristics that were similar in trend to, but differing in magnitude from, the corresponding effects produced on unswept wings. Notably, the data indicated that a given percent-span aileron would be most effective in producing roll when it spans the center portion of the wing semispan.

At values of wing angle of attack below approximately 14°, the rolling moment produced by the spoiler-aileron configuration generally increased with increase in the angle of attack, and the yawing moment was favorable; also, in this angle-of-attack range, the spoiler aileron generally produced larger rolling moments with flap deflected than with flap undeflected.

INTRODUCTION

The plain-flap type of control device is being considered and incorporated in the design of high-speed aircraft having swept wings. The design engineer on such aircraft is greatly hampered, however, by a lack of data upon which to base estimates of the various lift and lateral-control design parameters. In order to help alleviate this difficulty, the National Advisory Committee for Aeronautics is currently investigating flap-type controls on swept wings with the ultimate objective of obtaining flap and aileron design criterions similar to those available on unswept wings (references 1 to 6).

The data presented and discussed herein are the results of a low-speed lift and lateral-control investigation of 16.7-percent-chord plain flaps and ailerons having various spans, spanwise locations, and trailing-edge angles on a tapered low-drag semispan wing having a leading-edge sweep angle of 51.3°. The present investigation, which was performed in the Langley 300 MPH 7- by 10-foot tunnel, is an extension of the investigation reported in reference 7. The model used in the present investigation and that reported in reference 7 were essentially the same, differing only in the plan form of the wing tip. The characteristics of the wing in pitch were determined through a large angle-of-attack range for various flap deflections with the flaps sealed and unsealed. Rolling-moment, yawing-moment, hinge-moment and internal-seal-pressure characteristics of the various span ailerons were determined for a large range of aileron deflections and angles of attack with the ailerons sealed. The effect of aileron-end treatment (inboard end of aileron cut off parallel to the plane of symmetry rather than normal to the aileron hinge axis) on the lateral control and hinge-moment characteristics of one of the aileron configurations was also investigated. In addition, the lateral-control effectiveness of a spoiler configuration (previously developed on another sweptback wing, reference 8), investigated in conjunction with a full-span plain unsealed flap deflected various amounts, was determined.

Included herein is a comparison between the aerodynamic and lateral control characteristics of the subject wing and the raked-tip wing of reference 7.

SYMBOLS

The forces and moments measured on the wing are presented about the wind axes, which, for the conditions of these tests (zero yaw), correspond to the stability axes. The X-axis is in the plane of symmetry of the model and is parallel to the tunnel free-stream air flow. The Z-axis is in the plane of symmetry of the model and is perpendicular to the X-axis. The Y-axis is perpendicular to both the X- and Z-axes. All three axes intersect at the intersection of the chord plane and the plane of symmetry

of the model at the chordwise location shown in figure 1. This position corresponds to the aerodynamic center of the plain wing and is located at 29.9 percent of the mean aerodynamic chord.

C_L lift coefficient $\left(\frac{\text{Twice lift of semispan model}}{qS}\right)$

ΔC_L increment of lift coefficient

C_D drag coefficient (D/qS)

C_m pitching-moment coefficient $\left(\frac{\text{Twice pitching moment of semispan model about Y-axis}}{qS\bar{c}}\right)$

ΔC_m increment of pitching-moment coefficient

C_l rolling-moment coefficient (L/qSb)

C_n yawing-moment coefficient (N/qSb)

C_h flap or aileron hinge-moment coefficient $(H/2qM)$

P seal-pressure coefficient $\left(\frac{\text{Pressure below aileron seal} - \text{Pressure above aileron seal}}{q}\right)$

D twice drag of semispan model, pounds

L rolling moment, resulting from aileron deflection or spoiler projection, about X-axis, foot-pounds

N yawing moment, resulting from aileron deflection or spoiler projection, about Z-axis, foot-pounds

H flap or aileron hinge moment, foot-pounds

M area-moment of flap or aileron rearward of and about the hinge axis, cubic feet (see table I)

q free-stream dynamic pressure, pounds per square foot $\left(\frac{1}{2}\rho V^2\right)$

S twice area of semispan wing model, 18.90 square feet

b twice span of semispan model, 8.05 feet

A aspect ratio of wing, 3.43 (b^2/S)

$\bar{c}$ wing mean aerodynamic chord (M.A.C.),

$$2.49 \text{ feet} \left(\frac{2}{S} \int_0^{b/2} c^2 \, dy \right)$$

c local wing chord, feet

$\bar{x}$ distance along X-axis from leading edge of root chord to leading edge of mean aerodynamic chord,

$$2.20 \text{ feet} \left(\frac{2}{S} \int_0^{b/2} cx \, dy \right)$$

y lateral distance from plane of symmetry, measured parallel to Y-axis, feet

x longitudinal distance from leading edge of wing root chord to wing leading edge at any spanwise station, measured parallel to X-axis, feet

b_f span of flap, measured parallel to Y-axis, feet

b_a span of aileron, measured parallel to Y-axis, feet

V free-stream velocity, feet per second

ρ mass density of air, slugs per cubic foot

α angle of attack of wing with respect to chord plane at root of model, degrees

δ_f flap deflection relative to wing chord plane, measured perpendicular to flap hinge axis (positive when trailing edge is down), degrees

δ_a aileron deflection relative to wing chord plane, measured perpendicular to aileron hinge axis (positive when trailing edge is down), degrees

ϕ flap or aileron trailing-edge angle, measured in a plane approximately perpendicular to flap or aileron hinge axis, degrees

Λ wing sweep angle, angle between wing leading edge and a line parallel to Y-axis, degrees

$C_l/\Delta\alpha$ rolling-moment coefficient produced by 1° difference in angle of attack of various right and left portions of a complete wing (reference 5)

$\Delta\alpha/\Delta\delta$ effective change in the angle of attack over the flapped portion of a wing produced by a unit change in flap deflection

$$C_{h_\alpha} = \left(\frac{\partial C_h}{\partial \alpha}\right)_{\delta_a}$$

$$C_{h_{\delta_a}} = \left(\frac{\partial C_h}{\partial \delta_a}\right)_{\alpha}$$

$$C_{l_{\delta_a}} = \left(\frac{\partial C_l}{\partial \delta_a}\right)_{\alpha}$$

$$P_{\delta_a} = \left(\frac{\partial P}{\partial \delta_a}\right)_{\alpha}$$

The subscripts δ_a and α indicate the factor held constant. All slopes were measured in the vicinity of $\delta_a = 0^\circ$ and $\alpha = 0^\circ$.

Subscripts:

i	inboard
o	outboard
f	flap
a	aileron
max	maximum

The subscripts 1 to 5 have been used with the seal-pressure coefficient P to indicate the spanwise station at which the pressure coefficient was measured. (See fig. 2.)

The lift, drag, and pitching-moment coefficient data presented herein represent the aerodynamic effects of deflection in the same direction of the flaps or spoiler on both semispans of the complete wing. The rolling-moment and yawing-moment coefficient data represent the aerodynamic moments on a complete wing produced by the deflection of the aileron (or projection of a spoiler) on only one semispan of the complete wing.

CORRECTIONS

All the test data have been corrected for jet-boundary and reflection-plane effects. Blockage corrections, to account for the constriction effects produced by the wing model and wing wake, have also been applied to the test data.

No corrections have been applied to the data to account for the small amount of wing twist produced by aileron deflection or the tare effects of the root-fairing body.

APPARATUS AND MODEL

The semispan-sweptback-wing model was mounted vertically in the Langley 300 MPH 7- by 10-foot tunnel, as shown in figure 3. The root chord of the model was adjacent to the ceiling of the tunnel which served as a reflection plane. The model was mounted on the six-component balance system in such a manner that all forces and moments acting on the model could be measured. A small clearance was maintained between the model and the tunnel ceiling so that no part of the model came in contact with the tunnel structure. A root fairing, consisting of a body of revolution, was attached to the root of the model in order to deflect the spanwise flow of air that enters the tunnel test section through the clearance hole between the model and the tunnel ceiling.

The model was constructed of laminated mahogany over a welded steel framework to the plan-form dimensions shown in figure 1. The model was sweptback 51.3° at the leading edge, had an aspect ratio of 3.43 and a taper ratio of 0.44, and had neither twist nor dihedral. The wing sections normal to the 50-percent-chord line of the wing when in the unswept condition were NACA 65-012. Transition was fixed at the leading edge of the wing in order to duplicate more nearly full-scale conditions. The transition strip, consisting of No. 60 carborundum grains, extended over the forward 5 percent of the wing chord on both the upper and the lower surfaces along the entire span of the wing model. The carborundum grains were sparsely spread to cover from 5 to 10 percent of this area.

The semispan-wing model was equipped with plain radius-nose control surfaces (which were used either as lift-flaps or ailerons) that were 20 percent chord normal to the 50-percent-chord line of the wing when in the unswept condition and 16.7 percent chord parallel to the plane of symmetry of the swept wing. The flaps or ailerons were constructed around steel spars with joints (cut normal to the hinge axis) at three spanwise stations so that various spans of flap or aileron, occupying various spanwise locations, could be obtained (fig. 1 and table I). The modified plan form of the $0.404\frac{b}{2}$ outboard aileron (table I) had the inboard end of the aileron cut parallel to the plane of symmetry (fig. 4). The three mahogany flap and aileron profiles used had trailing-edge angles (in a plane approximately normal to the hinge axis) of 6° (true contour of trailing edge of NACA 65-012 airfoil), 14° (straight sides from hinge line to trailing edge of wing), and 25° (beveled trailing edge), and were built to the sections shown in figure 5. Except as noted, the various lift flaps did not have a seal across the gap ahead of the flap nose, whereas the various ailerons were sealed. The seal consisted of a plastic

impregnated cloth attached to both the wing and the control surface, across the gap ahead of the control-surface nose, except at the point of attachment of the flap or aileron actuating mechanism and at the control-surface support bearings. The seal extended and was attached to the bearing housing at the end of each flap or aileron chamber, and it is believed that the seal in each chamber was fairly complete. Pressure orifices were located above and below the seal in the wing block ahead of the aileron at the spanwise locations shown in figure 2. Two pairs of pressure orifices were located in each of the two center aileron sections, whereas only one pair of orifices was located in the inboard aileron section.

The spoiler-aileron configuration consisted of six spoiler segments, each having a span of $0.10\frac{b}{2}$ and a projection of 0.05c, attached to the upper surface of the wing in a stepped fashion with the span of each segment normal to the plane of symmetry (fig. 6). The midpoint of each spoiler segment was on the 0.70c line of the wing and the spoiler extended from $0.20\frac{b}{2}$ to $0.80\frac{b}{2}$.

A remotely controlled motor-driven flap-actuating mechanism was used to obtain the various flap and aileron deflections employed in the investigation. The control-surface deflections were constantly indicated on a meter by the use of a calibrated potentiometer which was mounted on the hinge axis near the outboard end of the aileron. A calibrated electrical resistance-type strain gage was employed to measure the flap and aileron hinge moments.

TESTS

All the tests were performed at an average dynamic pressure of approximately 20.5 pounds per square foot, which corresponds to a Mach number of 0.12 and a Reynolds number of 2,200,000 based on the wing mean aerodynamic chord of 2.49 feet.

Wing angle-of-attack tests with the unsealed flaps deflected various amounts from 0° to 60° were made through an angle-of-attack range from -10° to the wing stall angle, whereas corresponding tests with the sealed flaps at zero deflection were generally made through an angle-of-attack range from -10° to 10°. Additional lift, drag, pitching-moment, and hinge-moment coefficient data presented herein, for both the retracted and deflected conditions of the sealed flaps, were obtained in the course of obtaining the lateral-control-test data.

Lateral-control tests, with the various span ailerons having the various trailing-edge angles, generally were performed through an aileron-deflection range from -30° to 30° at constant angles of attack ranging from -4° to 28° in 4° increments.

Tests of the spoiler configuration were performed through an angle-of-attack range from -10° to the wing stall angle with the maximum span unsealed flap $\left(b_f = 0.925\frac{b}{2}\right)$ deflected 0°, 30°, and 60°.

RESULTS AND DISCUSSION

Wing Aerodynamic Characteristics

The static aerodynamic characteristics of the wing in pitch for several deflections of $0.521\frac{b}{2}$ and $0.925\frac{b}{2}$ unsealed inboard flaps are presented in figure 7, and corresponding data for several deflections of sealed flaps having various spans and spanwise locations are presented in figures 8 and 9. The incremental values of lift coefficient and pitching-moment coefficient resulting from flap deflection are shown in figures 10 and 11, respectively, for the flaps in both the unsealed and sealed conditions. In addition, the effects of flap span and spanwise location on the values of lift coefficient and pitching-moment coefficient obtained on the subject wing with the sealed flaps deflected 30° are shown in the summary figures presented as figures 12 and 13.

Lift characteristics.- The data presented in figures 7 to 10 and 12 show that increase in either the flap span or the flap deflection, within the range investigated, generally resulted in an increase in the lift at any given angle of attack and also in the maximum lift obtainable. The incremental lift produced by unit flap deflection tended to decrease as the flap deflection or the angle of attack increased and was generally larger at $\alpha = 0^\circ$ than at other angles of attack.

The values of ΔC_L obtained with the $0.521\frac{b}{2}$ and $0.925\frac{b}{2}$ unsealed flaps deflected 60° were, respectively, approximately 0.33 and 0.43 at $\alpha = 0^\circ$, approximately 0.29 and 0.35 at $\alpha = 12^\circ$, and approximately 0.07 and 0.21 at $C_{L_{max}}$ (figs. 7 and 10). The low value of $\Delta C_{L_{max}}$ shown here for the $0.521\frac{b}{2}$ flap as compared to the value of $\Delta C_{L_{max}}$ for the $0.925\frac{b}{2}$ flap has been noted previously in other investigations of partial-span and full-span flaps on swept-back wings and is thought to be associated with a premature stall occurring over the inboard portion of the wing when a trailing-edge flap is deflected. This phenomenon is more clearly illustrated by a comparison of the lift curves of figures 7 to 9, which reveals that the values of ΔC_L tend to decrease more rapidly for inboard flaps than for outboard or full-span flaps, as the wing stall is approached. The decrease in the values of ΔC_L produced by given flap deflections as α increased (figs. 7 to 10) was also noted in the swept-wing investigation reported in reference 7, but was not noted in

the investigations of unswept wings reported in references 1 and 2, and is therefore thought to be a phenomenon associated with sweptback wings. The data presented herein were obtained at a moderately low value of Reynolds number; however, the results of other wind-tunnel investigations have indicated that the rate of increase of $C_{L_{max}}$ with Reynolds number is less for sweptback wings than for unswept wings in the critical range of Reynolds number and is almost negligible when transition is fixed on the wing leading edge.

In addition to the increase in wing lift with flap span previously noted, figures 8, 9, and 12 also show that, at angles of attack below that for $C_{L_{max}}$, the lift effectiveness of a given percent-span outboard flap was less than that of a corresponding percent-span inboard flap. This is in excess of the effect that could be attributed to the larger ratio of flap area to wing area obtained with inboard flaps than with outboard flaps and agrees with corresponding results obtained on unswept wings (references 1 to 3) and with the results obtained in the swept-wing investigation reported in reference 7. It will be noted that with the flap sealed, the ratio of $\Delta C_{L_{b_{f=0.521\frac{b}{2}}}} \Big/ \Delta C_{L_{b_{f=0.925\frac{b}{2}}}}$ is almost constant at $\alpha = 0^\circ$, 12°, and at $C_{L_{max}}$ (figs. 8 and 10), but with the flap unsealed, this ratio is almost constant only at $\alpha = 0^\circ$ and 12° (figs. 7 and 10). Moreover, a comparison of the lift data of figures 7, 8, and 10 shows that, at angles of attack below that for $C_{L_{max}}$, the values of ΔC_L obtained with flaps sealed or unsealed were generally quite similar (fig. 10), thereby indicating that the beneficial effects on ΔC_L of sealing the flap obtained in previous investigations on unswept wings were not obtained on the subject wing.

Drag characteristics.- Increase in the flap span or the flap deflection of either the sealed or unsealed flaps generally produced larger values of drag coefficient at low given values of C_L and smaller values of drag coefficient at high given values of C_L (figs. 7 to 9). A comparison of the lift-drag ratios L/D obtained at the various flap deflections indicates that at values of C_L above approximately 0.6, a flap deflection of 30° provides almost the optimum value of L/D, and any increase in flap deflection does not improve this ratio, although it does increase the lift coefficient (fig. 7). Because of the importance of the L/D ratio for take-off and landing (as well as for cruising flight), and because of the increase in pitching moment with flap deflection (as will be discussed in the following section) it may be advantageous to limit the flap deflection to a moderate value on sweptback wings.

Sealing the flap produced no significant changes in the values of drag coefficient at given values of lift coefficient for a given percent-span flap (figs. 7 and 8).

Pitching-moment characteristics.- At values of lift coefficient above approximately 0.65, the subject wing had an unstable variation of pitching-moment coefficient with lift coefficient regardless of the flap span, flap deflection, or the condition of the flap-nose seal (figs. 7 to 9). Increase in either the flap span or the flap deflection generally produced negative increments of pitching-moment coefficient ΔC_m over the entire lift-coefficient range (figs. 7, 8, and 11). The values of ΔC_m reflected only a small effect of sealing the flap at large flap deflections, but sealing the flap produced about 20 percent less negative values of ΔC_m for the $0.925\frac{b}{2}$ flap at low flap deflections. The values of ΔC_m obtained at $\alpha = 0^\circ$ varied almost linearly with flap deflection at values of δ_f between 0° and 30° (fig. 11), although the variation of pitching-moment coefficient with flap deflection $C_{m_{\delta_f}}$ tended to decrease as the flap deflection increased (figs. 7 and 8). For outboard flaps, or flaps having their outboard end at $0.990\frac{b}{2}$, the data of figures 9 and 13 indicate that a nonlinear variation of C_m with flap span exists and that, for a given percent-span flap, ΔC_m was largest for a flap located over the center portion or the outboard portion of the wing and was almost negligible for a short-span flap spanning the inboard portion of the wing. Almost similar trends are shown by the variation of $C_{m_{\delta_f}}$ with flap span, although such data are not presented herein. This effect is associated with the longitudinal distance rearward of the aerodynamic center of the loading produced by flaps on swept wings.

Flap hinge-moment characteristics.- As would normally be anticipated, the hinge-moment data of figures 7 to 9 show that the values of the flap hinge-moment coefficient became more negative with increase in the lift coefficient (or the angle of attack) of the wing, and also with increase in the flap deflection. Only slight, and in some cases, inconsistent effects on the values of hinge-moment coefficient were produced by increasing the flap span, varying the spanwise position of the flaps, or sealing the flaps.

In general, changes in the wing angle of attack, flap deflection, flap span, or flap spanwise location, produced trends in the swept-wing lift, drag, pitching-moment, and flap hinge-moment characteristics that were similar to, but of different magnitude from, the trends produced on unswept wings, except possibily at large angles of attack near the wing stall.

Aileron-Control Characteristics

The variation of the aileron lateral control characteristics with aileron deflection or wing angle of attack for each of the combinations of aileron span and trailing-edge angle investigated is presented in figures 14 to 21. The lateral-control parameters $C_{l_{\delta_a}}$, $C_{h_{\delta_a}}$, and C_{h_α}, determined from the data in figures 14 to 17, 20, and 21 (for ailerons

having $y_{a_o} = 0.990\frac{b}{2}$), are shown plotted against the position of the inboard end of the aileron in figure 22 and against aileron trailing-edge angle in figure 23. A summary chart, presenting the values of the aforementioned lateral-control parameters and the values of the seal-pressure parameter P_{δ_a} obtained with each of the aileron combinations tested, as well as the values of the total rolling-moment coefficient produced by $\pm 30^\circ$ deflection of each aileron, is given in table II.

Rolling-moment characteristics.- The data of figures 14 to 21 show that the curves of rolling-moment coefficient against aileron deflection for a given aileron configuration are fairly linear and are almost identical for values of α at and below 8.3°, but that these curves generally become less linear and the values of C_l at given aileron deflections decrease with increase in α above 8.3°. The magnitude of the reduction in C_l (as α increased) appeared to increase as the span of an aileron having $y_{a_o} = 0.990\frac{b}{2}$ (outboard ailerons) increased, and is particularly large for the $0.513\frac{b}{2}$ (center-span) and $0.521\frac{b}{2}$ (inboard) ailerons. This phenomenon is thought to be associated with the premature stall that occurred when control surfaces were used on the inboard portion of the wing (see figs. 7 to 9) and indicates that an aileron on the subject wing would retain the greater part of its effectiveness through the α range when it is located near the wing tip.

As an indication of the maximum rolling effectiveness of the ailerons, assuming an aileron system with no differential linkage, the values of the total rolling-moment coefficient for $\pm 30^\circ$ aileron deflection at constant values of α have been computed for each of the aileron arrangements investigated and are listed in table II. Because the trends exhibited by these values of total C_l for $\delta_a = \pm 30^\circ$ are similar to the trends exhibited by the values of the aileron-effectiveness parameter $C_{l_{\delta_a}}$ for each of the aileron arrangements, only the variations of the parameter $C_{l_{\delta_a}}$ with aileron span, spanwise location, and trailing-edge angle will be dealt with in the following discussion of rolling-moment characteristics.

The variation of the aileron-effectiveness parameter $C_{l_{\delta_a}}$ with the position of the inboard end of the aileron, for ailerons having $\phi_a = 14^\circ$ and $y_{a_o} = 0.990\frac{b}{2}$ and with aileron trailing-edge angle, for outboard ailerons of $0.404\frac{b}{2}$, is shown in figures 22 and 23, respectively. As would be normally anticipated, $C_{l_{\delta_a}}$ increased with increasing aileron span and decreased with increasing aileron trailing-edge angle. (Corresponding effects have been determined previously on unswept wings (reference 4).) The variation of $C_{l_{\delta_a}}$ with aileron span was nonlinear, and the data of figure 22 and table II indicate that a given percent-span aileron would be most effective when spanning the

center portion of the wing semispan and least effective when spanning the inboard portion of the wing semispan. A comparison of the values of $C_{l_{\delta_a}}$ measured with the $0.513\frac{b}{2}$ center-span aileron and with the $0.521\frac{b}{2}$ inboard aileron (table II) with the values of $C_{l_{\delta_a}}$ estimated for these ailerons from the $C_{l_{\delta_a}}$ curve of figure 22 indicates excellent agreement. The estimated values of $C_{l_{\delta_a}}$ were obtained from figure 22 by taking the difference between the values of $C_{l_{\delta_a}}$ at the inboard and outboard ends of each aileron. Because of this excellent agreement between the measured and estimated values of $C_{l_{\delta_a}}$, it is indicated that the $C_{l_{\delta_a}}$ curve of figure 22 could be used to estimate accurately the aileron-effectiveness parameters of ailerons spanning various portions of the wing semispan on wings having plan forms similar to the wing investigated.

In the investigation reported in reference 9, the subject data and data obtained in other investigations have been analyzed and a method of computing control parameters for sweptback wings has been developed, which, for the subject wing, is represented by the relationship

$$C_{l_{\delta_a}} = \frac{C_l}{\Delta\alpha}\frac{\Delta\alpha}{\Delta\delta}\cos^2\Lambda$$

The variation of $C_{l_{\delta_a}}$ with aileron span calculated from this relationship is shown in figure 22. The variation of $C_l/\Delta\alpha$ with aileron span used in these calculations was obtained from reference 5 for a wing of aspect ratio 6 and a taper ratio of 0.5; these values approximately correspond to the geometric characteristics for the wing of the present paper when it is unswept. A value of 0.44 was used for $\Delta\alpha/\Delta\delta$ which corresponds to the value for a sealed aileron of 0.20c (normal or approximately normal to the hinge line). The theoretical curve of $C_{l_{\delta_a}}$ is in excellent agreement with the experimentally determined curve (as was shown in reference 9), except for short-span ailerons located near the wing tip, where the experimentally determined curve provides slightly smaller values of $C_{l_{\delta_a}}$.

Yawing-moment characteristics.- The total yawing-moment coefficient resulting from equal up and down deflection of the ailerons was generally adverse (sign of yawing moment opposite to sign of rolling moment) for all combinations of aileron span and trailing-edge angles tested (figs. 14 to 21). The magnitude of the adverse yawing-moment coefficient increased as the angle of attack increased, in one case becoming as much as 84 percent of the total rolling-moment coefficient. The ratio of adverse yawing moment to rolling moment was considerably larger for the subject

wing than the corresponding ratio obtained for unswept wings. Reference 10 indicates that these large adverse yawing moments would tend to reduce the rolling power of the ailerons and that these adverse yawing moments, when coupled with the low aileron effectiveness encountered at high values of lift coefficient and/or low airplane directional stability, may be quite deleterious. As would be expected, the yawing moment produced by any given equal up and down deflection of the ailerons increased with increasing aileron span. Variation of the aileron trailing-edge angle caused no significant changes in the yawing moments produced by the $0.404\frac{b}{2}$ outboard aileron (figs. 16, 20, and 21).

From considerations of either the total yawing moment or the ratio of yawing moment to rolling moment, there appears to be no advantage to be gained in the use of ailerons spanning the center portion or the inboard portion of the wing semispan. The center-span aileron ($0.513\frac{b}{2}$), while producing more rolling moment, also produced more adverse yawing moment than would probably be produced by a comparable span aileron located at the wing tip; however, the ratio of yawing moment to rolling moment was almost identical for all configurations.

Aileron hinge-moment characteristics.- Hinge-moment-coefficient data obtained on the various spans of aileron (figs. 14 to 21) show that the values of the hinge-moment coefficient C_h, at given aileron deflections, generally became more negative as the wing angle of attack increased. The data also show that a fairly linear variation of C_h with δ_a was obtained for the $0.925\frac{b}{2}$ aileron at low angles of attack. The variation of C_h with δ_a, for the up-going aileron, generally became less as the value of α increased, as the aileron span of outboard ailerons decreased and, for the $0.404\frac{b}{2}$ outboard ailerons, as the aileron trailing-edge angle increased.

The values of the aileron hinge-moment parameters C_{h_α} and $C_{h_{\delta_a}}$ were only slightly affected by changes in the span or spanwise location of the ailerons (fig. 22 and table II). For ailerons having $y_{a_o} = 0.990\frac{b}{2}$ and $\phi_a = 14^\circ$, C_{h_α} and $C_{h_{\delta_a}}$ exhibited a slight shift toward more negative values as the aileron span was increased, and for the $0.513\frac{b}{2}$ center-span aileron and the $0.521\frac{b}{2}$ inboard aileron as well as for the $0.404\frac{b}{2}$ outboard aileron, the data indicated a slight shift toward more negative values of both C_{h_α} and $C_{h_{\delta_a}}$ when the spanwise position of the aileron was moved inboard. In addition, for outboard ailerons of $0.404\frac{b}{2}$, C_{h_α} and $C_{h_{\delta_a}}$ exhibited large changes toward less negative (or more positive) values as the aileron trailing-edge angle was increased (fig. 23). Corresponding effects on the values of C_{h_α} and $C_{h_{\delta_a}}$ produced by change in

aileron trailing-edge angle have been noted previously in other investigations on swept and unswept wings (references 7 and 4, respectively).

Internal seal-pressure characteristics.- The internal seal-pressure data obtained on the various span ailerons having a trailing-edge angle of 14° (figs. 14 to 19 and table II) show that the most linear variation of P with δ_a and the highest value of P at any given value of δ_a were invariably obtained on each aileron at the spanwise station located nearest the inboard end of the aileron. In addition, for each span of aileron, the values of P for given aileron deflections and the values of P_{δ_a} generally decreased in proceeding from the inboard pressure-orifice stations to the outboard stations. Increasing the wing angle of attack had an inconsistent effect upon P_{δ_a} but generally produced a shift of the pressure curves toward more positive values of pressure coefficient. For a constant aileron span $\left(b_a = 0.404\frac{b}{2}\right)$, increasing the aileron trailing-edge angle generally produced slightly smaller values of P_{δ_a} and produced only negligible changes in the values of P at given aileron deflections (figs. 16, 20, and 21 and table II).

The seal-pressure data indicate, in general, that sealed internal balances will provide hinge-moment balancing effects on a highly sweptback wing through a moderate aileron-deflection range and a large angle-of-attack range up to and through the angle of wing stall. Calculations of the balancing moments of various sizes of sealed internal balance made by the methods and data presented in reference 11 and the data presented in the present paper showed that an internal balance which would permit ±20° aileron deflection on the wing investigated would provide considerable balancing effects through the wing angle-of-attack range; however, this would also limit the rolling power of the ailerons, which may be serious at low speeds. In order to increase the deflection range of the ailerons above ±20°, and thereby the available rolling moment, the size of the overhanging balance would necessarily be shortened with an accompanying loss in available balancing power of the internal balance.

Characteristics of the modified $0.404\frac{b}{2}$ aileron.- As has been previously noted, and as shown in figure 1, the ailerons tested in the main part of this investigation were formed by segments the ends of which, with the exception of the ends at the $0.065\frac{b}{2}$ and $0.990\frac{b}{2}$ stations, were cut perpendicular to the aileron hinge line. In order to determine the effects of aileron end treatment or changes in aileron plan form on aileron control characteristics, the $0.404\frac{b}{2}$ outboard aileron having a trailing-edge angle of 6° was modified by cutting the inboard end of the aileron parallel to the plane of symmetry (fig. 4). A comparison of the data for the modified aileron configuration with that of the original aileron configuration (figs. 24 and 25 and table II) shows that the modification resulted in approximately a 9-percent reduction in the rolling power of the aileron, no notable change in the yawing-moment

characteristics, and a negligible reduction in the value of the hinge-moment parameter C_{h_α}. The main effect of the modification was a reduction in the variation of hinge moment over the aileron deflection range; this reduction amounted to approximately 55 percent in the value of $C_{h_{\delta_a}}$.

Spoiler Control Characteristics

The aerodynamic and lateral control characteristics of the wing equipped with the spoiler configuration shown in figure 6 and with the $0.925\frac{b}{2}$ unsealed flap deflected 0°, 30°, and 60° are shown in figure 26. As has been previously noted, the spoiler configuration used for these tests is similar to one of the more satisfactory configurations developed in the investigation reported in reference 8.

A comparison of the aerodynamic characteristics of the flapped wing-spoiler configuration with the characteristics of the plain flapped wing (fig. 7(b)) shows that the addition of the spoiler configuration on both semispans of the complete swept wing (for possible use as a speed brake or a glide-path control) generally produced the same effects on the values of C_L, C_D, C_m, and C_h at values of α below approximately 16° as are produced on unswept wings. Addition of the spoiler configuration to the swept wing reduced the values of C_L over the entire angle-of-attack range; in addition, the values of C_D were increased, and the values of C_m and C_h generally became more positive (or less negative) at low angles of attack, and opposite trends were exhibited by these coefficients at large angles of attack. The spoiler configuration produced only small changes in the incremental values of C_L, C_D, C_m, and C_h resulting from deflection of the flap.

The variation of spoiler-aileron rolling-moment coefficient with angle of attack was irregular for all three flap deflections; the values of C_l generally increased with increase in α at values of α below approximately 14° and tended to decrease with increase in α above $\alpha = 14°$. Except in the high angle-of-attack range, the values of C_l produced by spoiler projection generally were greatest with the flap deflected. The yawing-moment coefficients produced by spoiler projection were favorable over most of the angle-of-attack range but became adverse at angles of attack greater than approximately 12°.

It is rather difficult to make a direct comparison between the relative effectiveness of the one spoiler configuration investigated and the effectiveness of the ailerons investigated, principally because the spoiler was tested at only one projection and the configuration tested may not be optimum for the subject wing. However, considering the variation of the rolling-moment characteristics over the projection range of this spoiler configuration on another wing (reference 8) — which would probably be quite similar on the subject wing — it appears

that the present spoiler configuration at a maximum projection of approximately 0.08c would probably provide as much rolling moment over the angle-of-attack range as the $0.404\frac{b}{2}$ outboard aileron (which represents a fairly typical aileron configuration) deflected ±20° (to allow for adequate internal balancing). A comparison of this nature is not complete, however, because the spoilers exhibited more favorable yawing-moment characteristics and would have more favorable stick-force characteristics than the $0.404\frac{b}{2}$ aileron, particularly at high speeds. It should be remembered that the comparative analysis of the effectiveness of the two lateral control devices is based on data obtained only at low speed and, as such, is not intended to apply in the transonic speed range wherein wings of this plan form are designed to fly.

Effect of Wing-Tip Shape

Reference 7 presents the results of an investigation, similar to that reported herein, performed with essentially the same wing model as the present model, except that the wing model of reference 7 was equipped with a raked tip. For purposes of identification, the wing of reference 7 will be referred to in the ensuing discussion as the "raked-tip wing" and the wing of the present investigation will be referred to as the "swept-tip wing."

Comparison of wing aerodynamic characteristics.- The variation of the wing angle of attack and drag, and pitching-moment coefficients with lift coefficient for the raked-tip wing with the largest span of flap tested at 0° and 30° deflections were almost identical to the corresponding characteristics of the swept-tip wing with the $0.925\frac{b}{2}$ flap at similar deflections. This rather complete lack of significant changes in the wing aerodynamic characteristics as a result of changing the tip shape has been noted previously in several unpublished investigations. This phenomenon, plus the fact that the aspect ratios of the swept-tip and raked-tip wings under discussion were about the same, leads to the belief that any major changes in the wing aerodynamic characteristics resulting from a change in the wing-tip shape are the result of changes in the wing aspect ratio. In addition, it is considered somewhat surprising that the variation of the increment of lift coefficient with flap deflection produced by the largest span flap on the raked-tip wing was almost in perfect agreement with the results for the $0.925\frac{b}{2}$ flap on the swept-tip wing, because the ratios of area and span of the largest span flap on the raked-tip wing to the area and span of the raked-tip wing are smaller than the corresponding ratios for the swept-tip wing.

Comparison of aileron lateral control characteristics.- In general, the C_l, C_n, C_h, and P data obtained on the swept-tip and raked-tip wings were quite similar and exhibited the same trends with change in aileron deflection and wing angle of attack. Also, in general, the effect of variation of the wing-tip shape on the variation of the lateral-control parameters $C_{h_{\delta_a}}$, C_{h_α}, and $C_{l_{\delta_a}}$ with aileron trailing-edge

angle and on the variation of $C_{h_{\delta_a}}$ and C_{h_α} with aileron span was negligible. For any given span of aileron, the rolling-effectiveness parameter $C_{l_{\delta_a}}$ for the swept-tip wing was slightly greater than the $C_{l_{\delta_a}}$ values for the raked-tip wing. This effect seems logical when one considers the comparative spans and spanwise locations of the ailerons tested on both wings. From a comparison of these low-speed data, it appears, therefore, that the wing with the swept tip would be preferred because the wing with this tip has, for equal aspect ratio and taper ratio, more physical length of trailing edge upon which to install ailerons and high-lift devices than the comparable raked-tip wing, and because it would provide more satisfactory performance (as a result of its larger area) for an airplane.

CONCLUSIONS

A wind-tunnel investigation was performed at low speed to determine the aerodynamic characteristics of a 51.3° sweptback semispan wing equipped with 16.7-percent-chord plain flaps and ailerons having various spans, spanwise locations, and trailing-edge angles. In addition, a spoiler-aileron configuration was tested on the semispan wing in conjunction with a 92.5-percent-span flap. The results of the investigation led to the following conclusions:

1. In general, changes in the wing angle of attack, flap deflection, flap span, or flap spanwise location produced trends in the swept-wing lift, drag, pitching-moment, and flap hinge-moment characteristics that were similar to, but of different magnitude from, the trends produced on unswept wings, except possibly at large angles of attack near the wing stall. In the low and moderate lift-coefficient range, a seal installed across the 0.5-percent-chord gap ahead of the flap nose produced no significant changes in the lift, drag, pitching-moment, and hinge-moment characteristics of the wing obtained with the flap unsealed.

2. The incremental value of lift coefficient ΔC_L obtained with 52.1-percent span and 92.5-percent span unsealed flaps deflected 60° were, respectively, approximately 0.33 and 0.43 at zero angle of attack, approximately 0.29 and 0.35 at an angle of attack of 12°, and approximately 0.07 and 0.21 at maximum lift.

3. As would be normally anticipated the effectiveness of the ailerons, as shown by the variation of rolling-moment coefficient with aileron deflection $C_{l_{\delta_a}}$, increased as the aileron span increased and decreased as the trailing-edge angle of a given aileron was increased. The data indicated that a given percent-span aileron would be most effective when spanning the center portion of the wing semispan, but

would retain the greater part of its effectiveness through the angle-of-attack range when spanning the outboard portion of the wing semispan.

4. The total yawing moment, resulting from equal up and down deflections of the ailerons, was generally adverse for all combinations of aileron span and trailing-edge angle tested and became more adverse as the wing angle of attack or the aileron span increased. Variation of the trailing-edge angle caused no significant changes in the yawing moments produced by a given span of aileron.

5. The values of the aileron hinge-moment parameters C_{h_α} and $C_{h_{\delta_a}}$ were only slightly affected by changes in the span or spanwise location of the ailerons; C_{h_α} and $C_{h_{\delta_a}}$ exhibited a slight shift toward more negative values as the aileron span was increased toward the wing root section and as the spanwise location of a given span of aileron was moved inboard. In addition, for a given span of aileron, C_{h_α} and $C_{h_{\delta_a}}$ exhibited large changes toward less negative (or more positive) values as the aileron trailing-edge angle was increased.

6. Increase in the wing angle of attack had an inconsistent effect on the variation of seal-pressure coefficient with aileron deflection P_{δ_a} but generally produced a shift of the curves of the pressure coefficient against aileron deflection toward more positive values of pressure coefficient. Increase in the aileron trailing-edge angle generally resulted in slightly smaller values of P_{δ_a} but had a negligible effect on the values of pressure coefficient obtained at given aileron deflections. The seal-pressure data indicate, in general, that sealed internal balances will provide hinge-moment balancing effects on a highly sweptback wing through a moderate aileron-deflection range and a large angle-of-attack range up to and through the angle of wing stall.

7. Data obtained on a 40.4-percent-span outboard aileron modified by making the inboard end of the aileron parallel to the plane of symmetry (the original aileron had its inboard end normal to the aileron hinge line) shows that the only notable changes resulting from the modification were an approximately 9-percent reduction in the rolling effectiveness of the aileron and a 55-percent reduction in the parameter $C_{h_{\delta_a}}$.

8. The rolling moment produced by the spoiler-aileron configuration generally increased with increase in wing angle of attack α at values of α below approximately 14° and, in this α range, generally was greater with the flap deflected than with the flap undeflected. Also, in the aforementioned α range, the spoiler aileron produced favorable yawing moments.

9. A comparison made between the data obtained on the subject swept wing and data obtained on a raked-tip version of the subject wing indicated no major differences existed in the trends and magnitudes of the coefficients obtained.

Langley Aeronautical Laboratory
National Advisory Committee for Aeronautics
Langley Field, Va.

REFERENCES

1. House, R. O.: The Effects of Partial-Span Plain Flaps on the Aerodynamic Characteristics of a Rectangular and a Tapered Clark Y Wing. NACA TN No. 663, 1938.

2. House, Rufus O.: The Effects of Partial-Span Slotted Flaps on the Aerodynamic Characteristics of a Rectangular and a Tapered N.A.C.A. 23012 Wing. NACA TN No. 719, 1939.

3. Wenzinger, Carl J.: The Effects of Full-Span and Partial-Span Split Flaps on the Aerodynamic Characteristics of a Tapered Wing. NACA TN No. 505, 1934.

4. Langley Research Department (Compiled by Thomas A. Toll): Summary of Lateral-Control Research. NACA TN No. 1245, 1947.

5. Weick, Fred E., and Jones, Robert T.: Résumé and Analysis of N.A.C.A. Lateral Control Research. NACA Rep. No. 605, 1937.

6. Pearson, Henry A., and Jones, Robert T.: Theoretical Stability and Control Characteristics of Wings with Various Amounts of Taper and Twist. NACA Rep. No. 635, 1938.

7. Fischel, Jack, and Schneiter, Leslie E.: An Investigation at Low Speed of a 51.3° Sweptback Semispan Wing with a Raked Tip and with 16.7-Percent-Chord Ailerons Having Three Spans and Three Trailing-Edge Angles. NACA RM No. L8F29, 1948.

8. Schneiter, Leslie E., and Watson, James M.: Low-Speed Wind-Tunnel Investigation of Various Plain-Spoiler Configurations for Lateral Control on a 42° Sweptback Wing. NACA TN No. 1646, 1948.

9. Lowry, John G., and Schneiter, Leslie E.: Estimation of Effectiveness of Flap-Type Controls on Sweptback Wings. NACA TN No. 1674, 1948.

10. Fehlner, Leo F.: A Study of the Effect of Adverse Yawing Moment on Lateral Maneuverability at a High Lift Coefficient. NACA ARR, Sept. 1942.

11. Fischel, Jack: Hinge Moments of Sealed-Internal-Balance Arrangements for Control Surfaces. II – Experimental Investigation of Fabric Seals in the Presence of a Thin-Plate Overhang. NACA ARR No. L5F30a, 1945.

TABLE I.- DIMENSIONAL CHARACTERISTICS OF THE VARIOUS 0.167c FLAPS AND AILERONS TESTED ON THE 51.3° SWEPTBACK WING

Flap or aileron span	Flap or aileron spanwise location		M (ft^3)
	y_{f_i} or y_{a_i}	y_{f_o} or y_{a_o}	
$0.925\frac{b}{2}$	$0.065\frac{b}{2}$	$0.990\frac{b}{2}$	0.2131
$.686\frac{b}{2}$	$.304\frac{b}{2}$	$.990\frac{b}{2}$	.1399
$.404\frac{b}{2}$	$.586\frac{b}{2}$	$.990\frac{b}{2}$	.0637
$.173\frac{b}{2}$	$.817\frac{b}{2}$	$.990\frac{b}{2}$	.0225
$.521\frac{b}{2}$	$.065\frac{b}{2}$	$.586\frac{b}{2}$	.1494
$.513\frac{b}{2}$	$.304\frac{b}{2}$	$.817\frac{b}{2}$	.1174
[a] $.404\frac{b}{2}$	$.586\frac{b}{2}$	$.990\frac{b}{2}$	.0561

[a]Modified by cutting inboard end of aileron parallel to plane of symmetry.

TABLE II.- SUMMARY OF THE LATERAL CONTROL CHARACTERISTICS OF 0.167c AILERONS OF VARIOUS SPANS ON THE 51.3° SWEPTBACK WING

Aileron span, b_a	ϕ_a (deg)	$C_{l_{\delta_a}}$	$C_{h_{\delta_a}}$	C_{h_α}	P_{δ_a}					Total C_l for $\delta_a = \pm 30°$			
					Sta. 1	Sta. 2	Sta. 3	Sta. 4	Sta. 5	$\alpha \approx 0°$	$\alpha \approx 8.3°$	$\alpha \approx 12.5°$	$\alpha \approx 20.8°$
$0.925\frac{b}{2}$	14	0.00118	-0.0064	-0.0024	0.025	0.033	0.030	0.033	0.027	0.0574	0.0562	0.0495	0.0436
$.686\frac{b}{2}$	14	.00105	-.0060	-.0015	------	.033	.031	.033	.027	.0514	.0503	.0414	.0417
$.404\frac{b}{2}$	14	.00057	-.0057	-.0011	------	------	------	.030	.024	.0299	.0298	.0250	.0240
$.173\frac{b}{2}$	14	.00022	-------	-------	------	------	------	------	------	.0139	.0134	.0129	.0096
$.521\frac{b}{2}$	14	.00063	-.0067	-.0025	.024	.026	.023	------	------	.0323	.0315	.0265	.0190
$.513\frac{b}{2}$	14	.00081	-.0064	-.0011	------	.031	.027	.028	.023	.0433	.0425	.0358	.0308
$.404\frac{b}{2}$	25	.00048	-.0035	.0015	------	------	------	.027	.021	.0276	.0243	.0268	.0255
$.404\frac{b}{2}$	6	.00059	-.0069	-.0015	------	------	------	.030	.026	.0310	.0276	.0276	.0242
[a] $.404\frac{b}{2}$	6	.00054	-.0031	-.0014	------	------	------	------	------	------	--------	---------	---------

[a] Modified by cutting inboard end parallel to plane of symmetry.

NACA

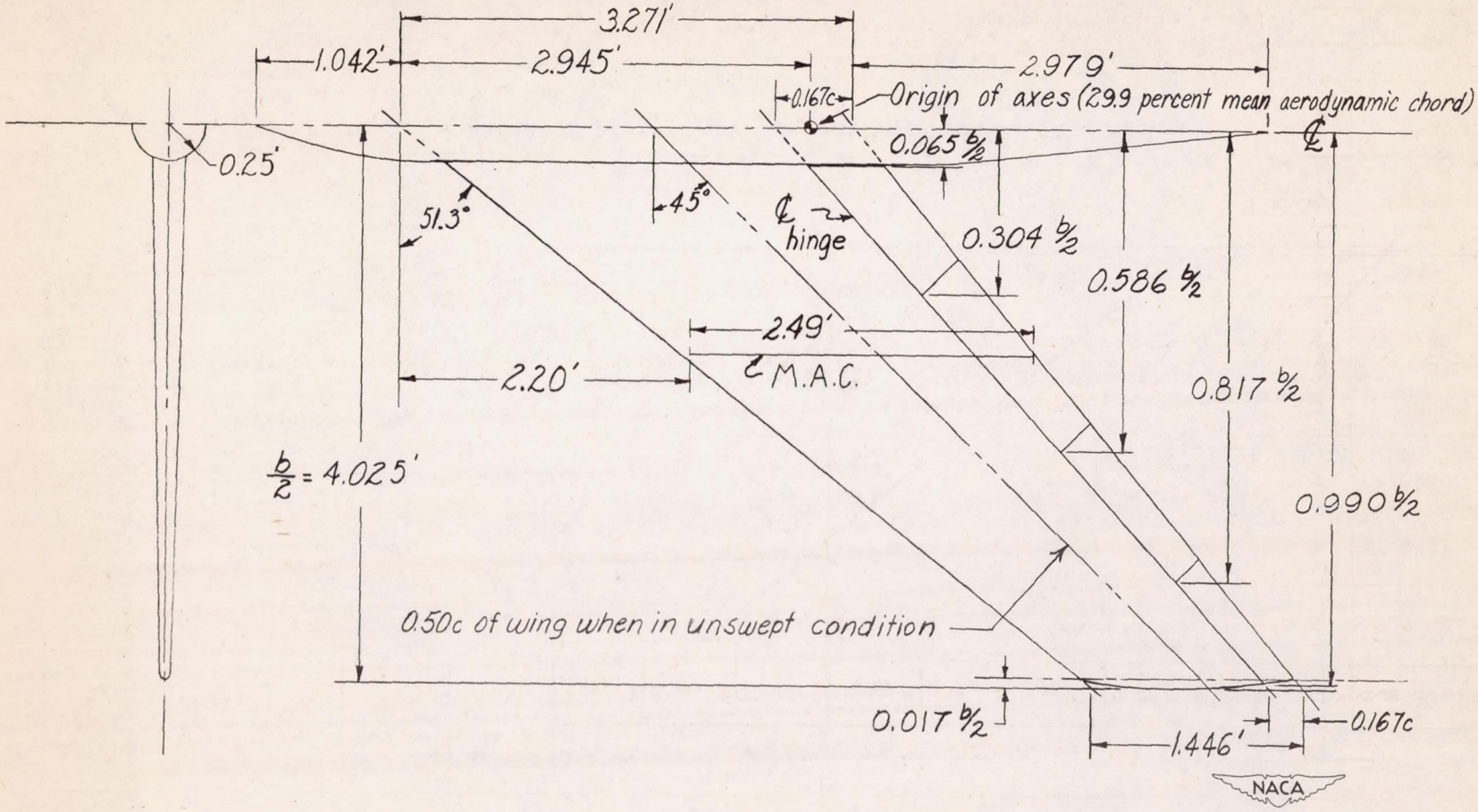


Figure 1.- Sketch of the 51.3° sweptback semispan wing model. S = 18.90 square feet; A = 3.43; taper ratio = 0.44. (All dimensions in feet, except as noted.)

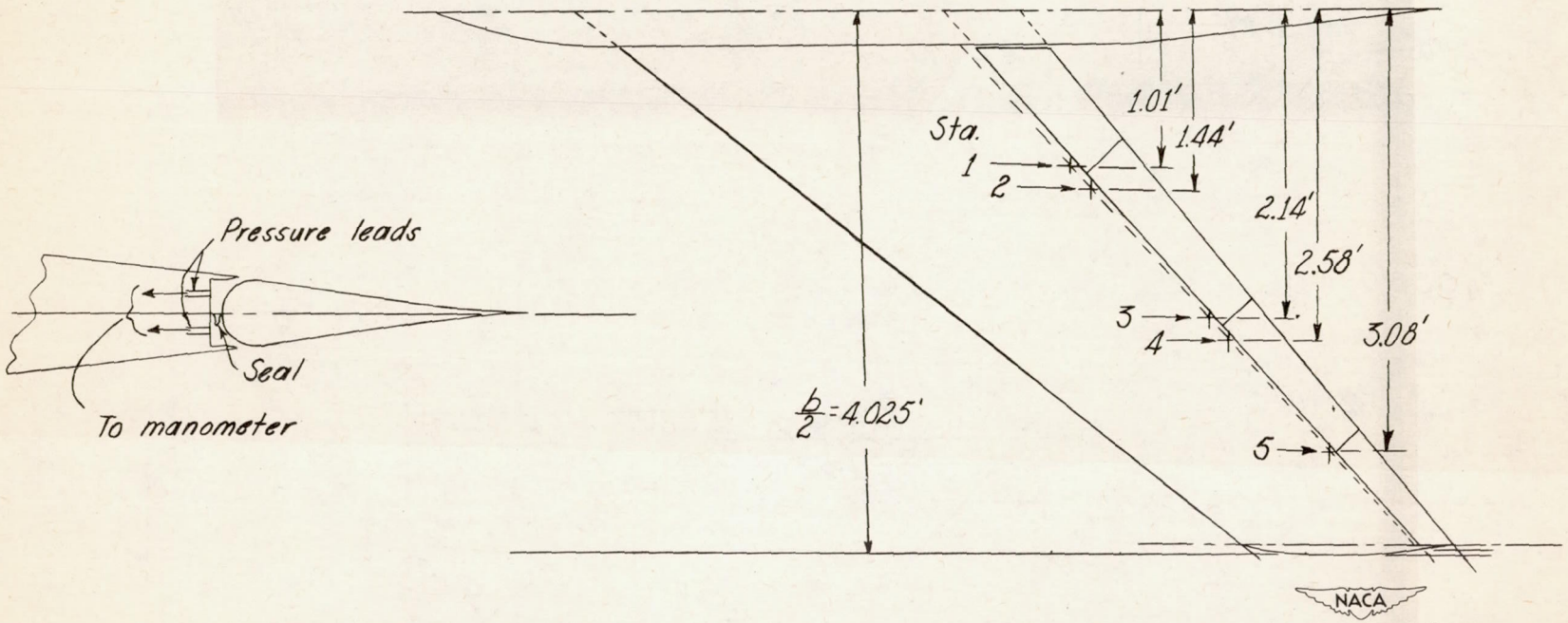


Figure 2.- Location of pressure orifices on the semispan wing model.

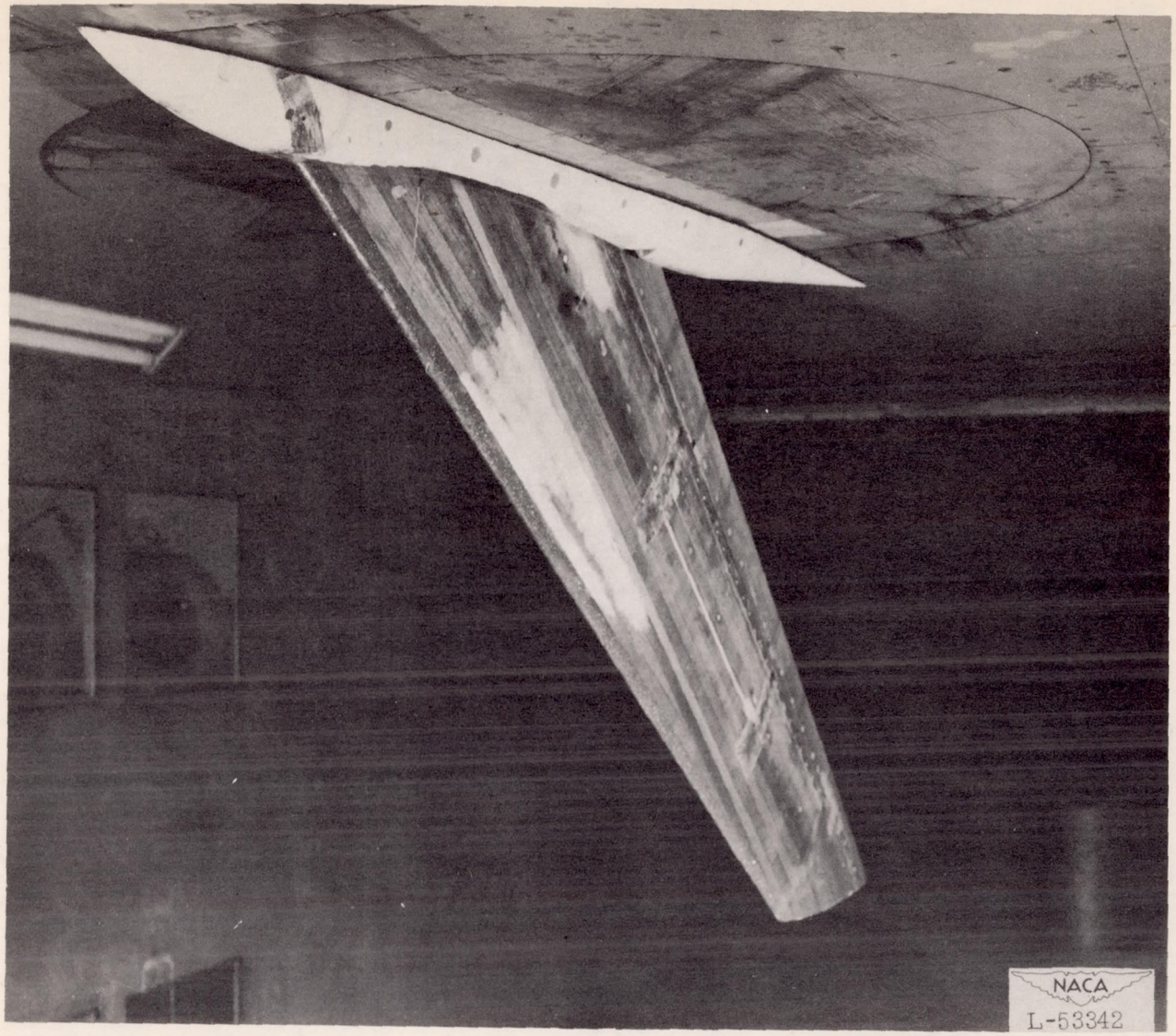


Figure 3.- The 51.3° sweptback semispan wing mounted near the ceiling in the Langley 300 MPH 7- by 10-foot tunnel.

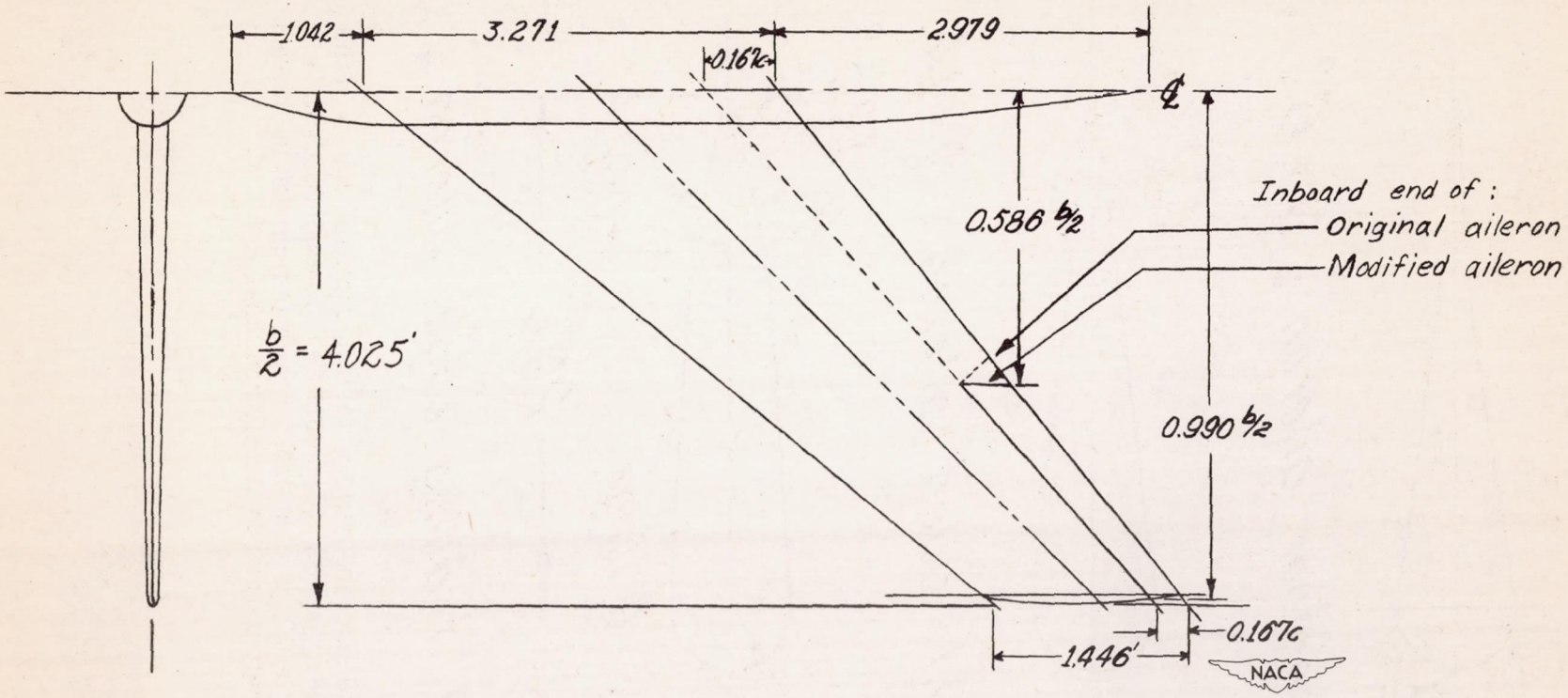


Figure 4.- Sketch of the 51.3° sweptback semispan wing showing the modified and original 0.404 $\frac{b}{2}$ ailerons tested.

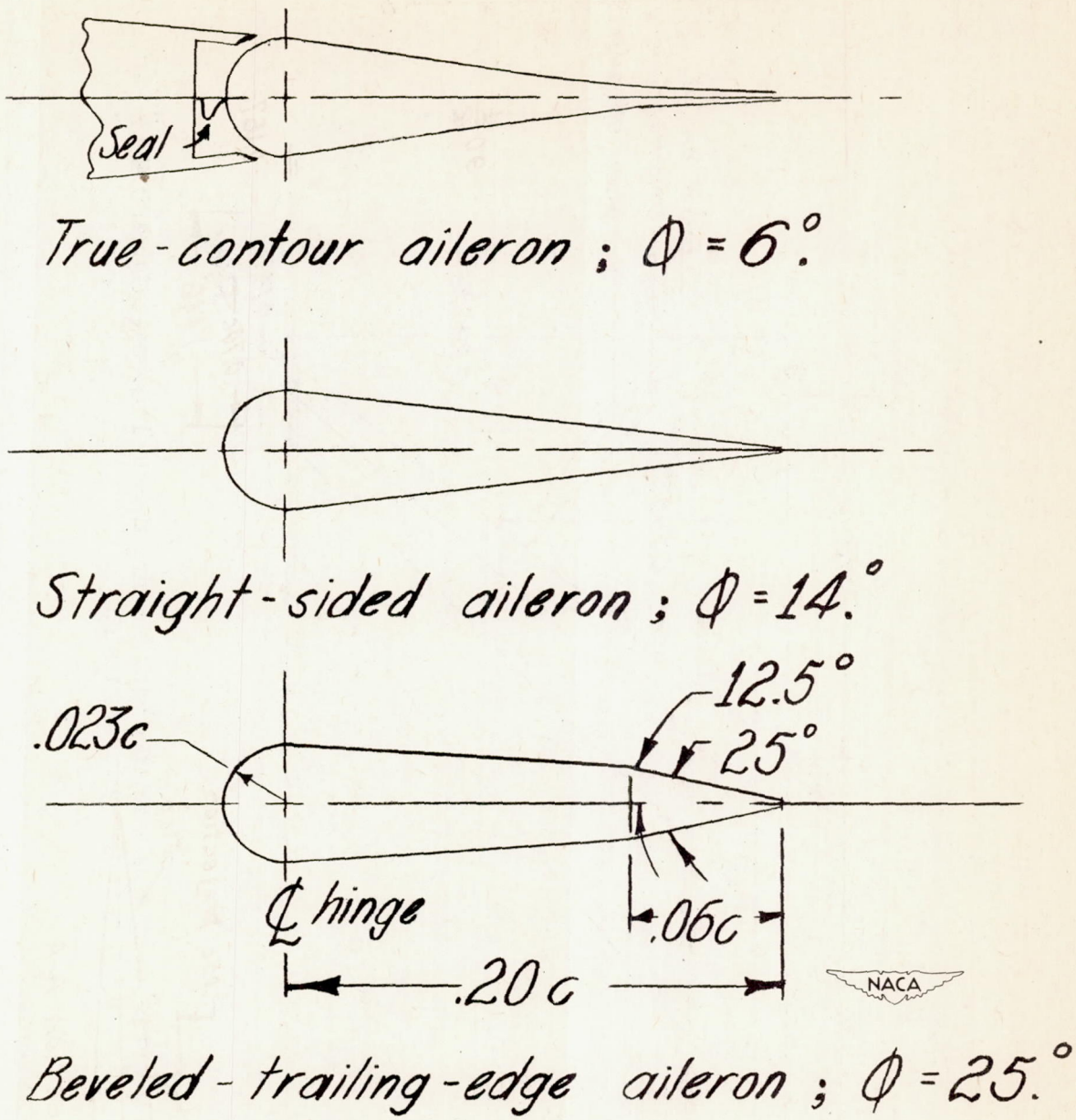


Figure 5.- Sketch of the flap and aileron contours tested on the 51.3° sweptback semispan wing model. (Contours and dimensions shown are in a plane normal to the 50-percent-chord line of the wing in the unswept condition or approximately normal to the aileron hinge line.)

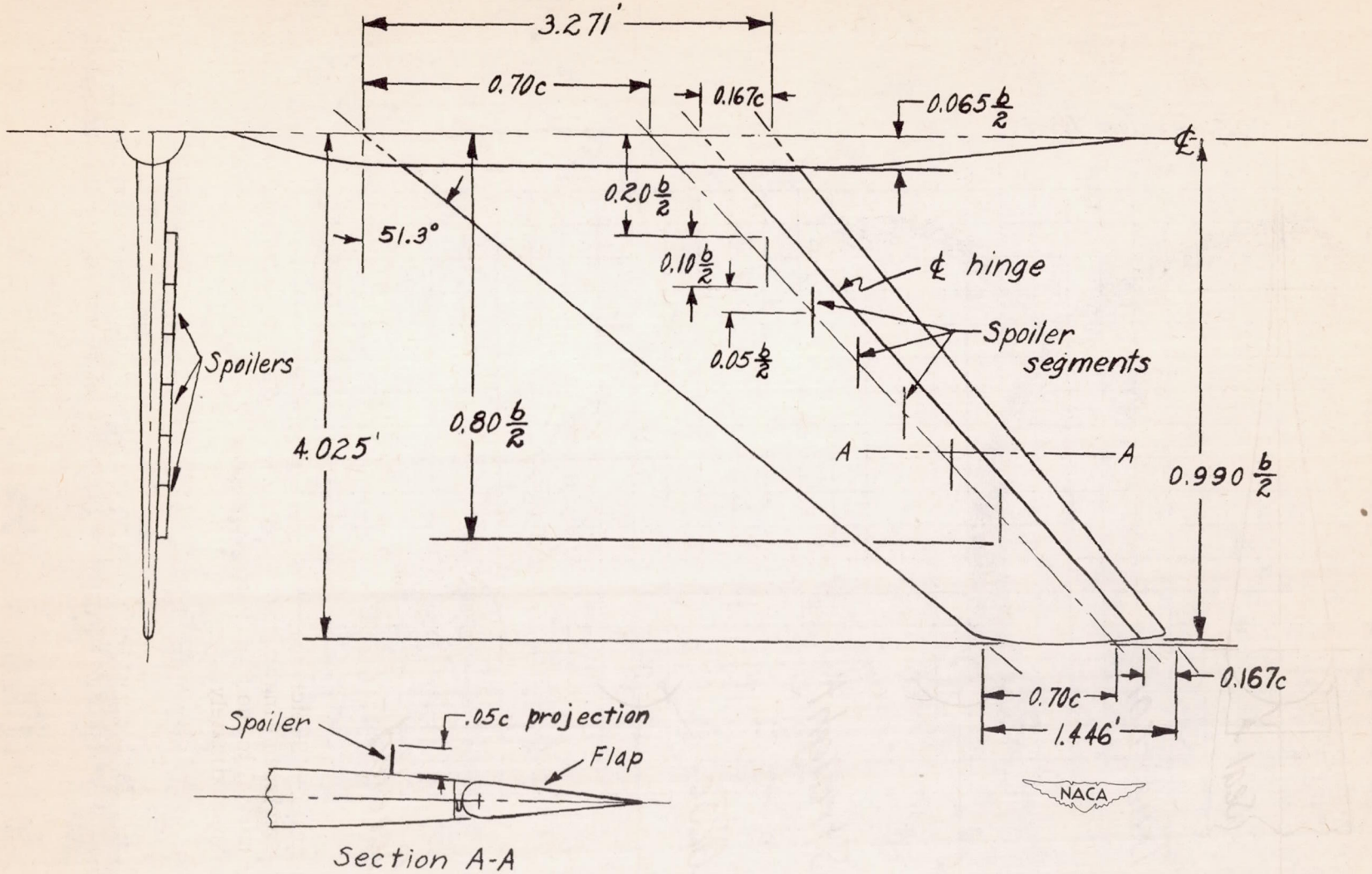
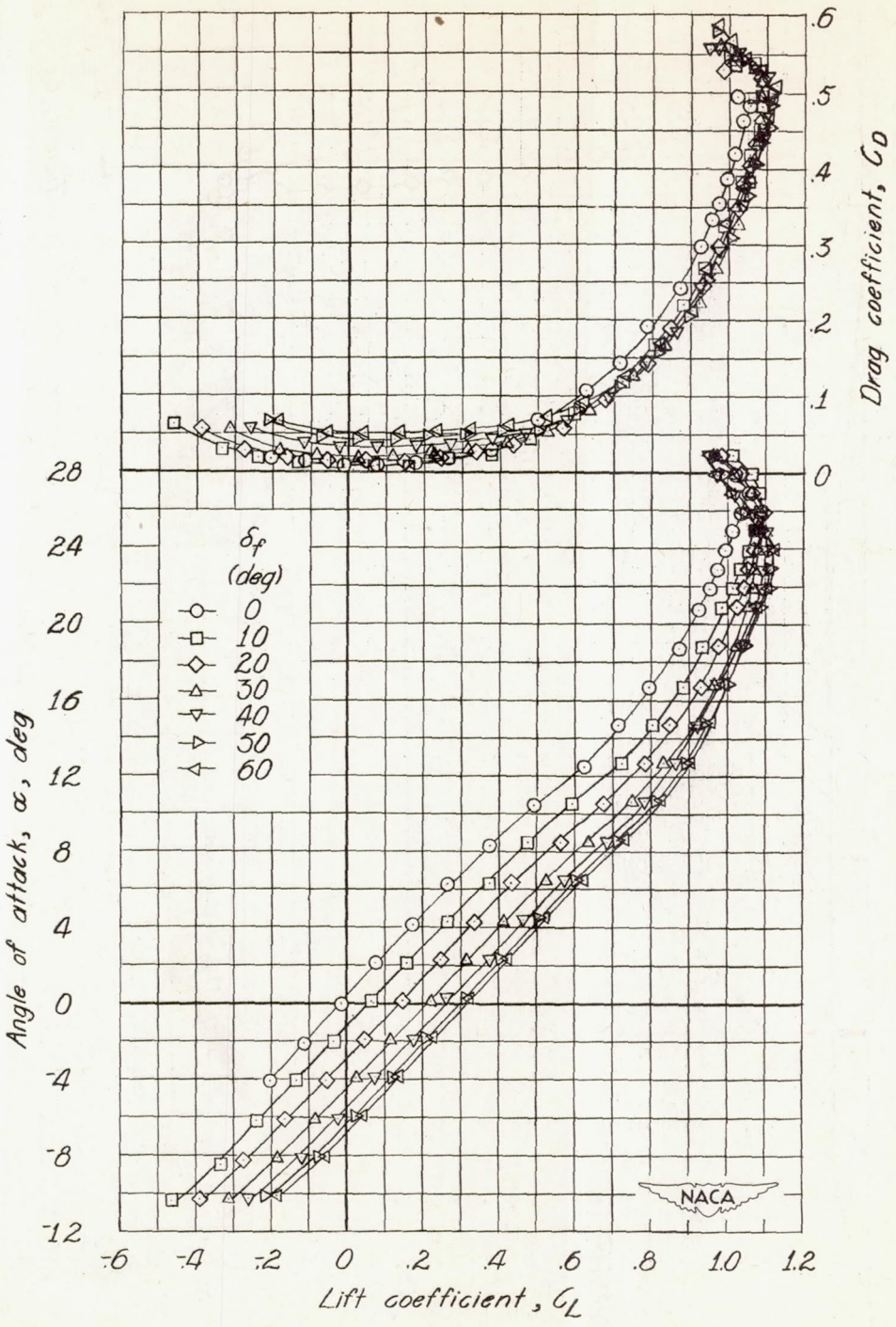
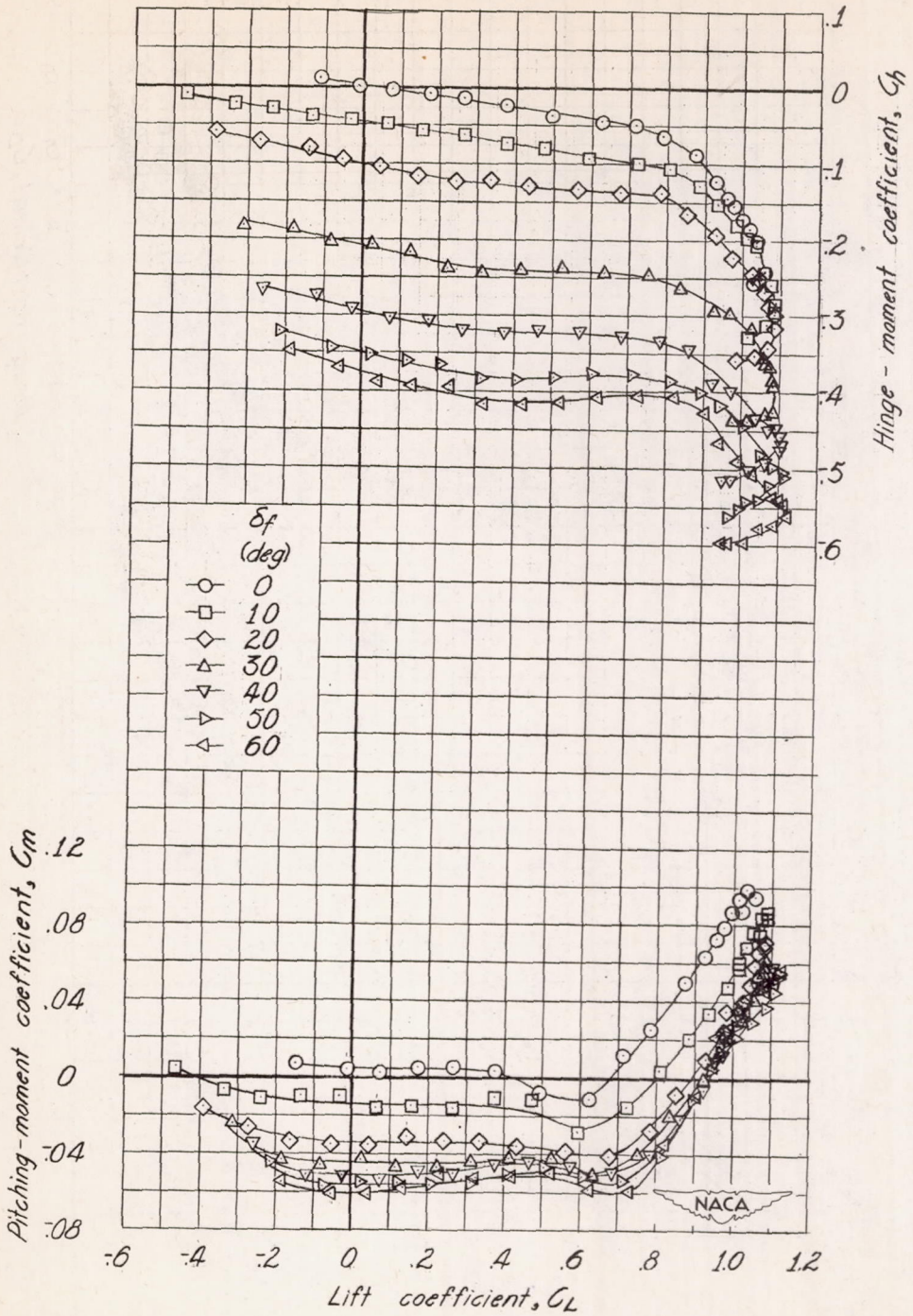


Figure 6.- Plan form and section of the spoiler configuration tested on the 51.3° sweptback semispan wing model.



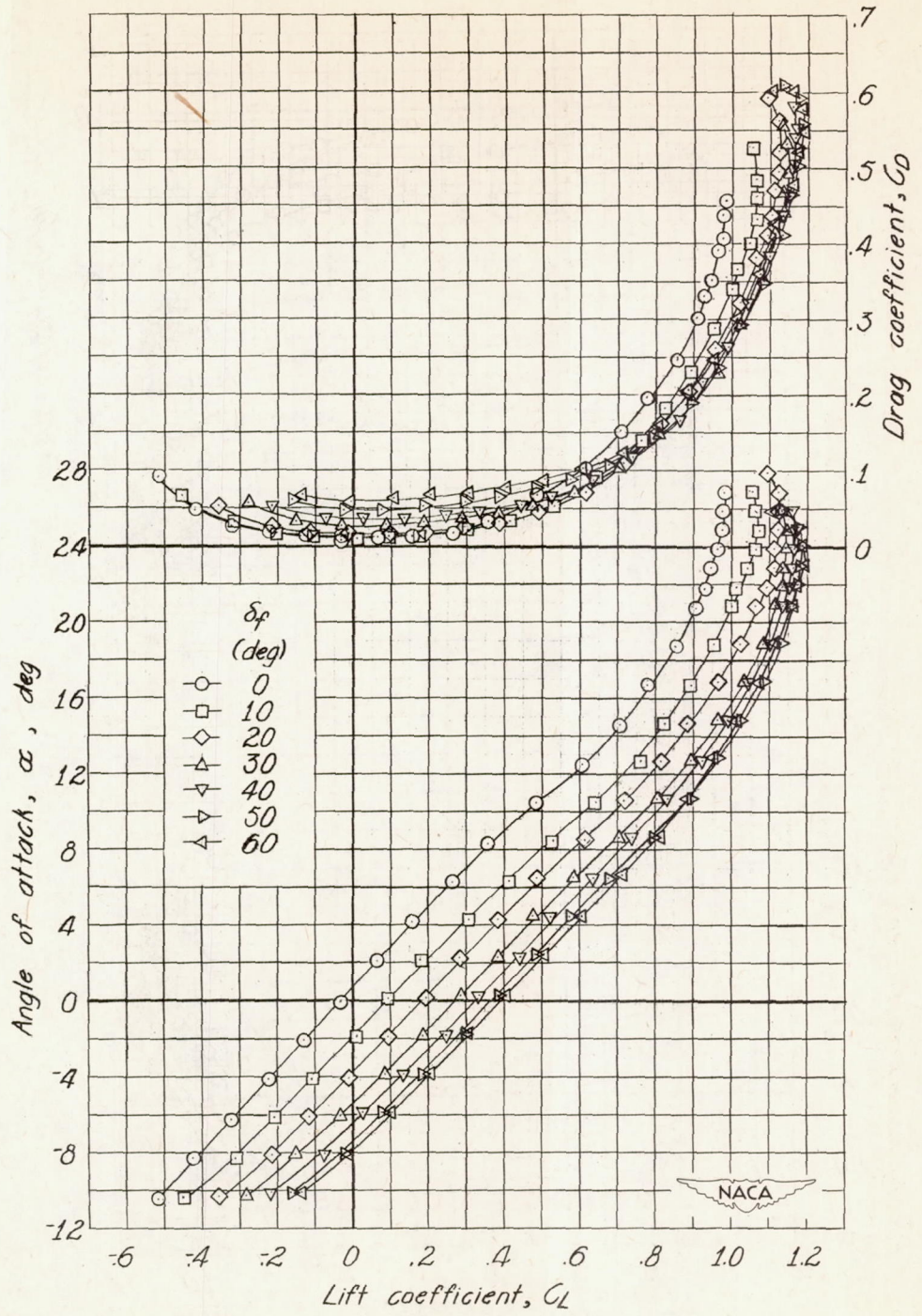
(a) Flap span, $0.521\frac{b}{2}$; $y_{f_i} = 0.065\frac{b}{2}$; $y_{f_o} = 0.586\frac{b}{2}$.

Figure 7.- Effect of flap deflection on the aerodynamic characteristics in pitch of the 51.3° sweptback wing. $\emptyset$ = 14° over entire wing span; flap unsealed.



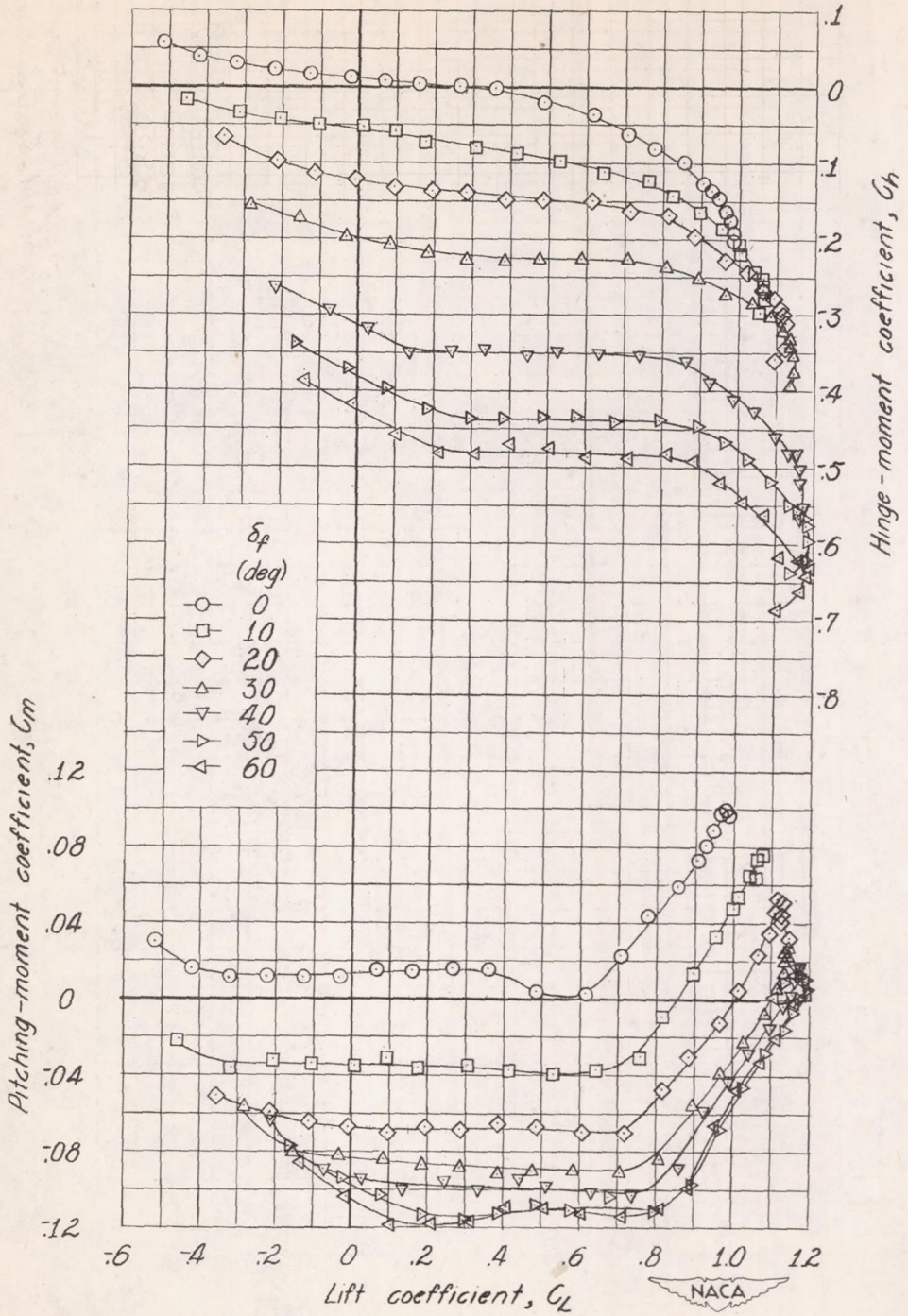
(a) Concluded.

Figure 7.- Continued.



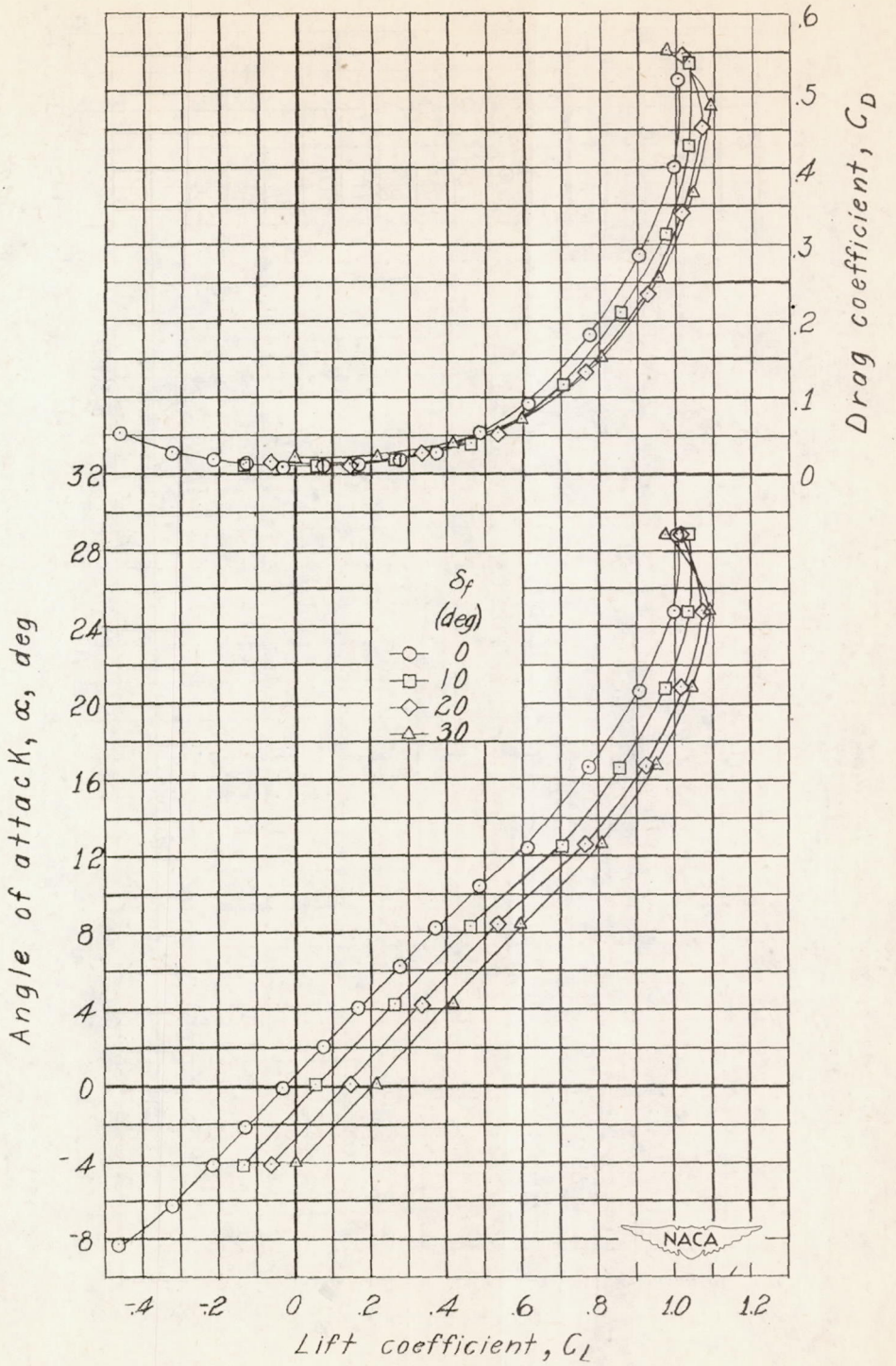
(b) Flap span, $0.925\frac{b}{2}$; $y_{f_i} = 0.065\frac{b}{2}$; $y_{f_o} = 0.990\frac{b}{2}$.

Figure 7.- Continued.



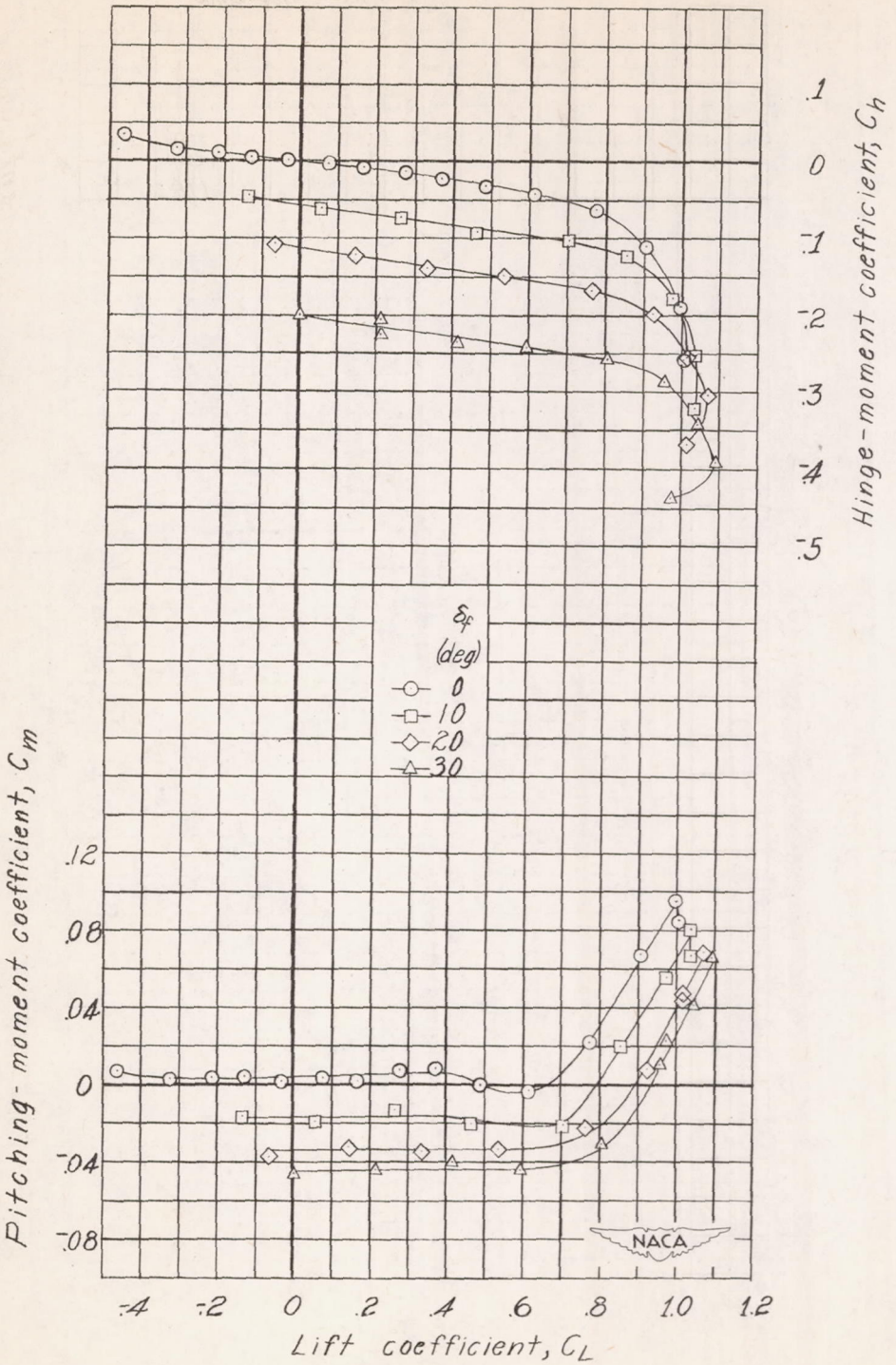
(b) Concluded.

Figure 7.- Concluded.



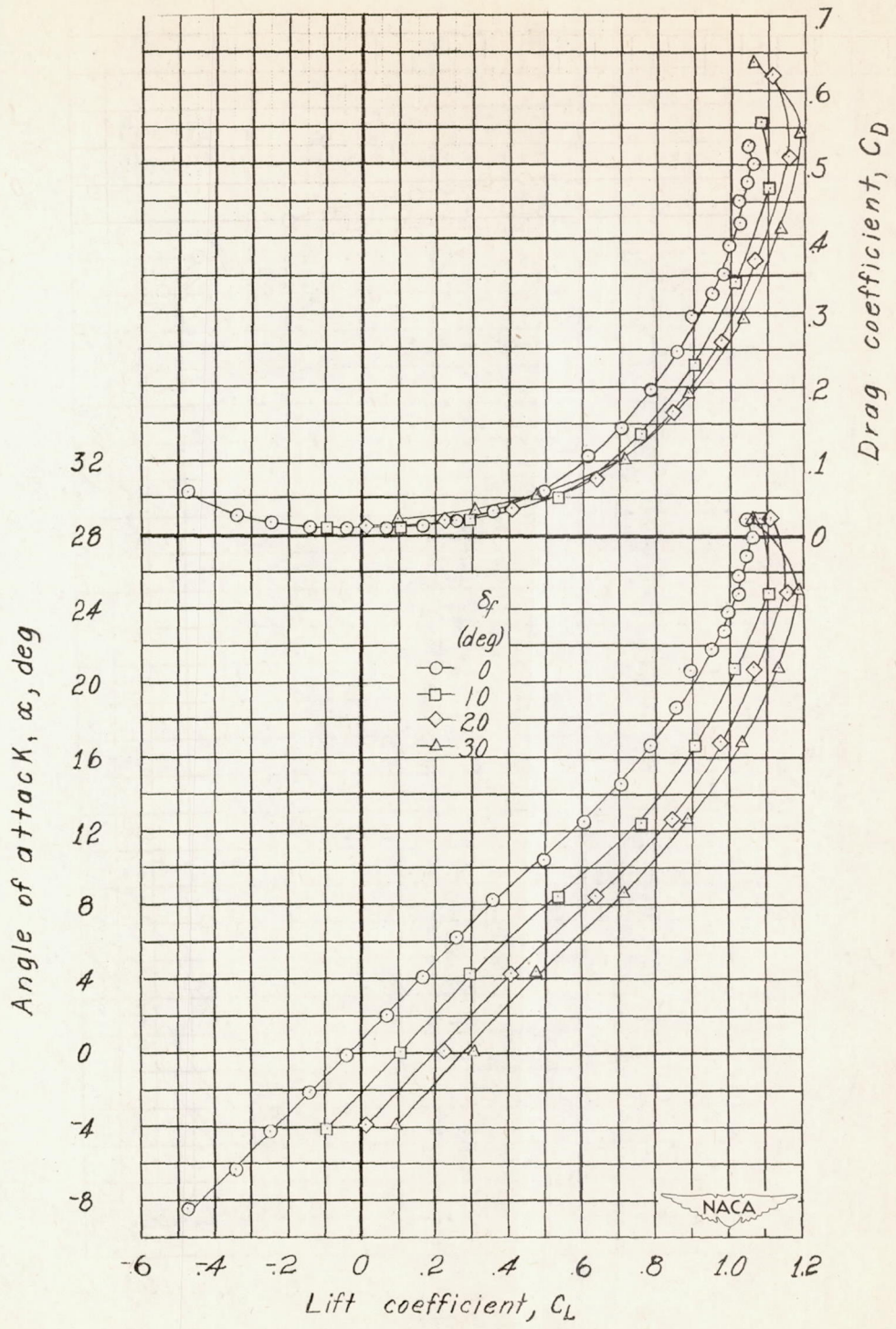
(a) Flap span, $0.521\frac{b}{2}$; $y_{f_i} = 0.065\frac{b}{2}$; $y_{f_o} = 0.586\frac{b}{2}$.

Figure 8.- Effect of flap deflection on the aerodynamic characteristics in pitch of the 51.3° sweptback wing. $\Phi = 14^\circ$ over entire wing span; flap sealed.



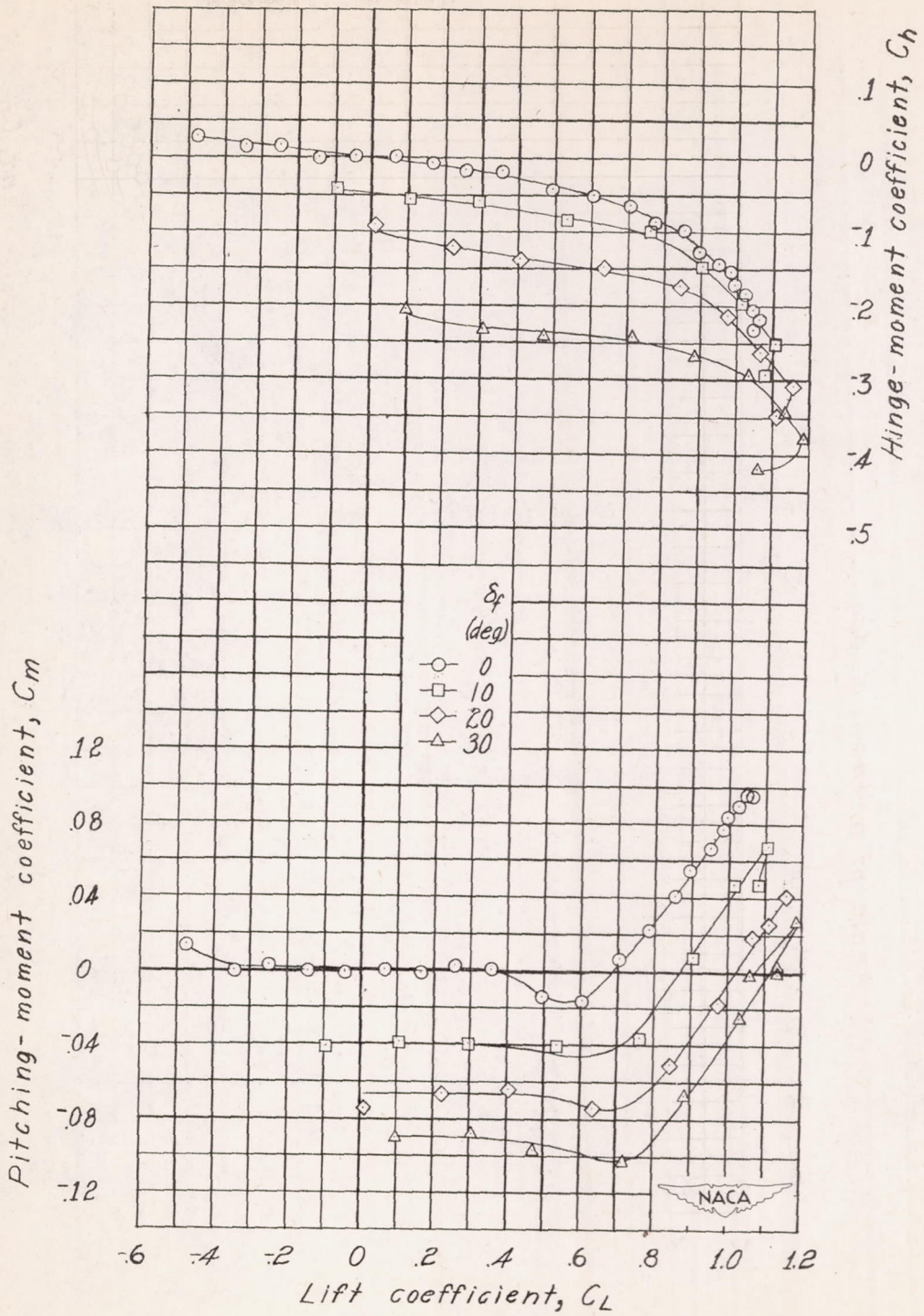
(a) Concluded.

Figure 8.- Continued.



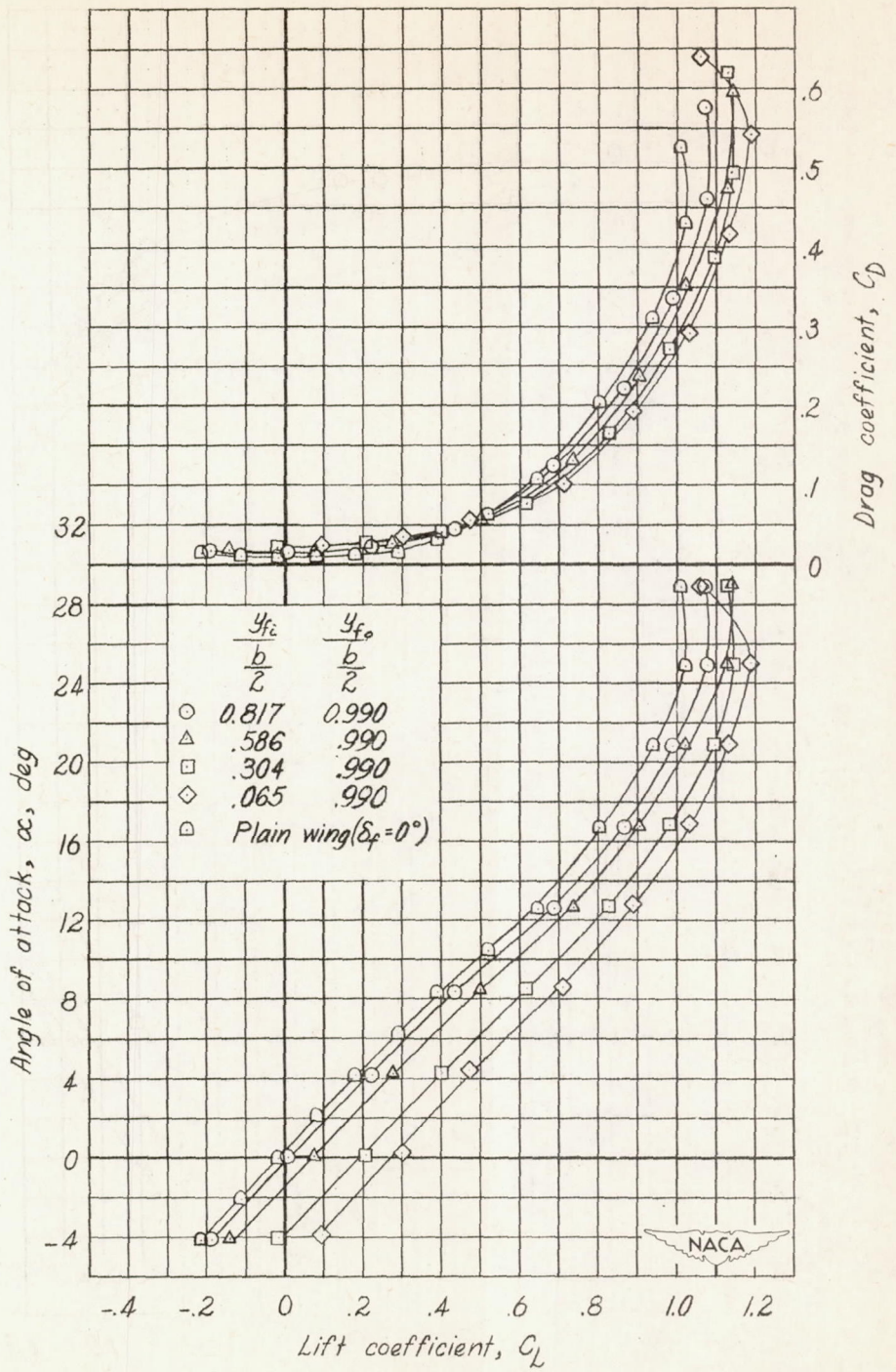
(b) Flap span, $0.925\frac{b}{2}$; $y_{f_i} = 0.065\frac{b}{2}$; $y_{f_o} = 0.990\frac{b}{2}$.

Figure 8.- Continued.



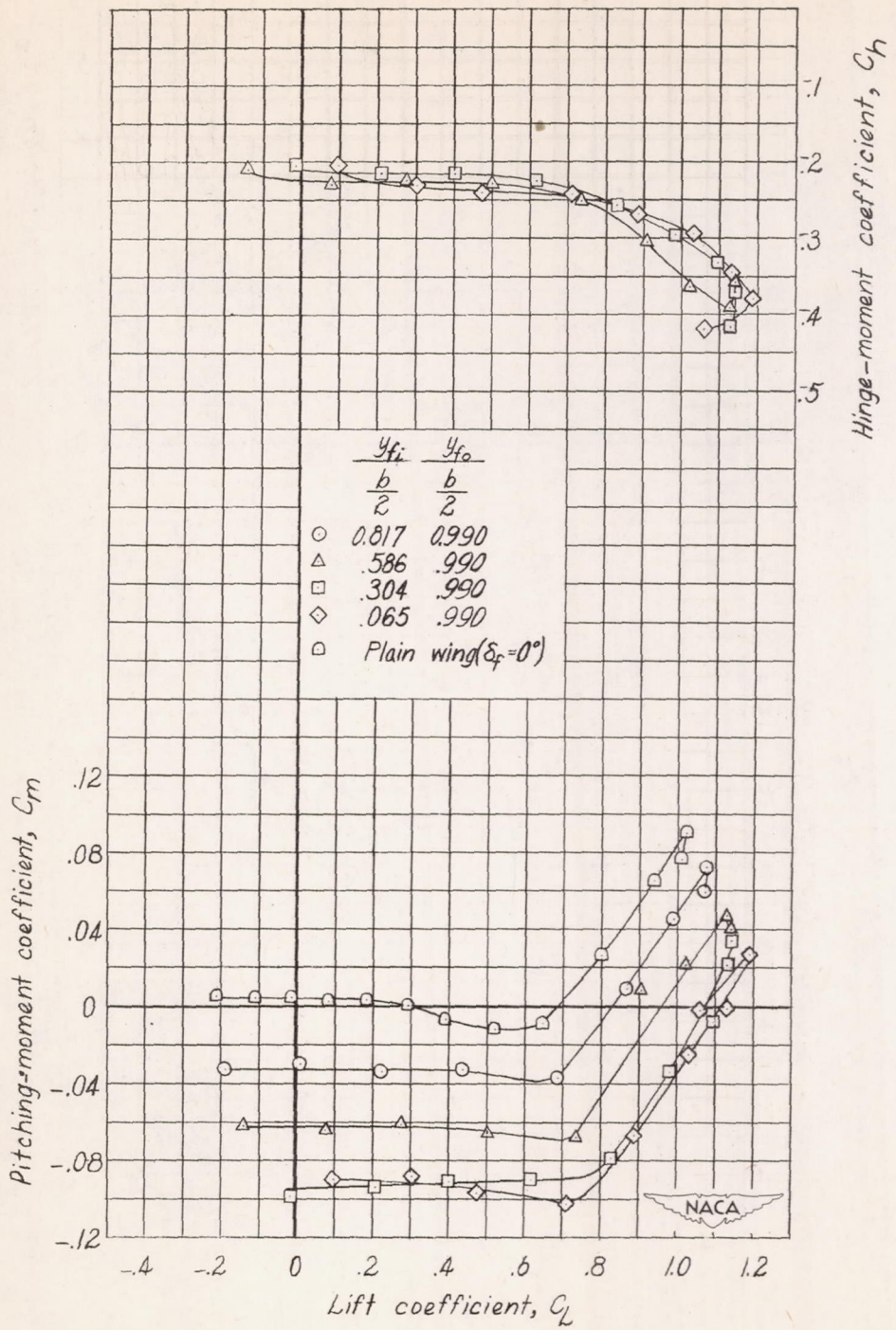
(b) Concluded.

Figure 8.- Concluded.



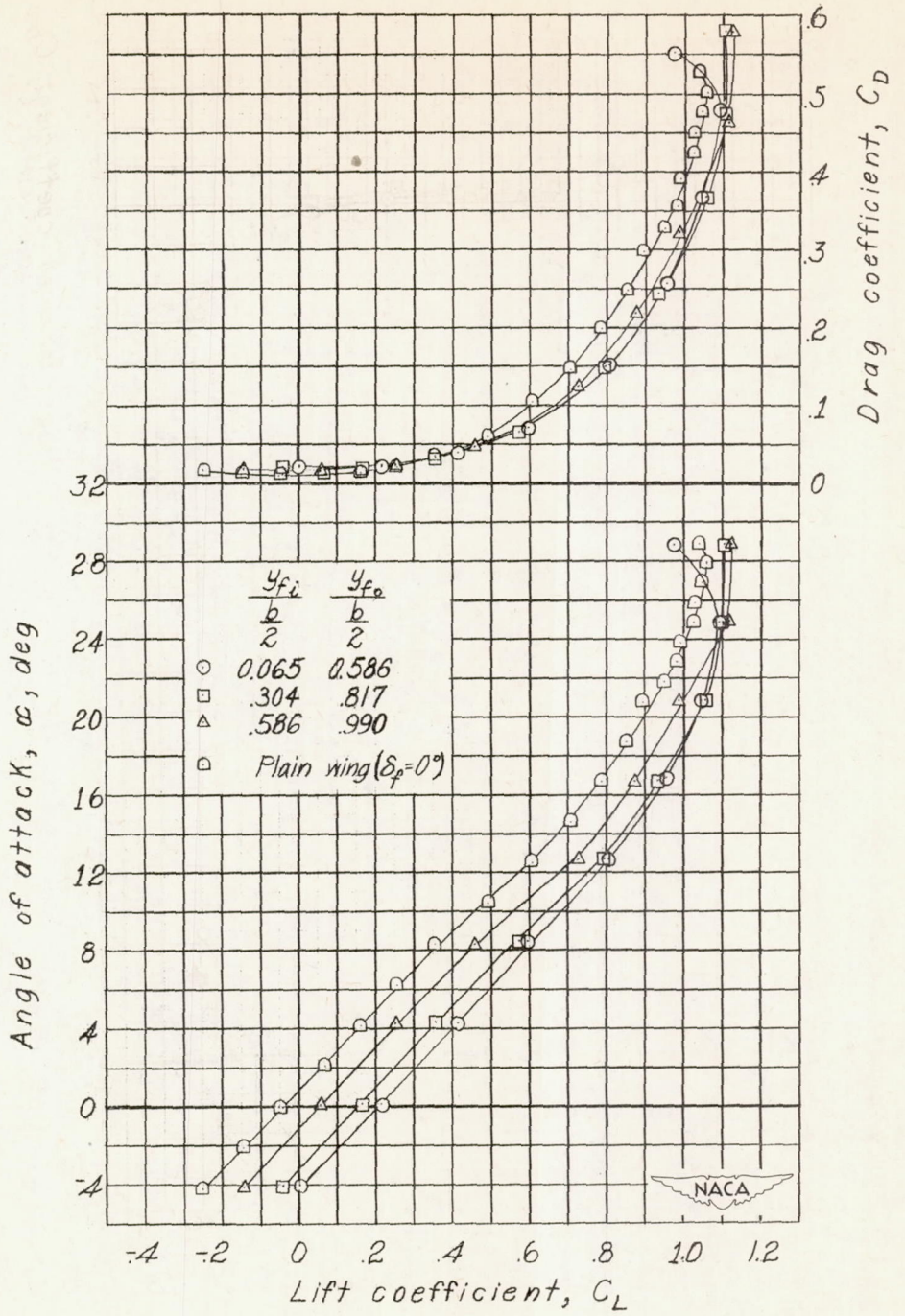
(a) $\emptyset = 14^\circ$ over flapped portion of wing; $\emptyset = 6^\circ$ over remainder of wing.

Figure 9.- Effect of flap span and spanwise location on the aerodynamic characteristics in pitch of the 51.3° sweptback wing. Flap sealed; $\delta_f = 30^\circ$.



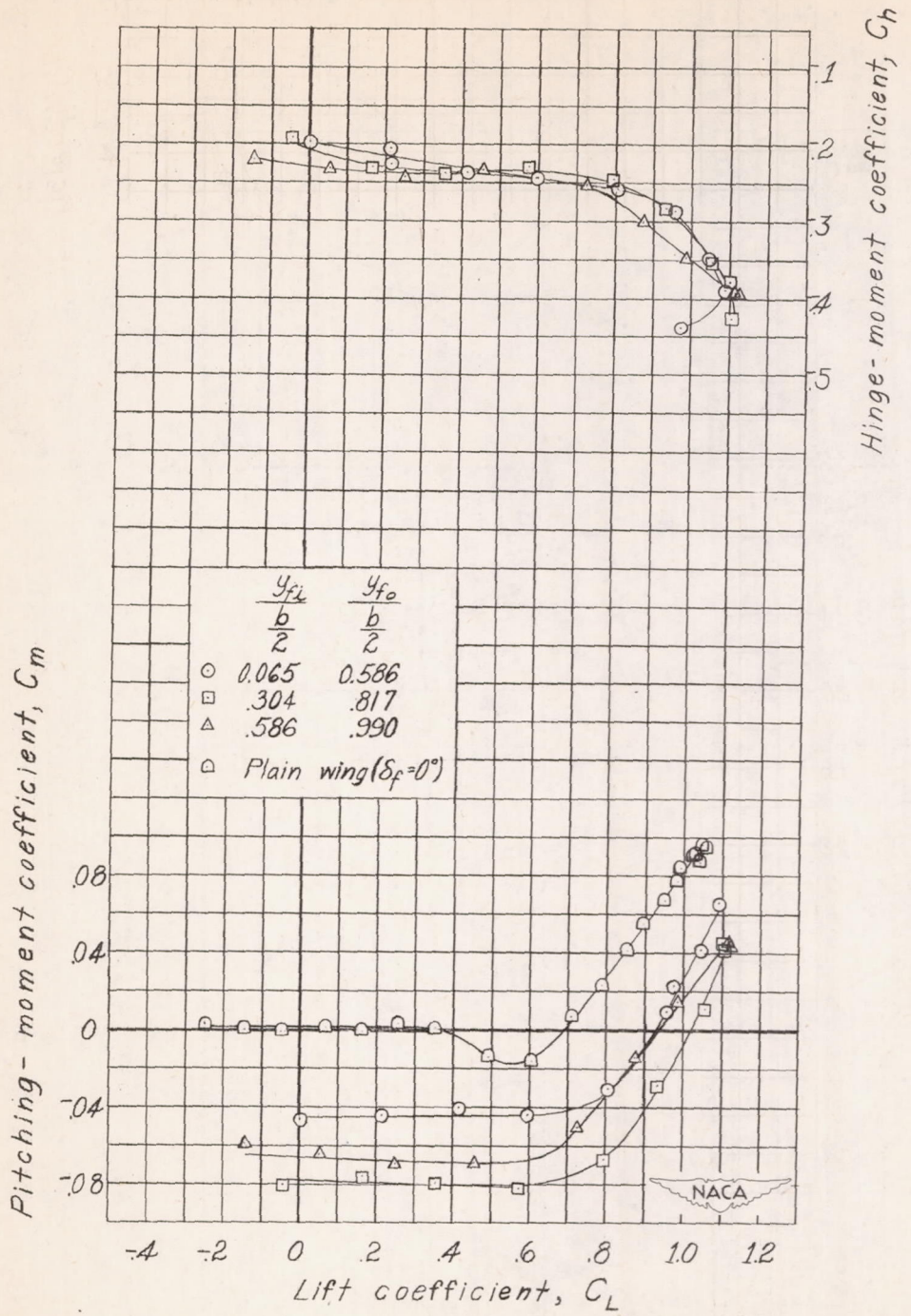
(a) Concluded.

Figure 9.- Continued.



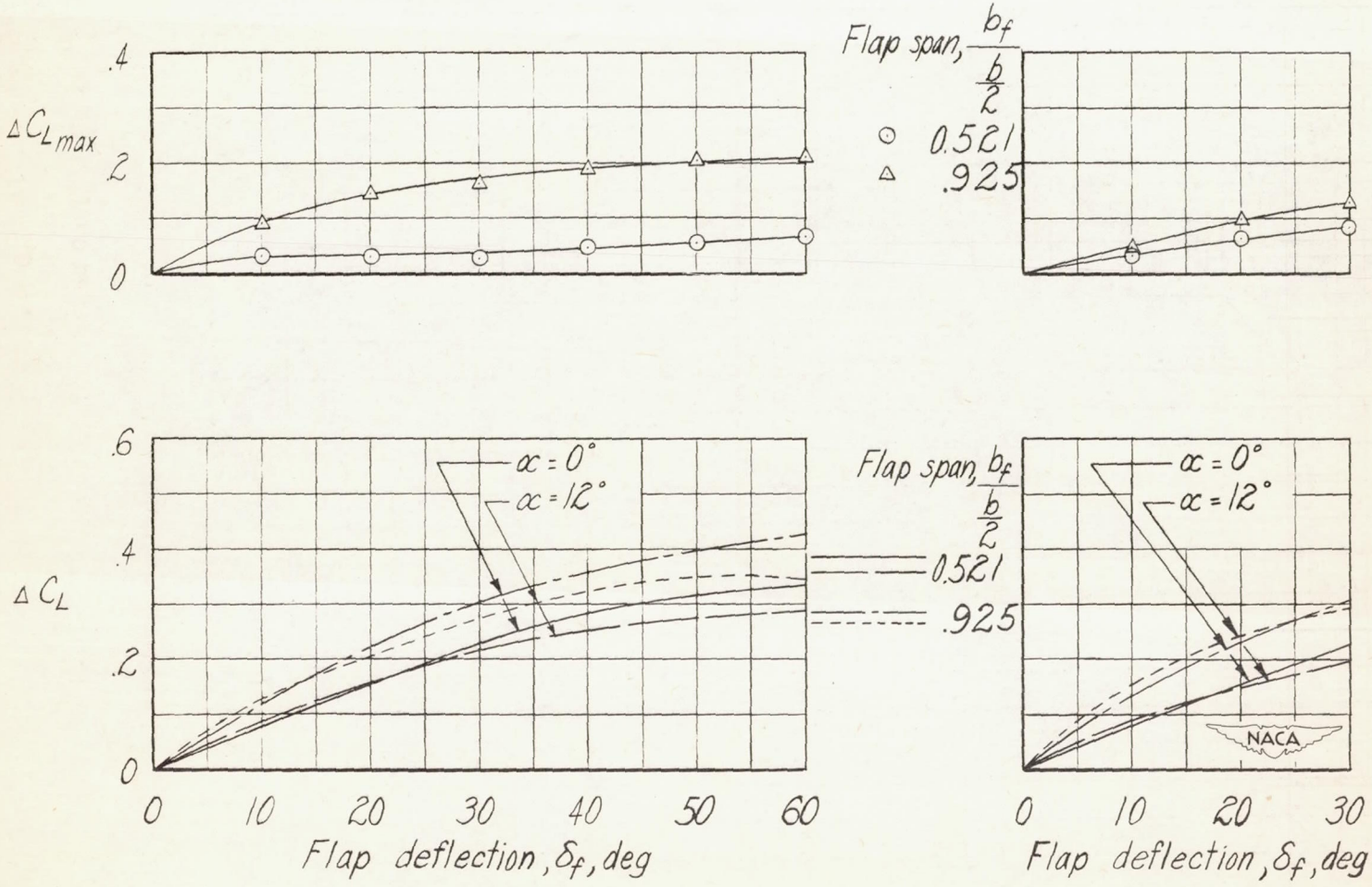
(b) $\phi = 14^{\circ}$ over entire wing span.

Figure 9.- Continued.



(b) Concluded.

Figure 9.- Concluded.



(a) Flap unsealed.

(b) Flap sealed.

Figure 10.- Variation of increment of lift coefficient ΔC_L with flap deflection for the 51.3° sweptback wing. $y_{f_i} = 0.065\frac{b}{2}$; $\phi = 14°$ over entire wing span.

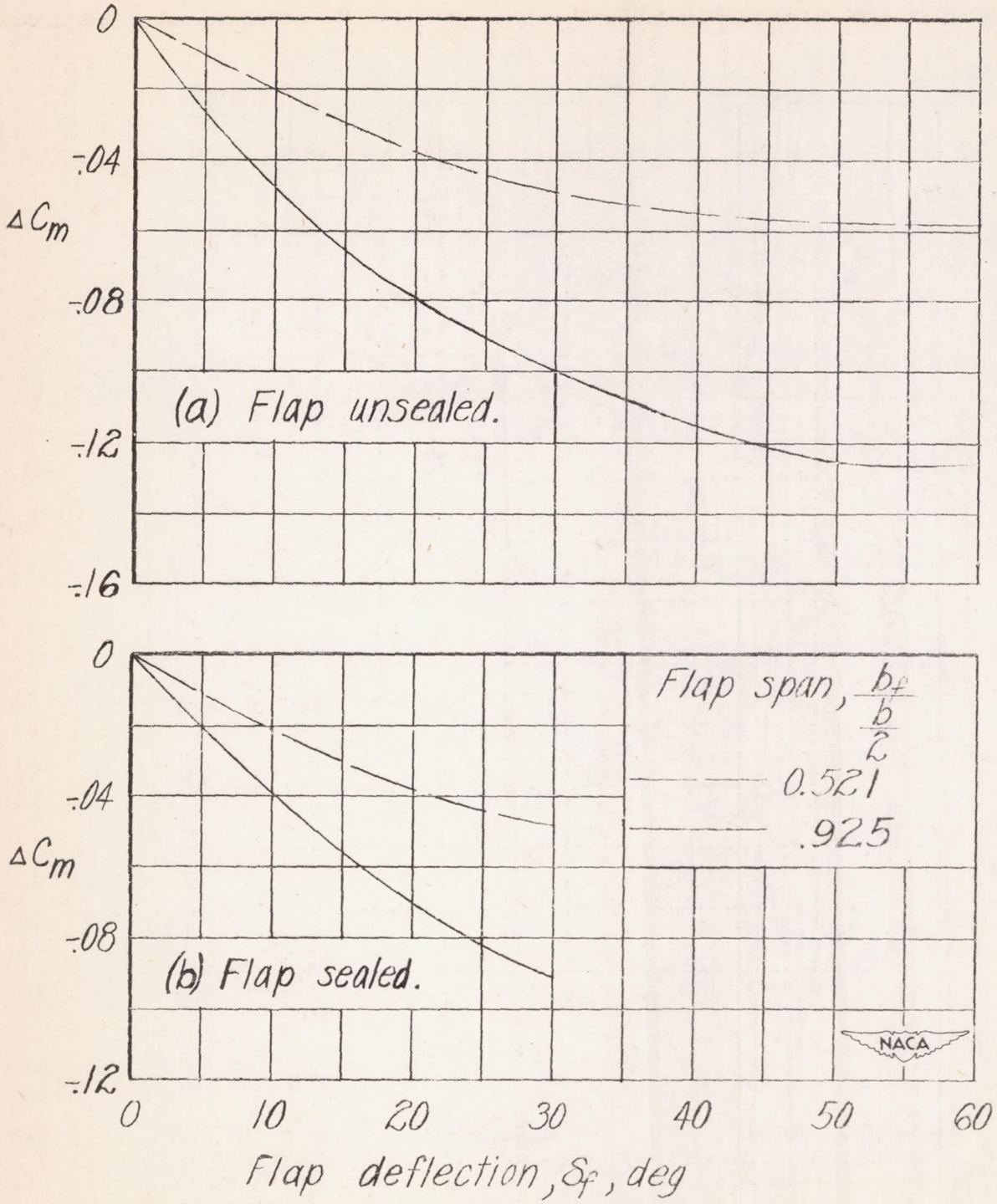


Figure 11.- Variation of increment of pitching-moment coefficient ΔC_m with flap deflection for the 51.3° sweptback wing at $\alpha = 0°$. $y_{f_i} = 0.065\frac{b}{2}$; $\phi = 14°$ over entire wing span.

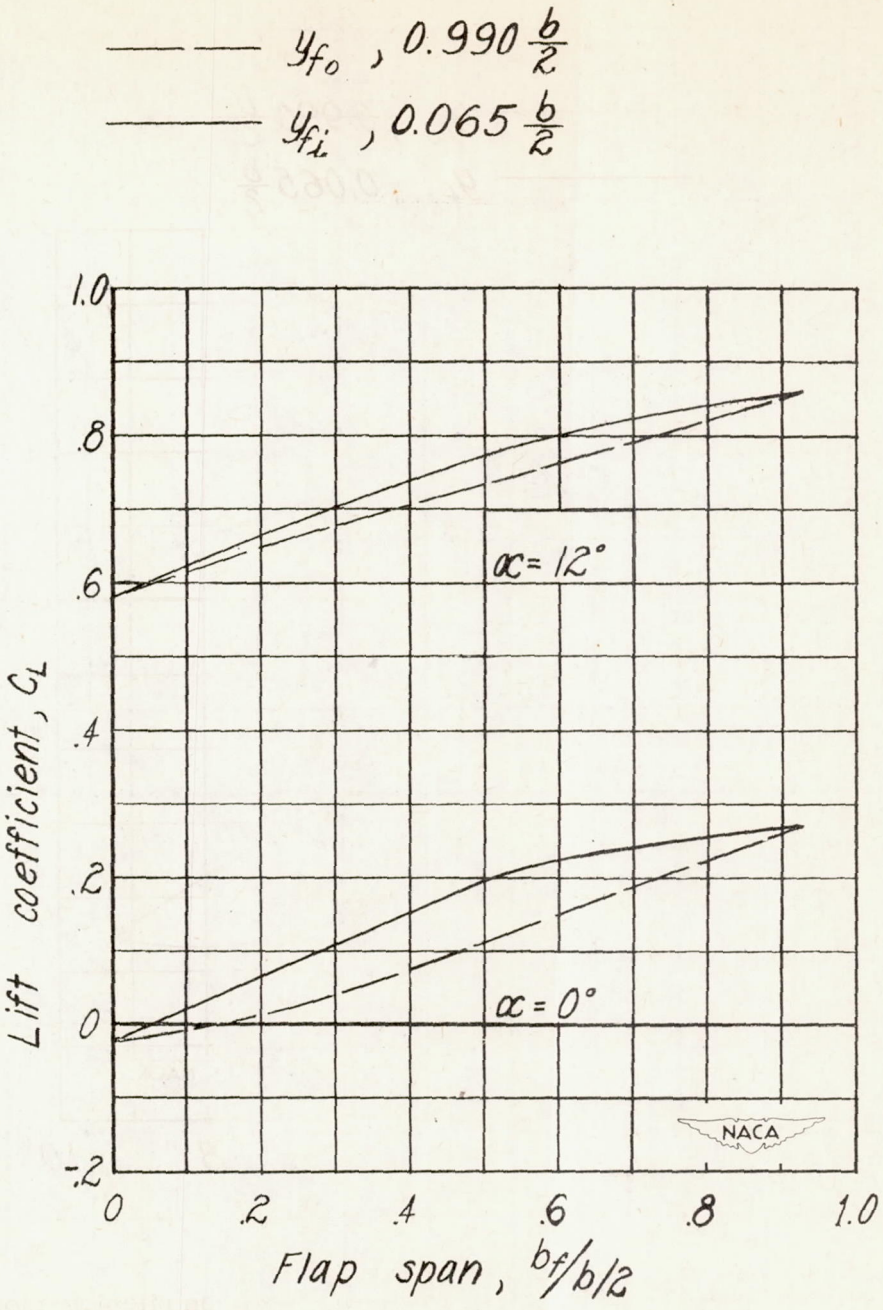


Figure 12.- Effects of flap span and spanwise location on lift coefficient of the 51.3° sweptback wing. Flap sealed; $\delta_f = 30°$; $\phi = 14°$ over entire wing span for $y_{f_i} = 0.065\frac{b}{2}$; $\phi = 14°$ over flapped portion of wing, and $\phi = 6°$ over remainder of wing for $y_{f_i} = 0.990\frac{b}{2}$.

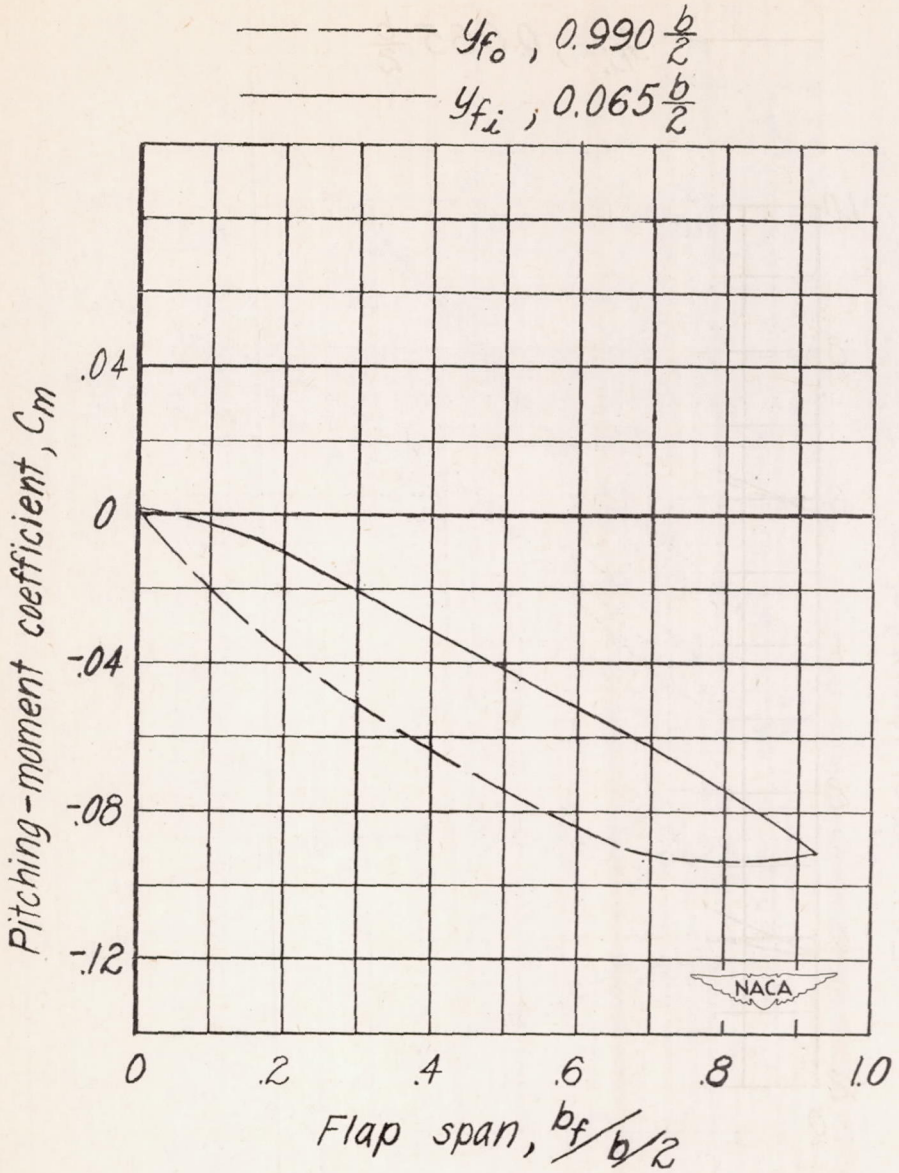


Figure 13.- Effect of flap span and spanwise location on pitching-moment coefficient of the 51.3° sweptback wing at $\alpha = 0°$. Flap sealed, $\delta_f = 30°$; $\emptyset = 14°$ over entire wing span for $y_{f_i} = 0.065\frac{b}{2}$; $\emptyset = 14°$ over flapped portion of wing, and $\emptyset = 6°$ over remainder of wing for $y_{f_o} = 0.990\frac{b}{2}$.

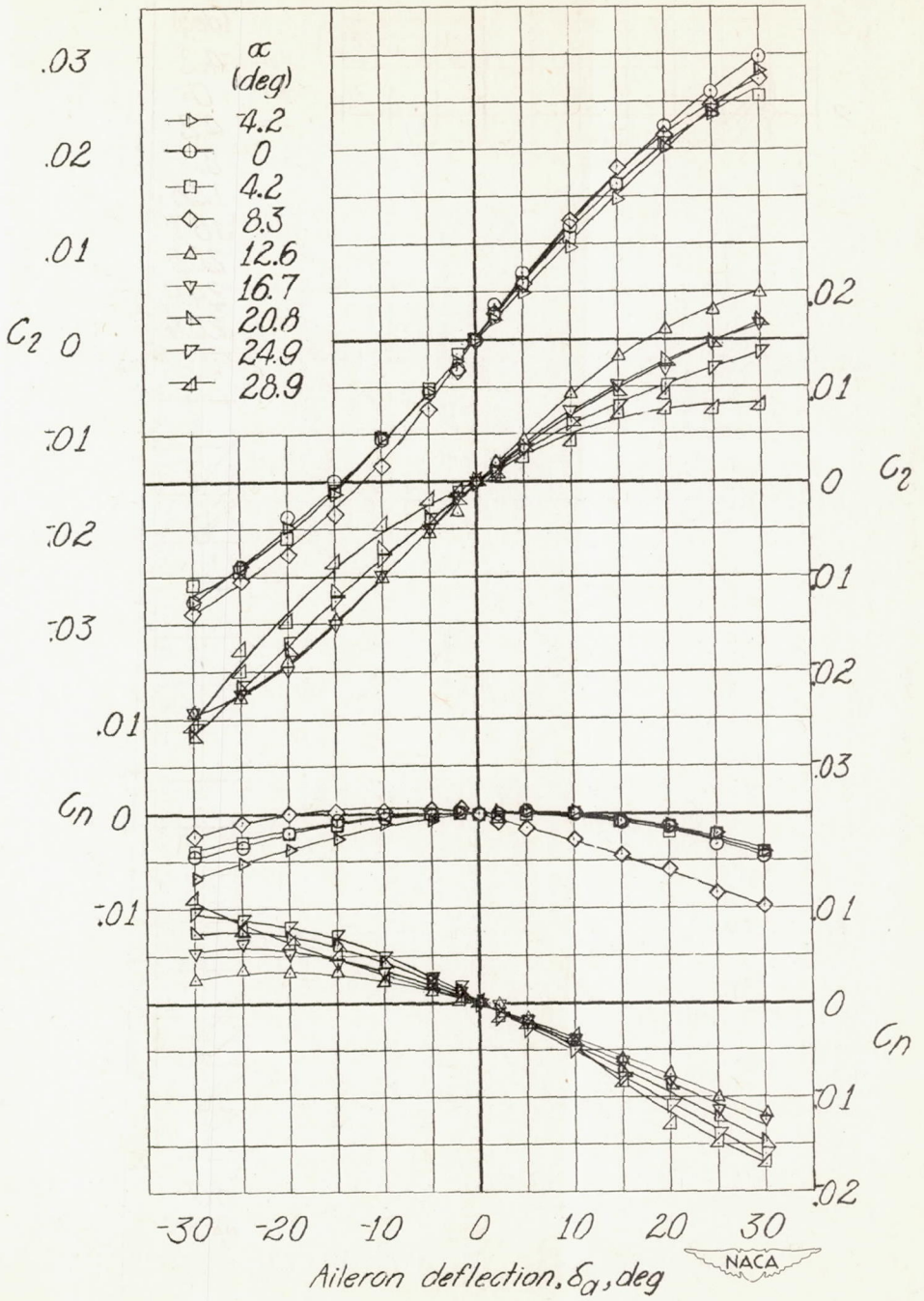


Figure 14.- Variation of lateral control characteristics with aileron deflection on the 51.3° sweptback wing. $b_a = 0.925\frac{b}{2}$; $y_{a_o} = 0.990\frac{b}{2}$; $\phi_a = 14°$.

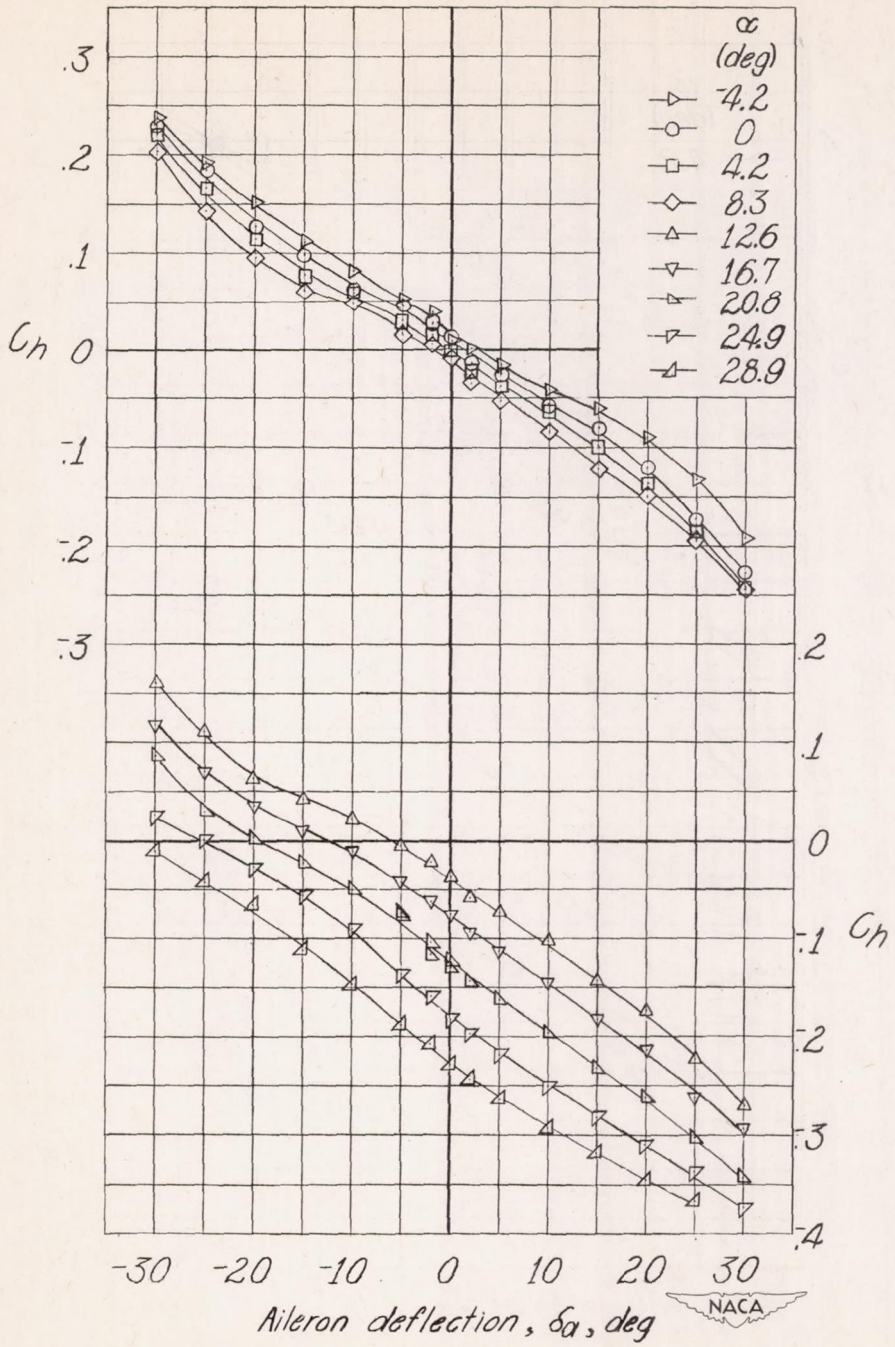


Figure 14.- Continued.

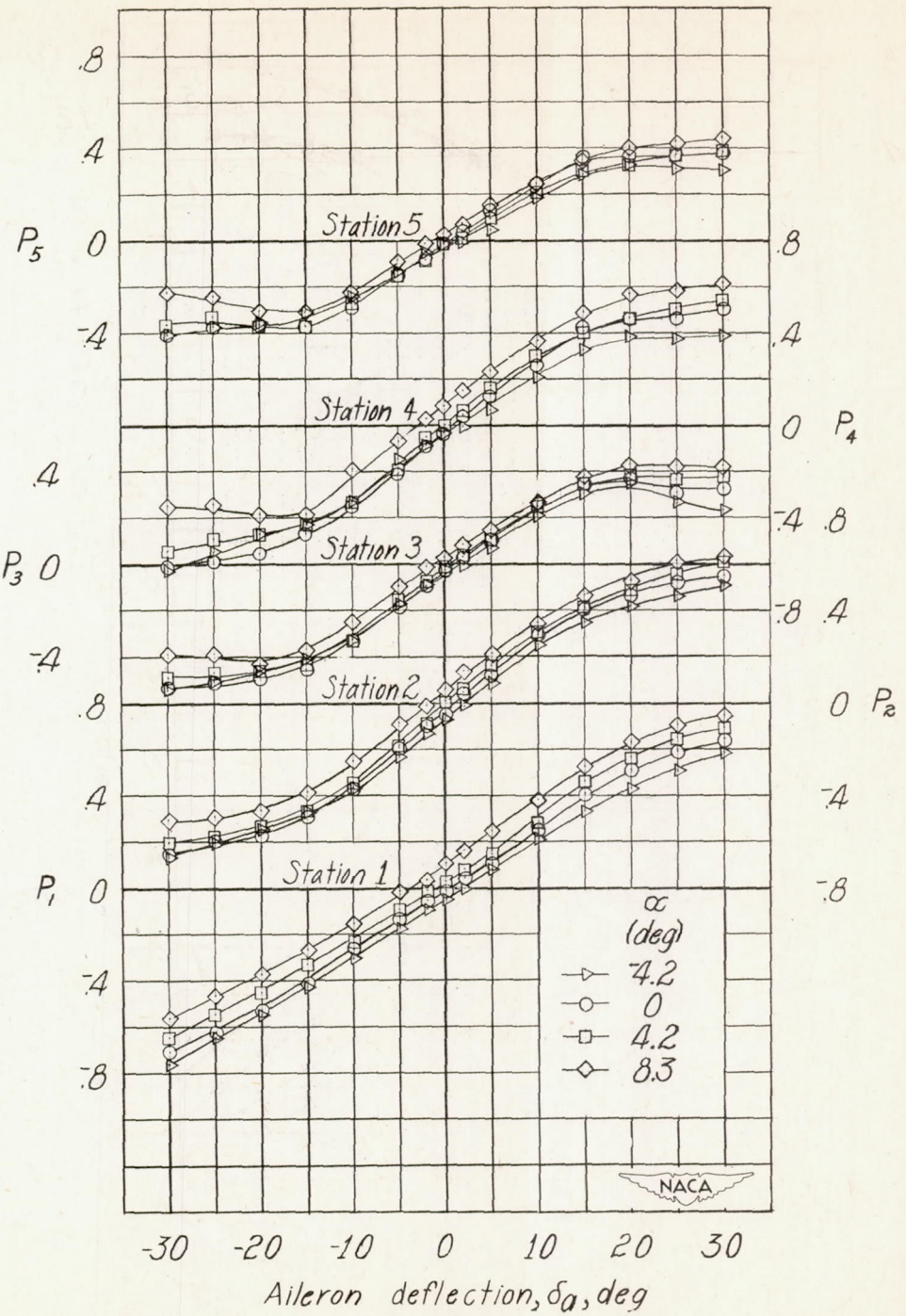


Figure 14.- Continued.

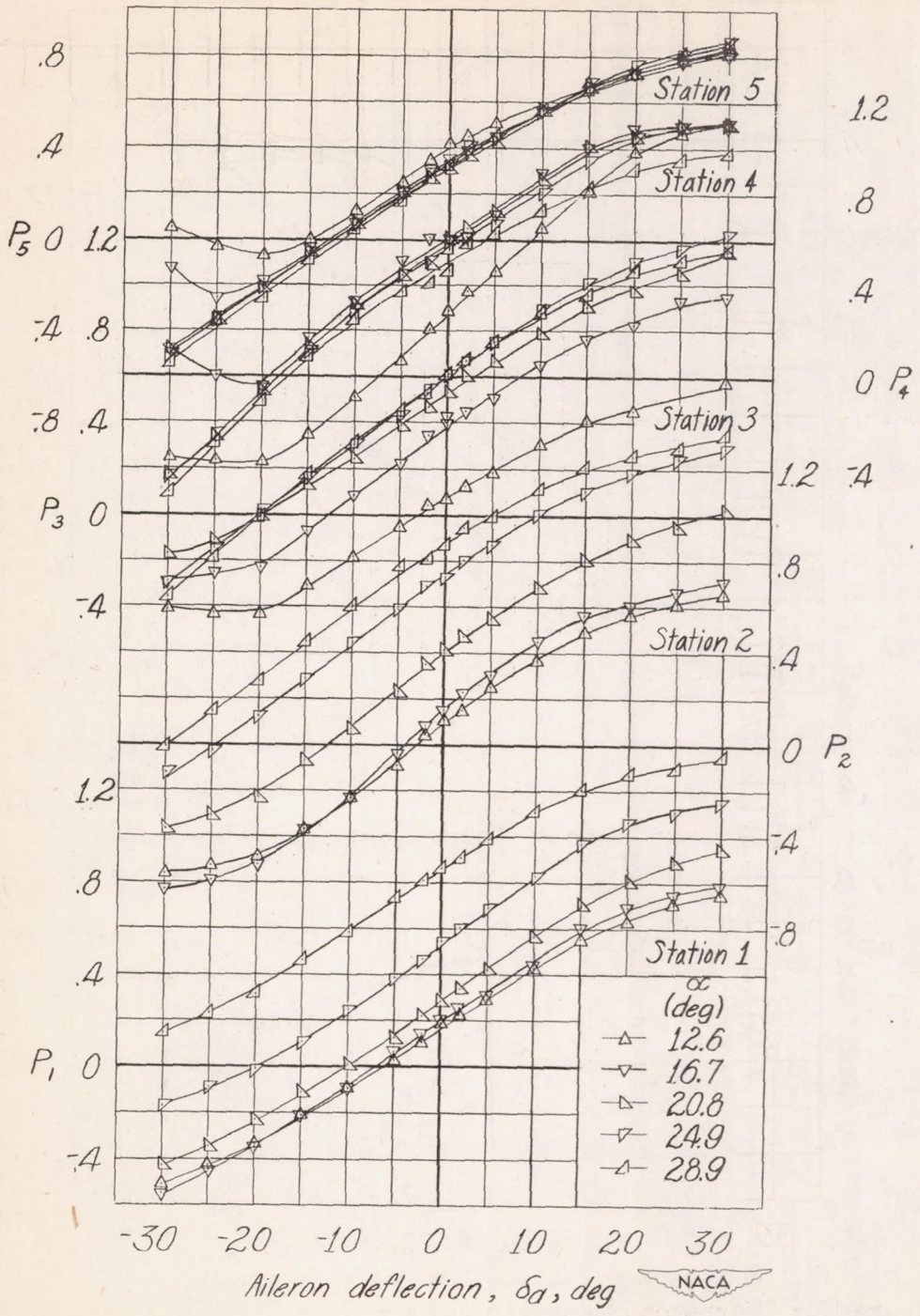


Figure 14.- Concluded.

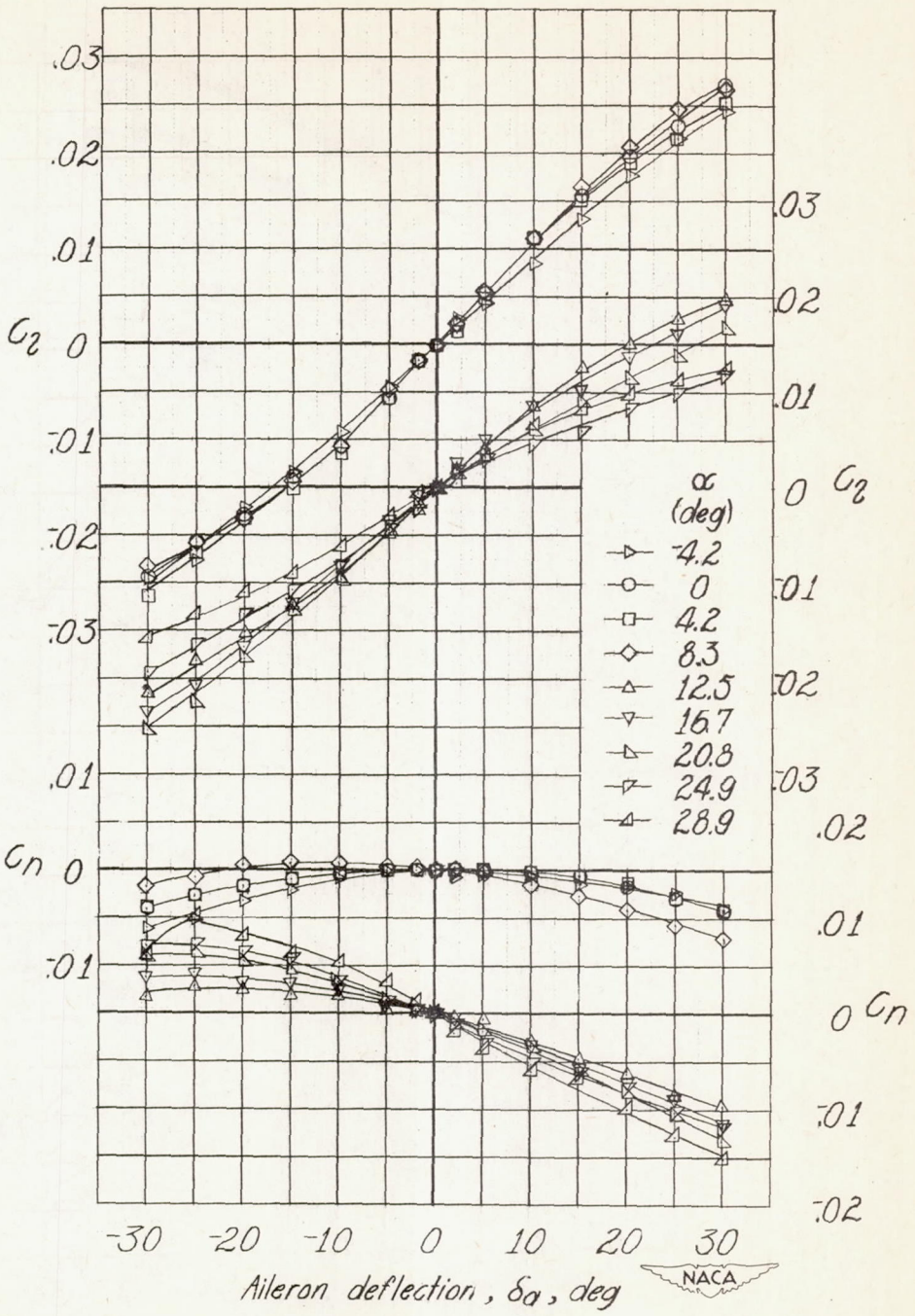


Figure 15.- Variation of lateral control characteristics with aileron deflection on the 51.3° sweptback wing. $b_a = 0.686\frac{b}{2}$; $y_{a_o} = 0.990\frac{b}{2}$; $\phi_a = 14°$, $\phi = 6°$ over remainder of wing span.

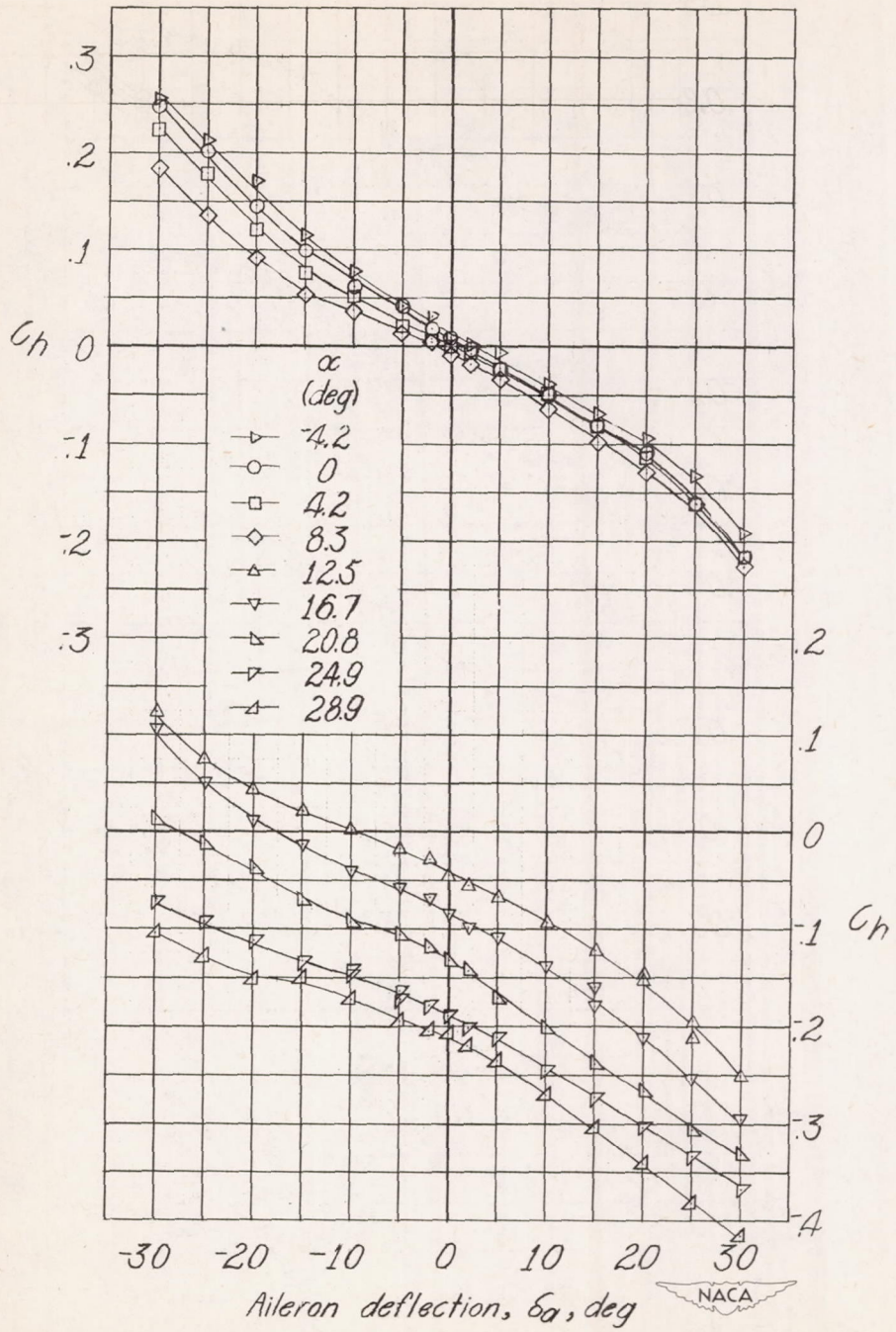


Figure 15.- Continued.

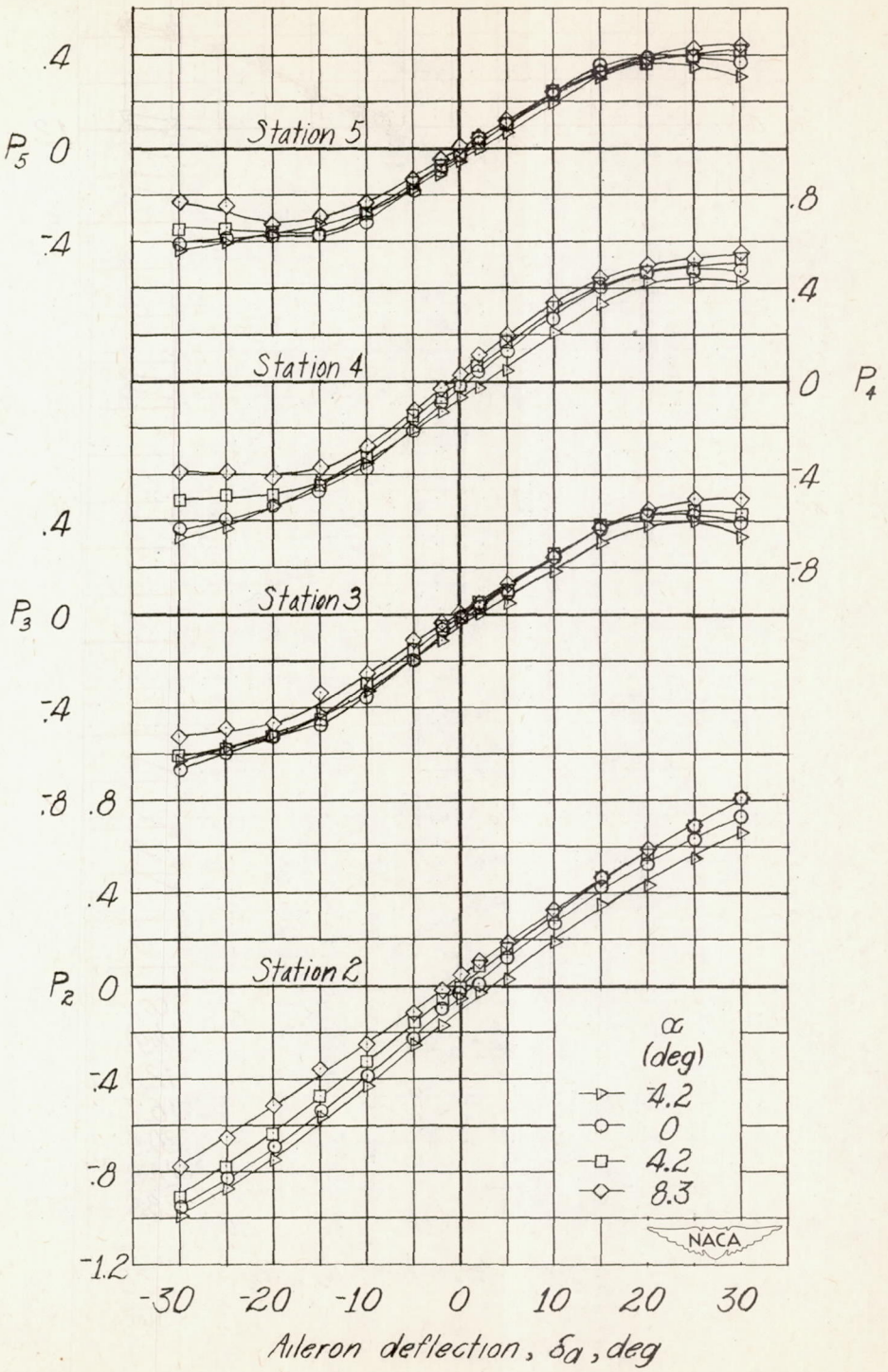


Figure 15.- Continued.

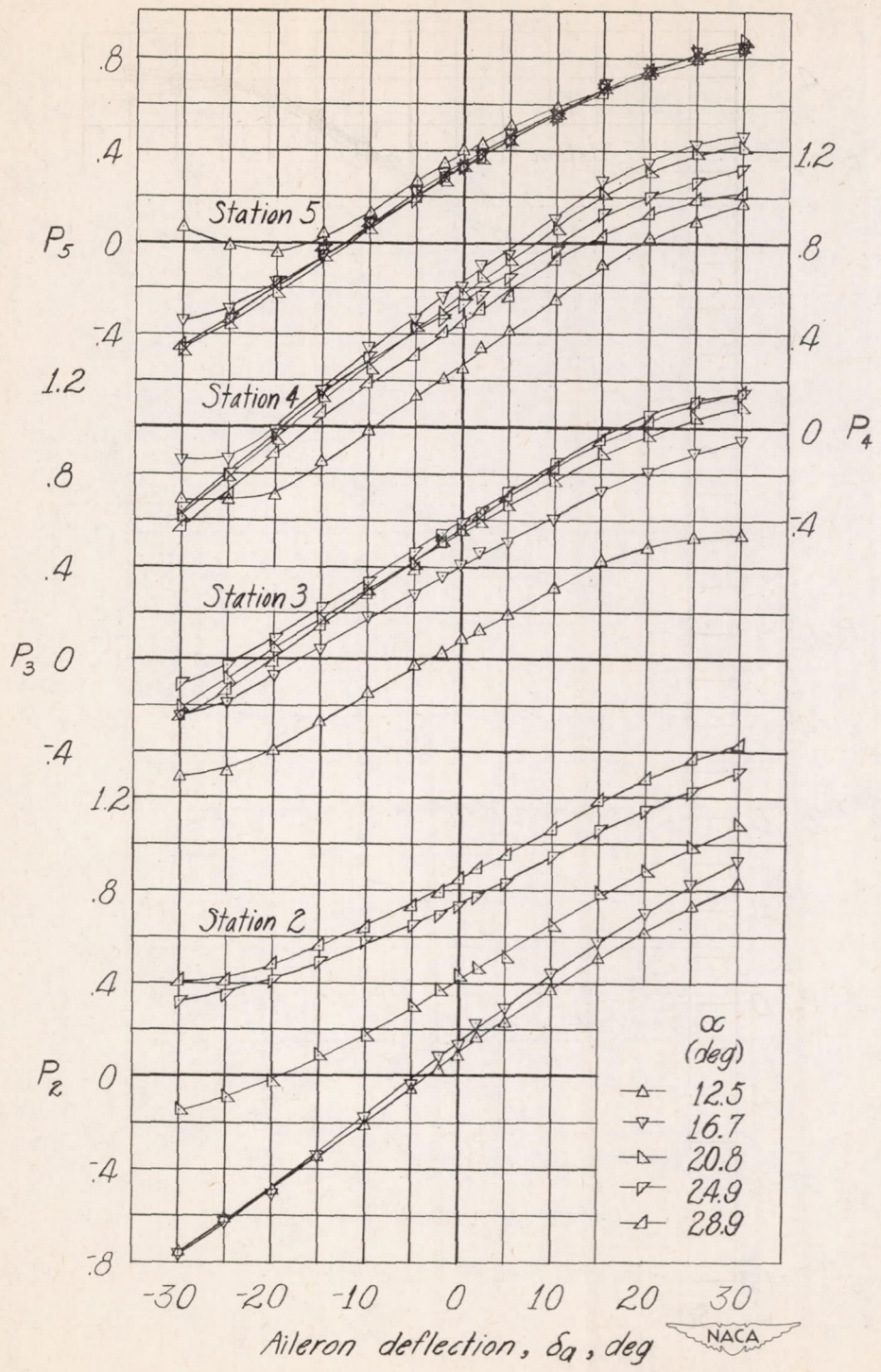


Figure 15.- Concluded.

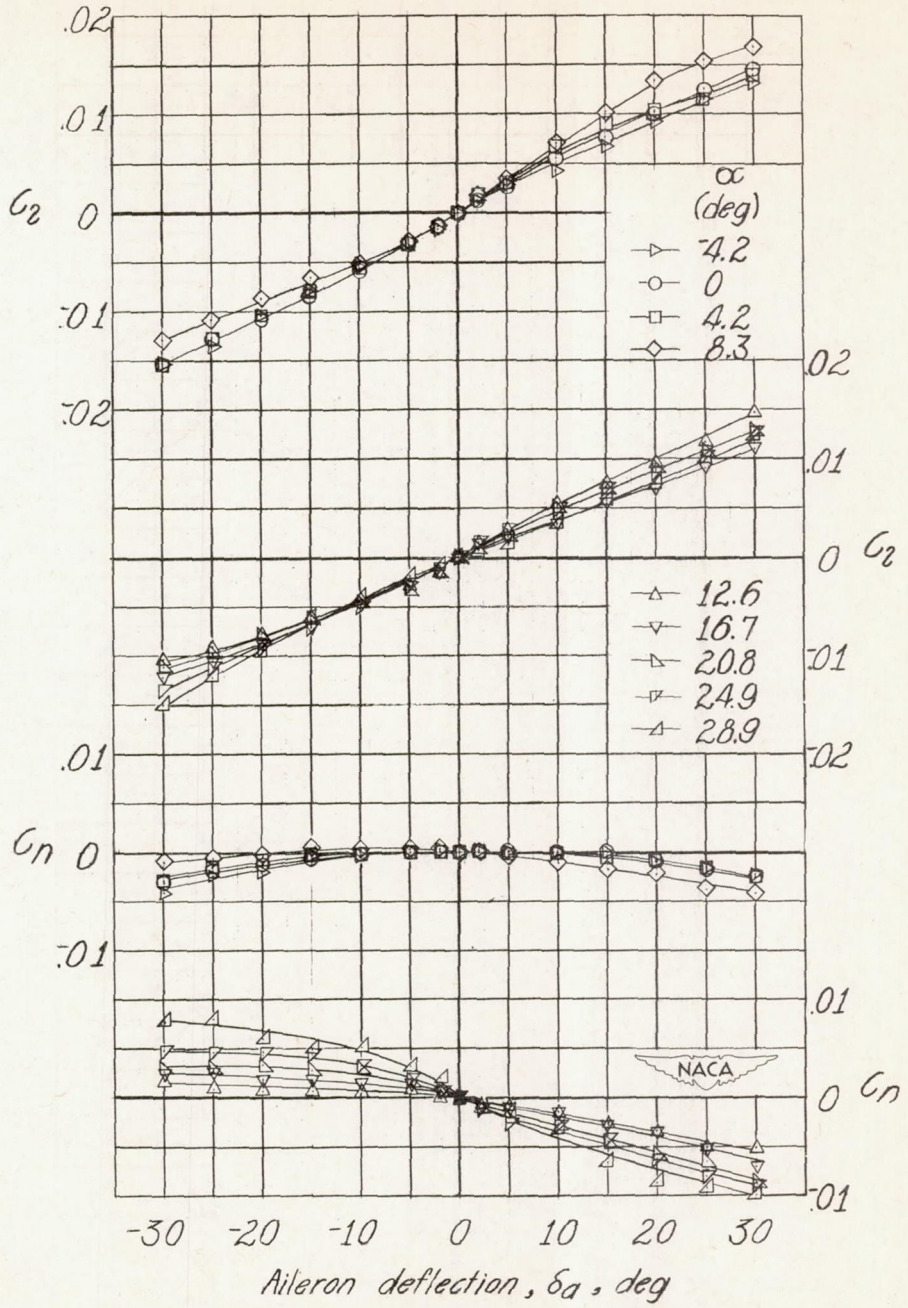


Figure 16.- Variation of lateral control characteristics with aileron deflection on the 51.3° sweptback wing. $b_a = 0.404\frac{b}{2}$; $y_{a_o} = 0.990\frac{b}{2}$; $\phi_a = 14°$, $\phi = 6°$ over remainder of wing span.

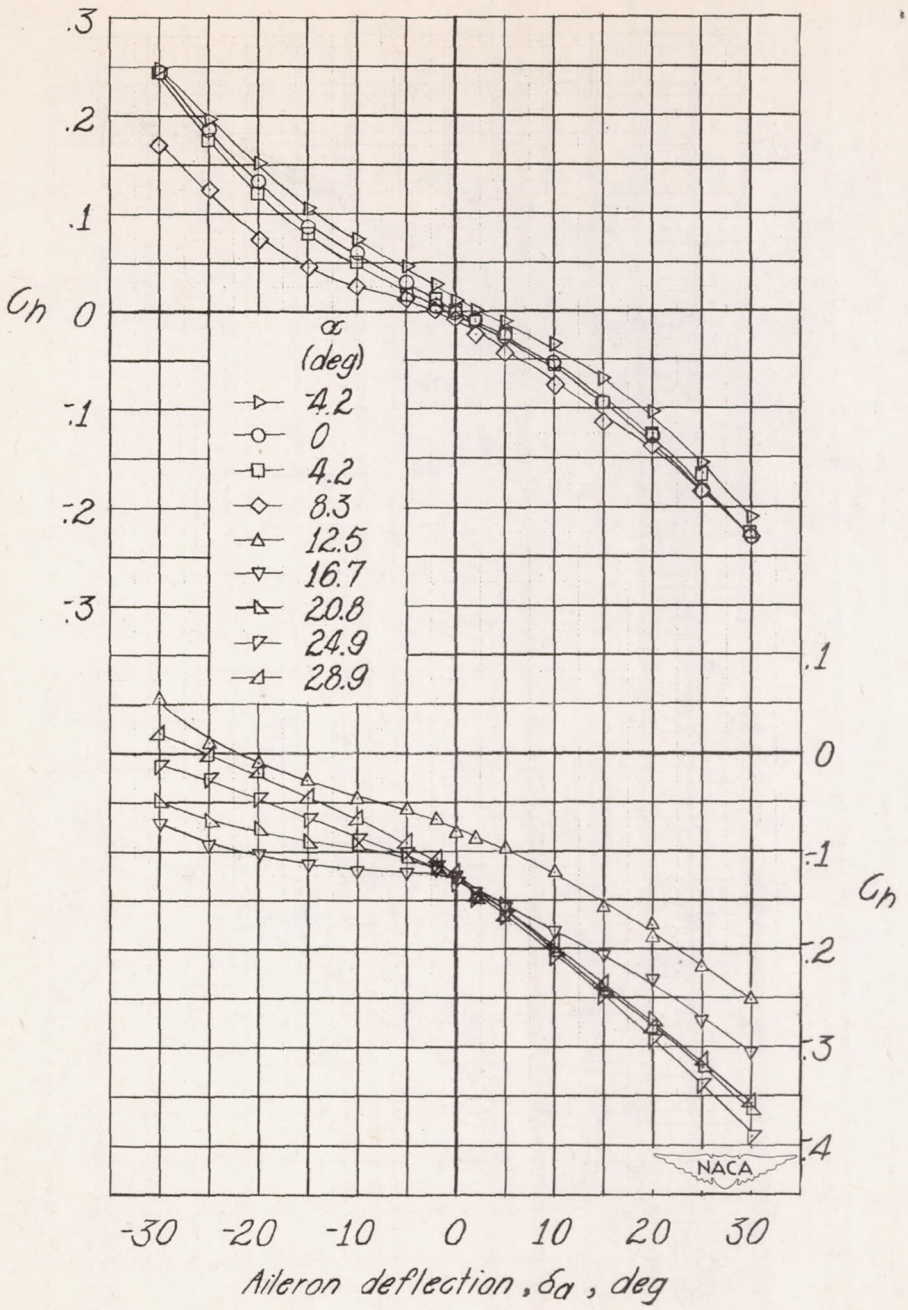


Figure 16.- Continued.

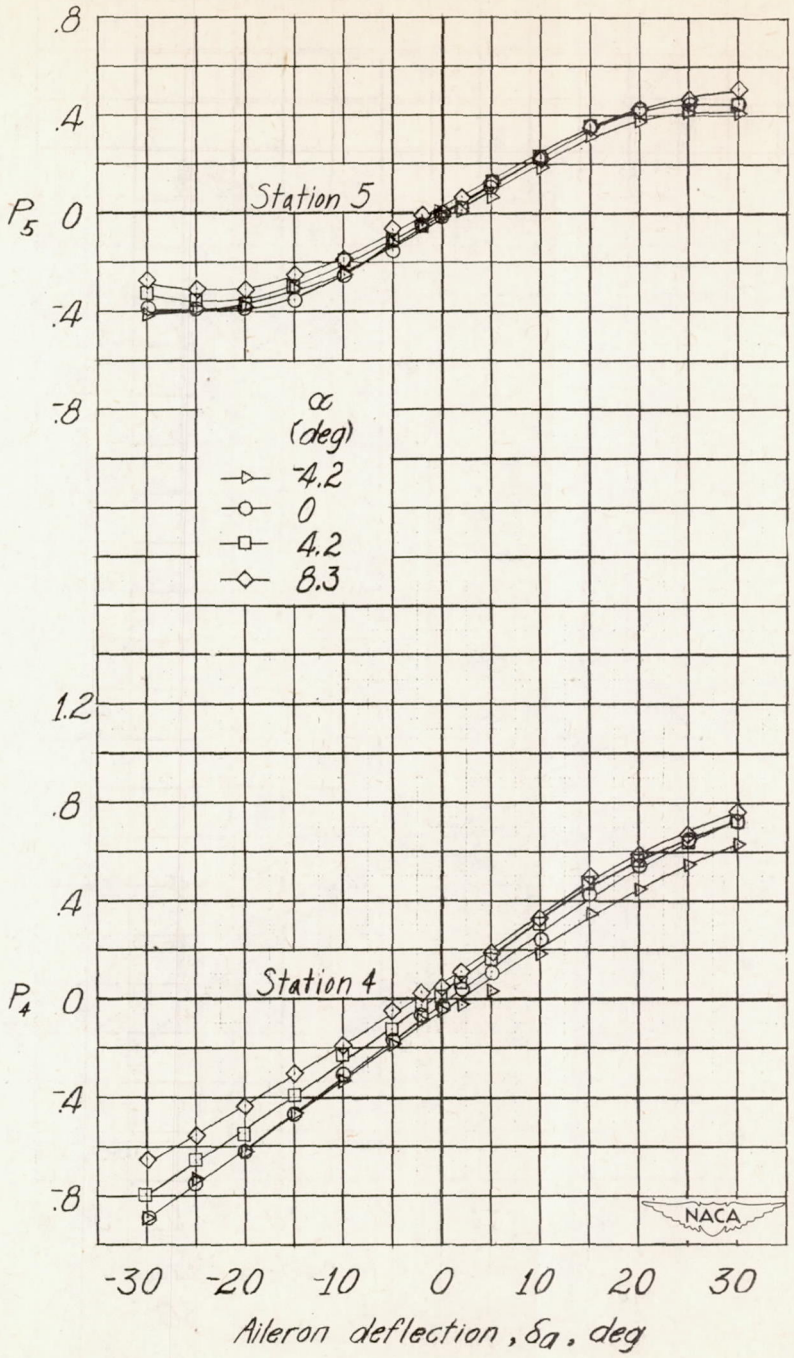


Figure 16.- Continued.

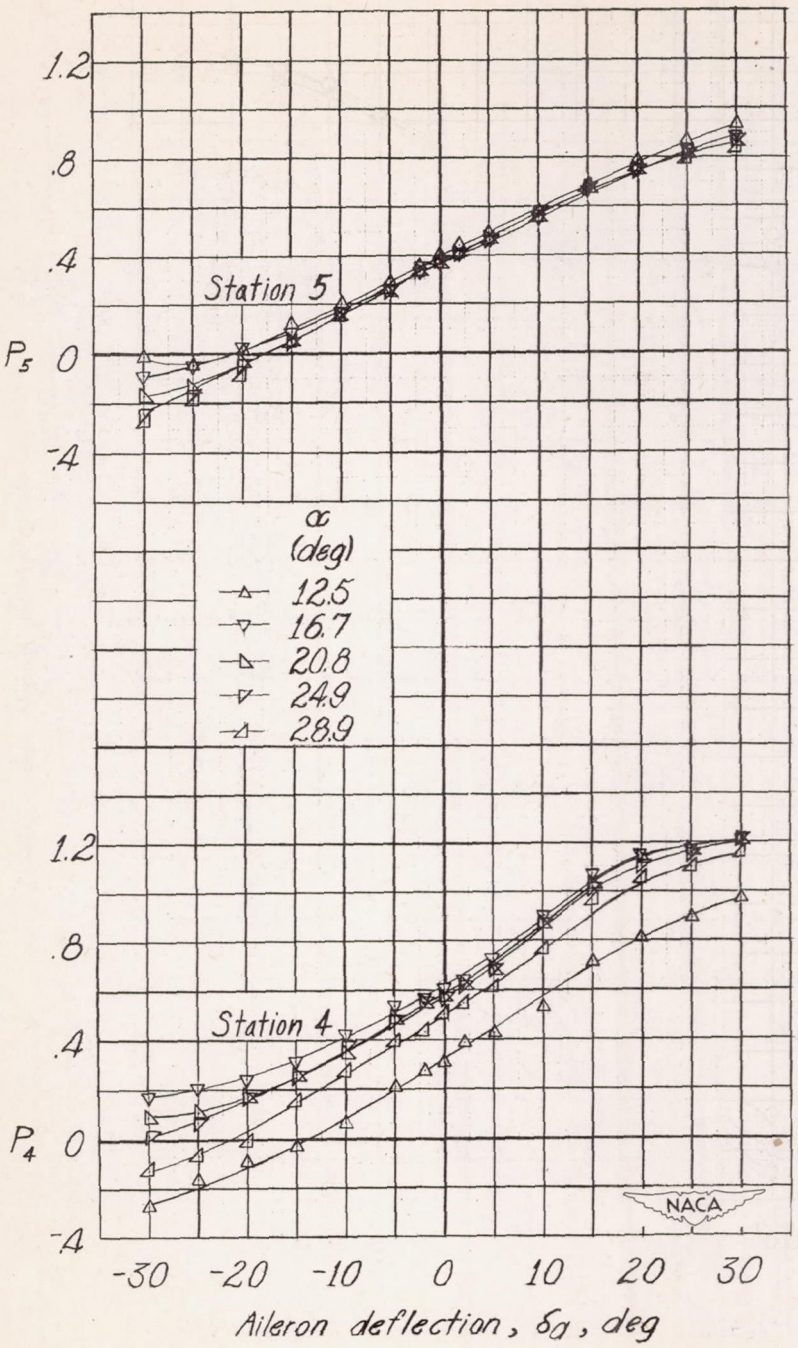


Figure 16.- Concluded.

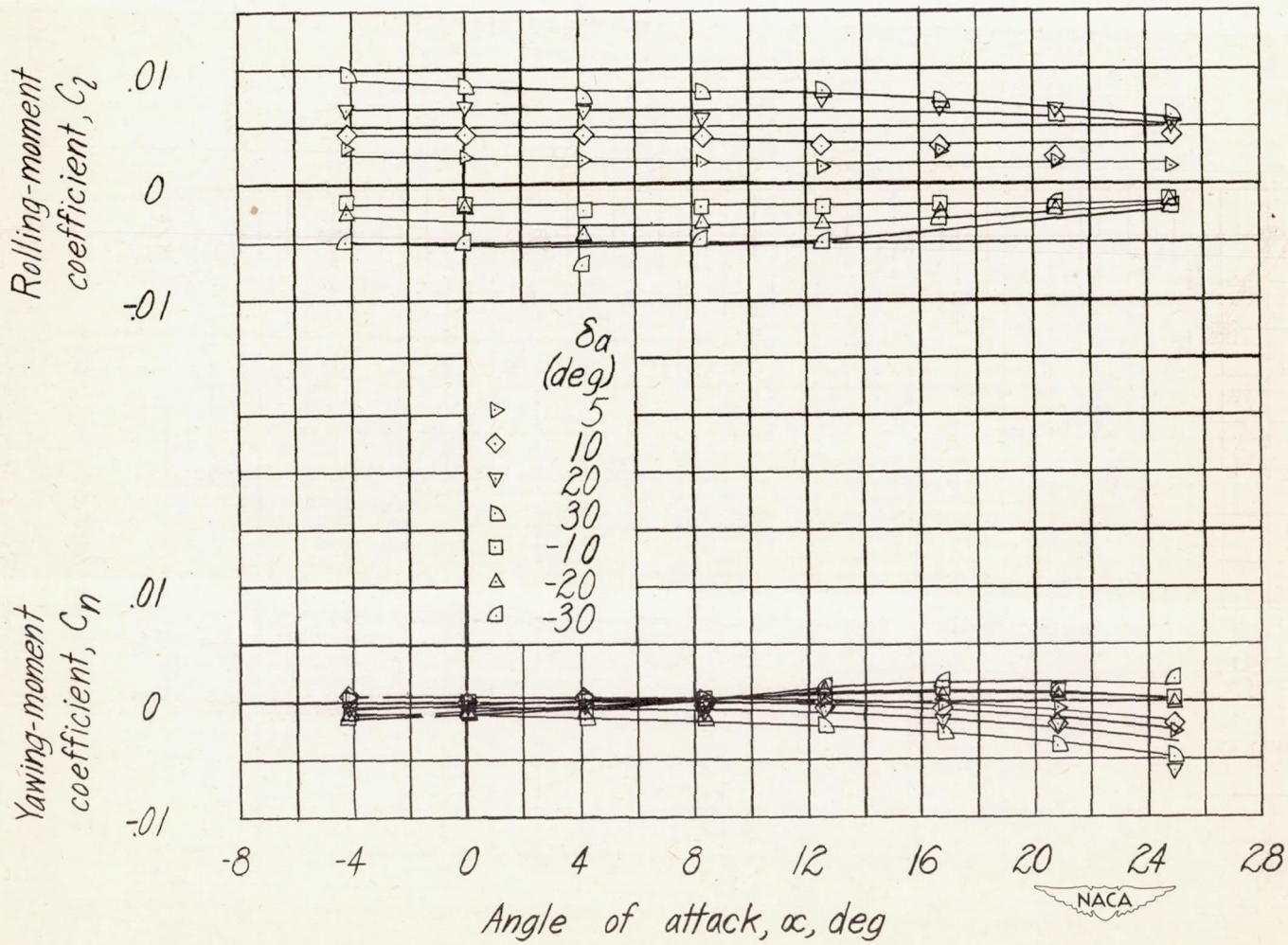


Figure 17.- Variation of lateral control characteristics with wing angle of attack for various aileron deflections on the 51.3° sweptback wing. $b_a = 0.173\frac{b}{2}$; $y_{a_o} = 0.990\frac{b}{2}$; $\phi_a = 14°$, $\phi = 6°$ over remainder of wing span.

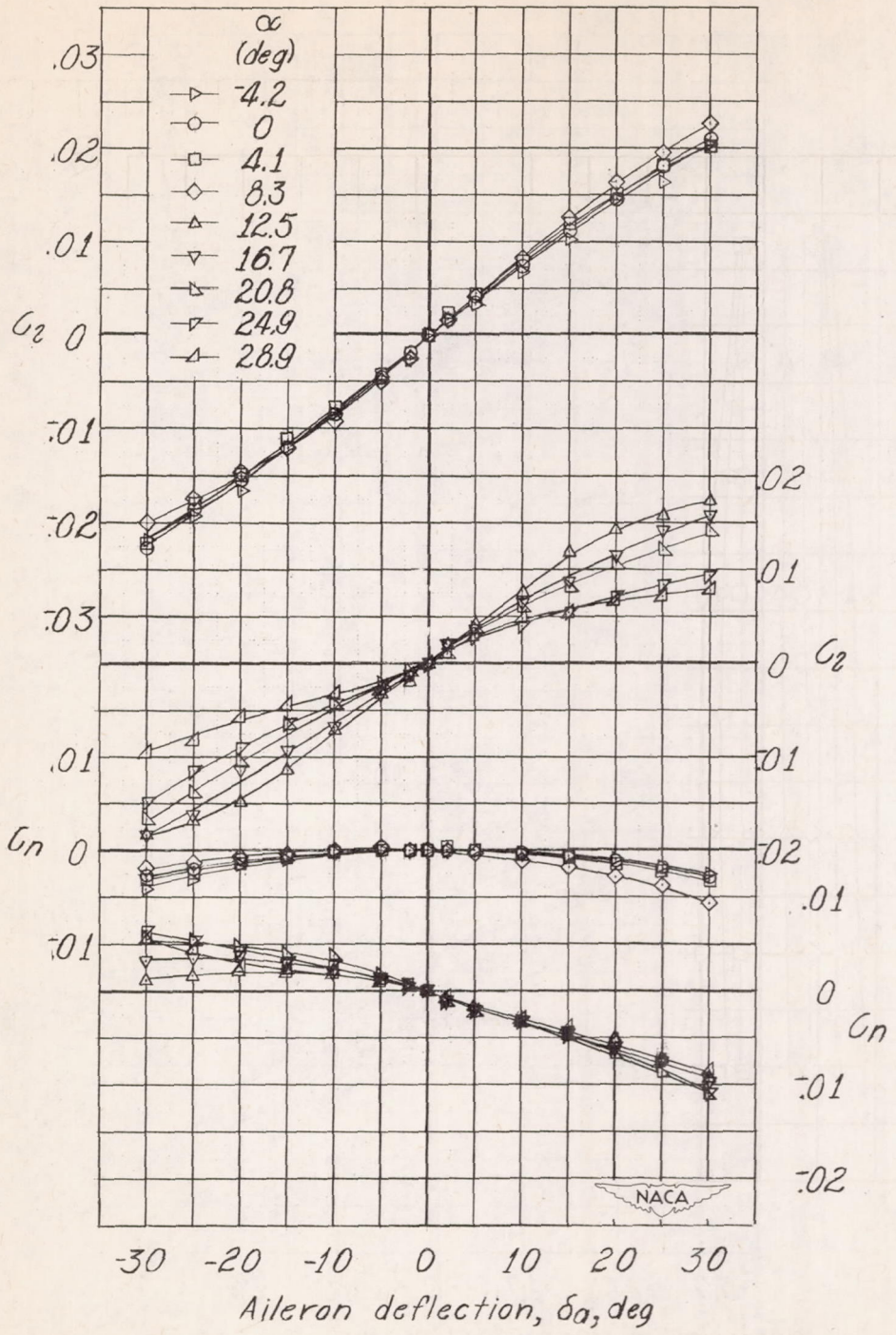


Figure 18.- Variation of lateral control characteristics with aileron deflection on the 51.3° sweptback wing. $b_a = 0.513\frac{b}{2}$; $y_{a_o} = 0.817\frac{b}{2}$; $\phi_a = 14°$; $\phi = 14°$ over remainder of wing span.

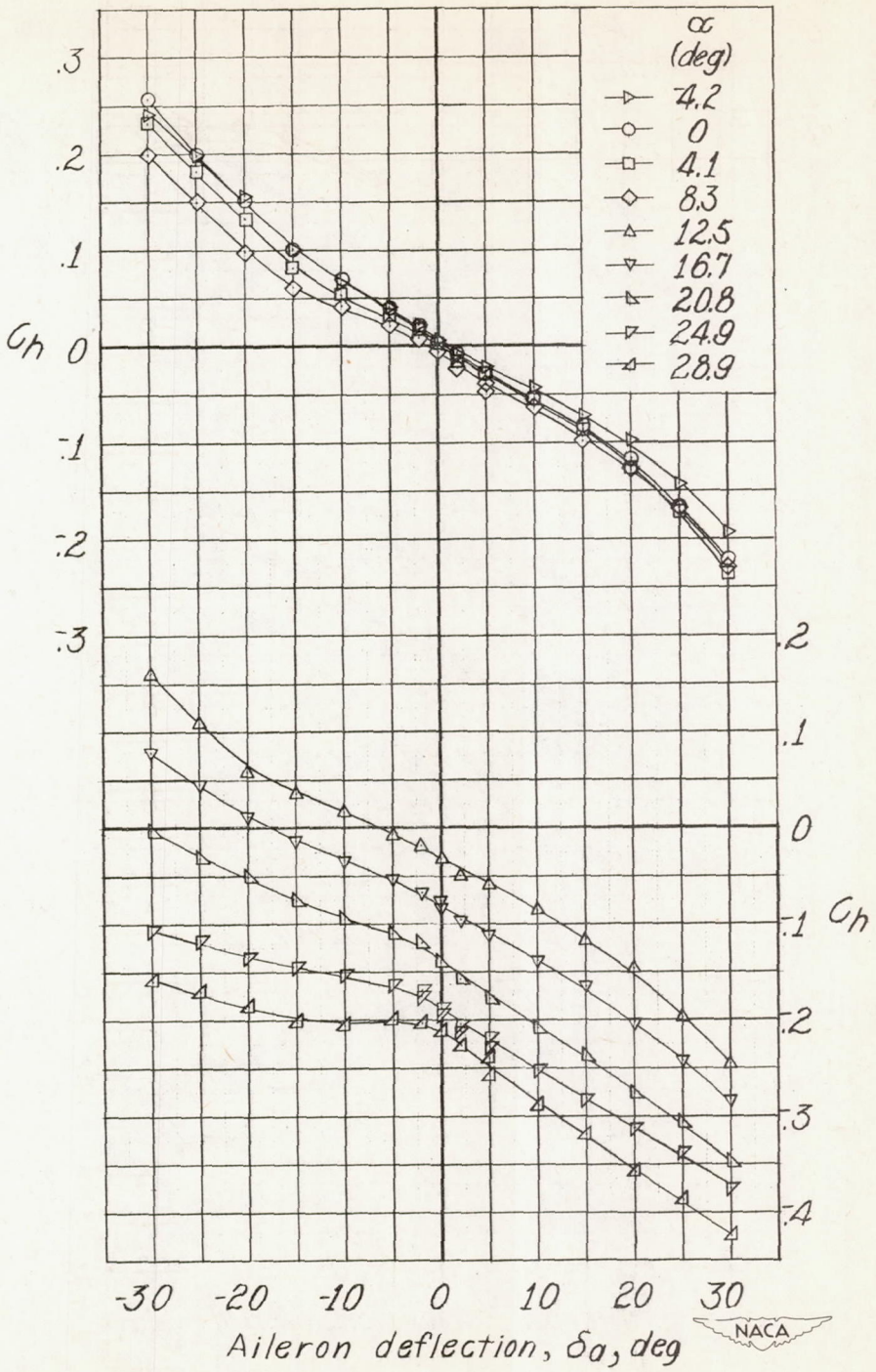


Figure 18.- Continued.

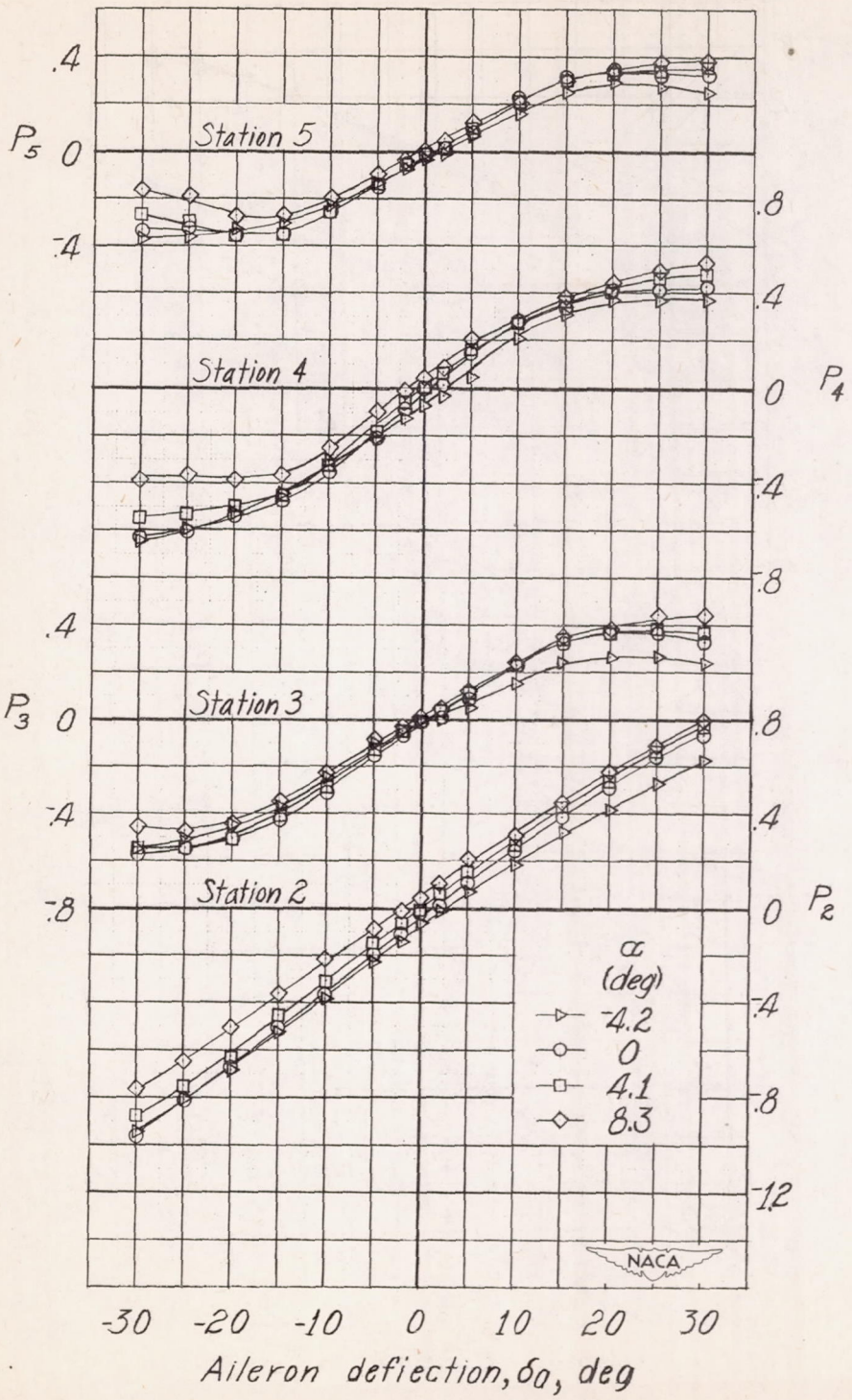


Figure 18.- Continued.

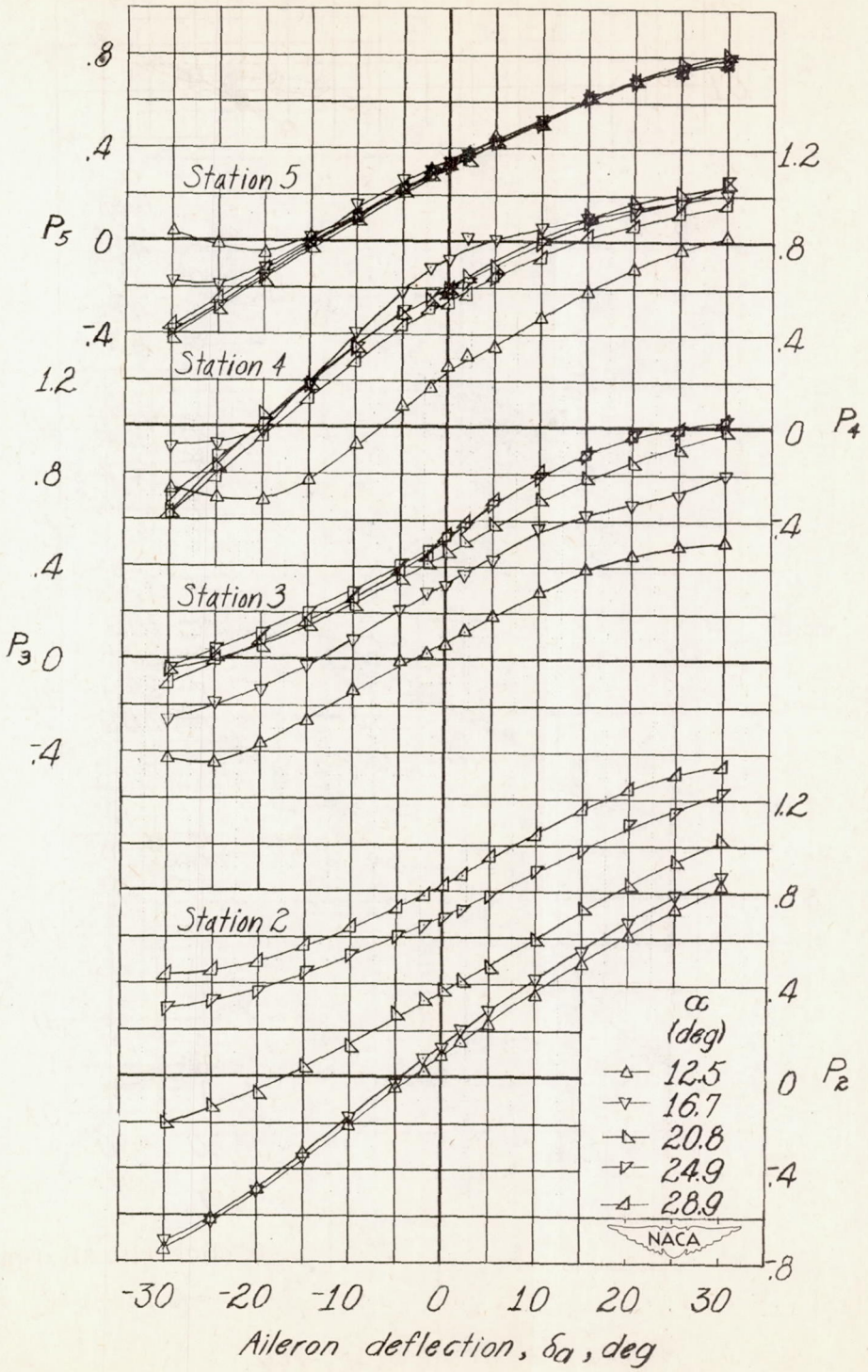


Figure 18.- Concluded.

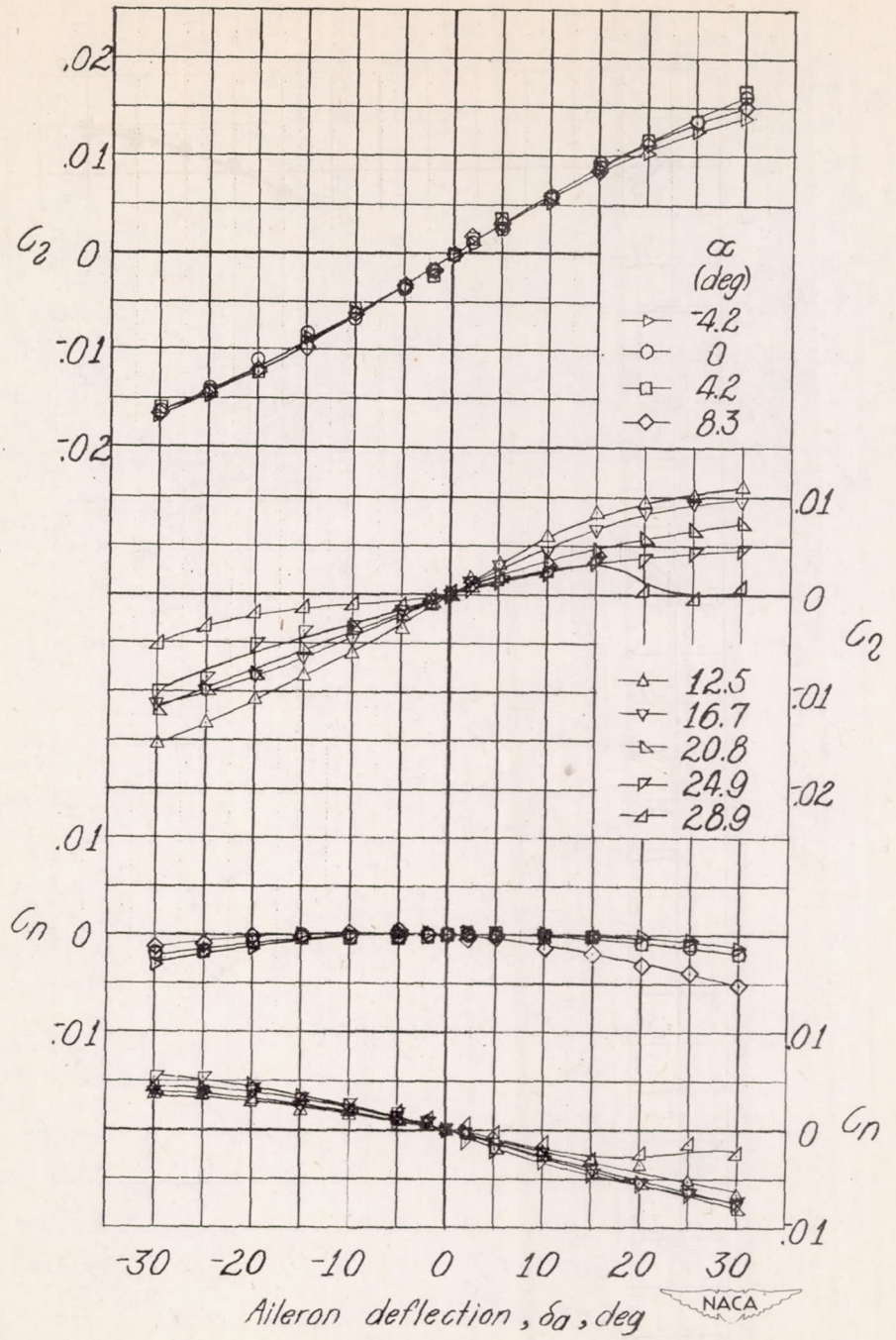


Figure 19.- Variation of lateral control characteristics with aileron deflection on the 51.3° sweptback wing. $b_a = 0.521\frac{b}{2}$; $y_{a_o} = 0.586\frac{b}{2}$; $\phi_a = 14°$, $\phi = 14°$ over remainder of wing span.

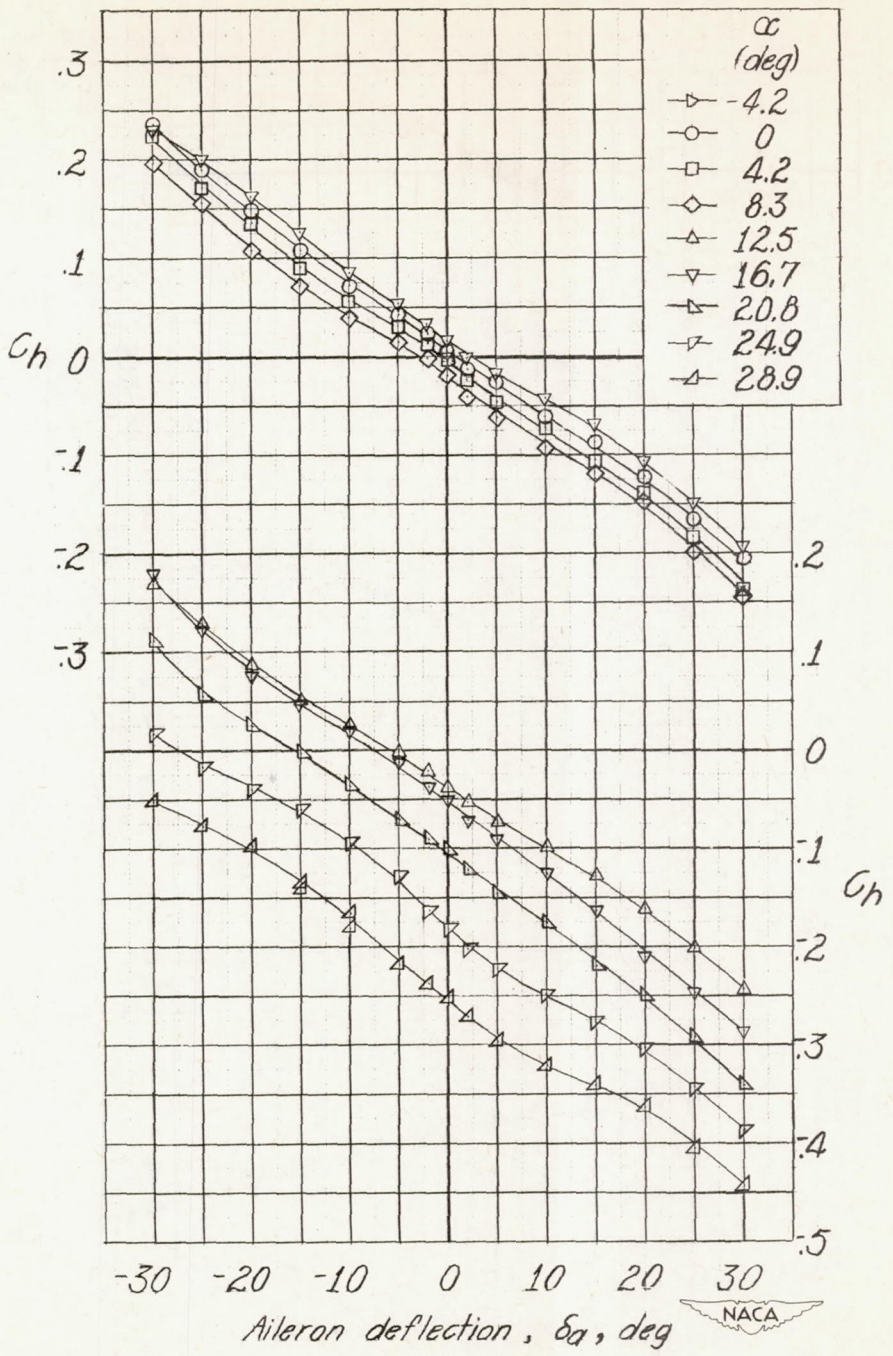


Figure 19.- Continued.

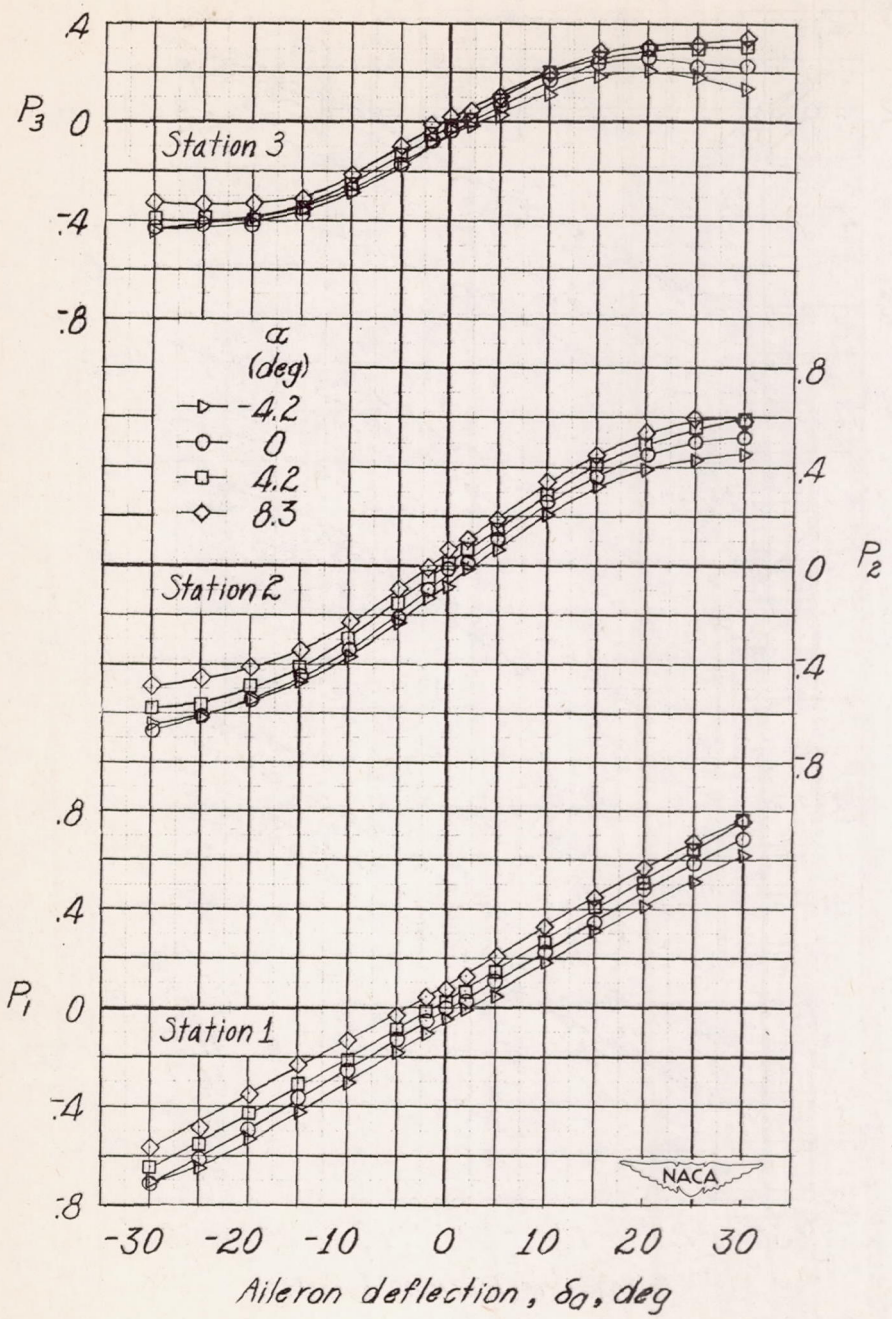


Figure 19.- Continued.

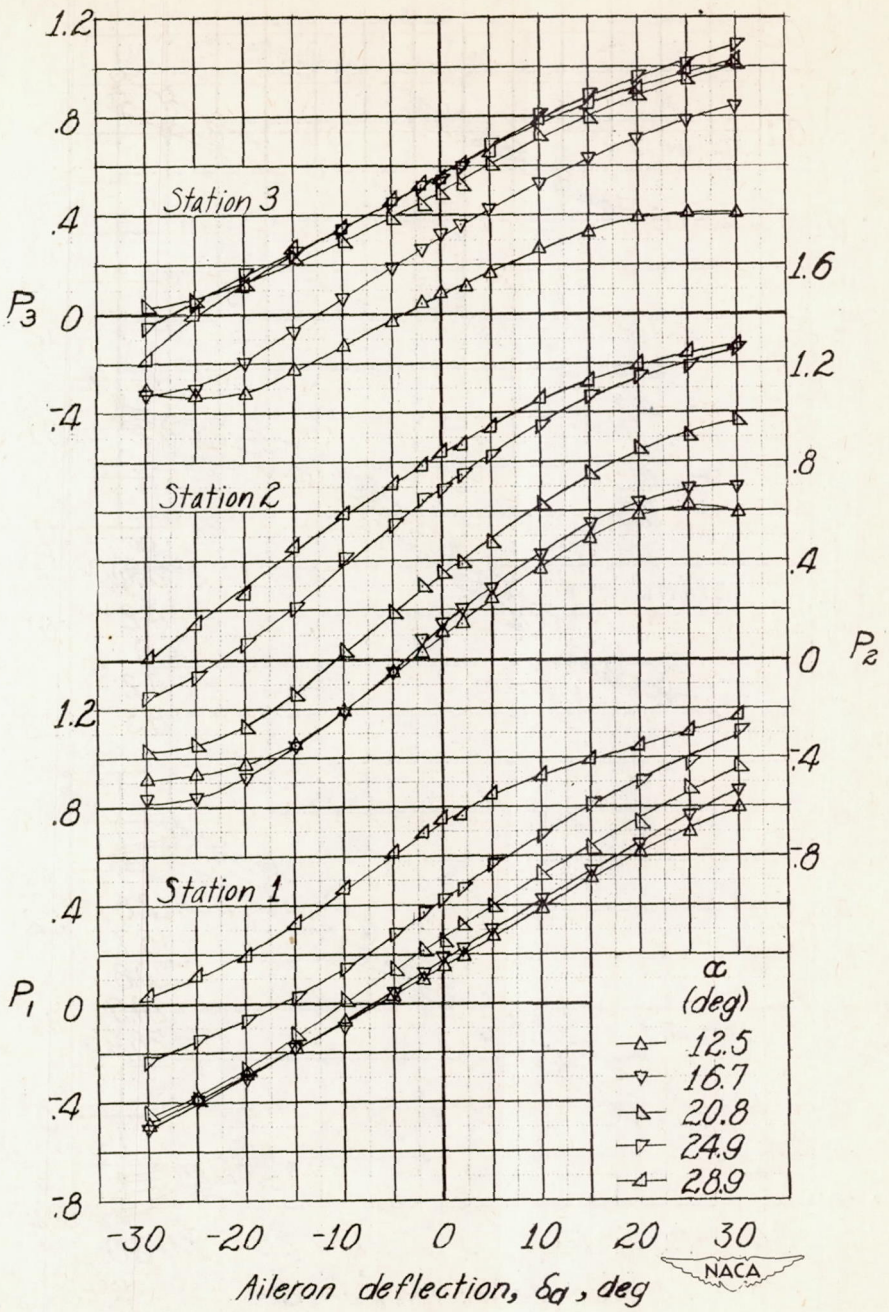


Figure 19.- Concluded.

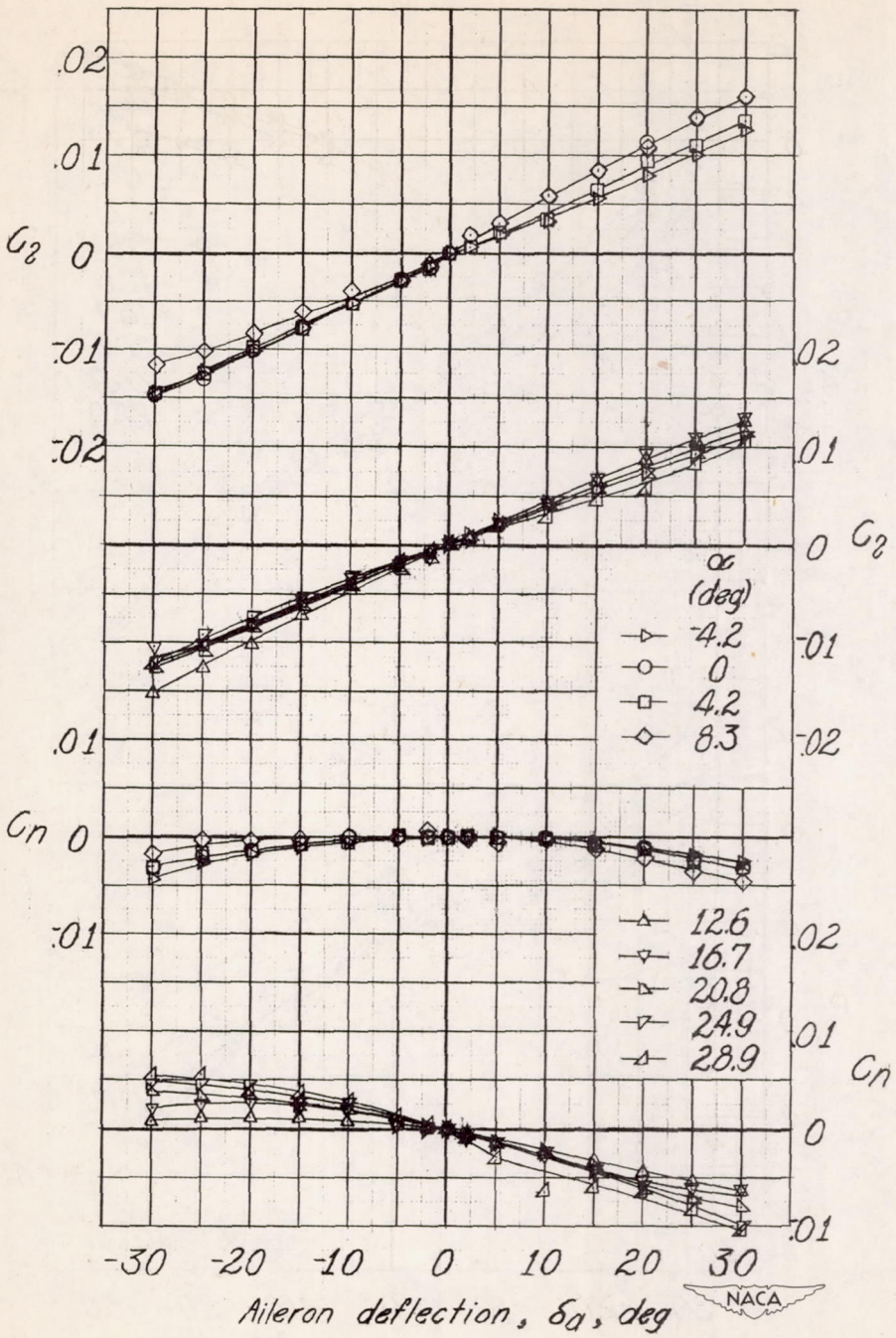


Figure 20.- Variation of lateral control characteristics with aileron deflection on the 51.3° sweptback wing. $b_a = 0.404\frac{b}{2}$; $y_{a_o} = 0.990\frac{b}{2}$; $\phi_a = 6°$, $\phi = 6°$ over remainder of wing span.

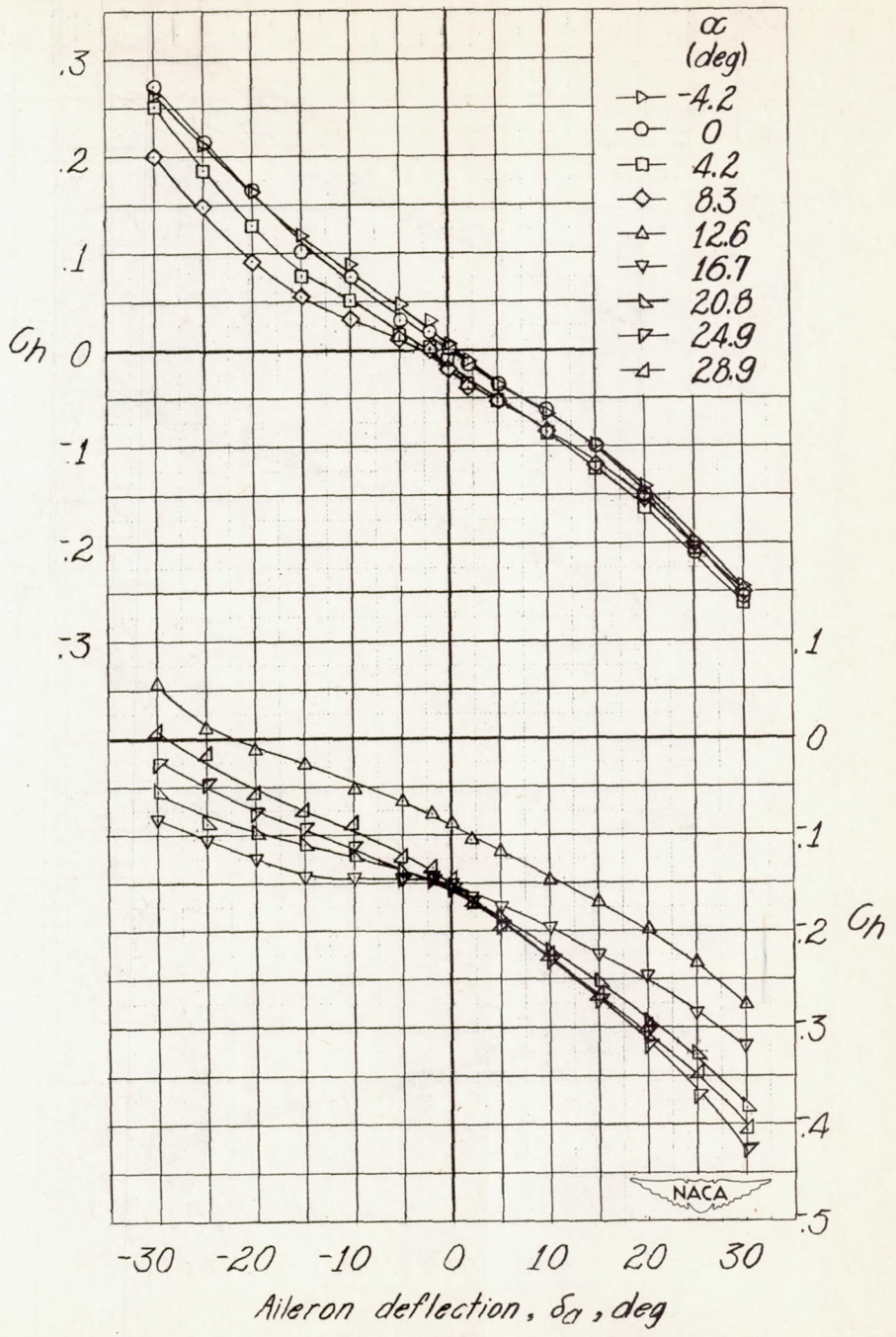


Figure 20.- Continued.

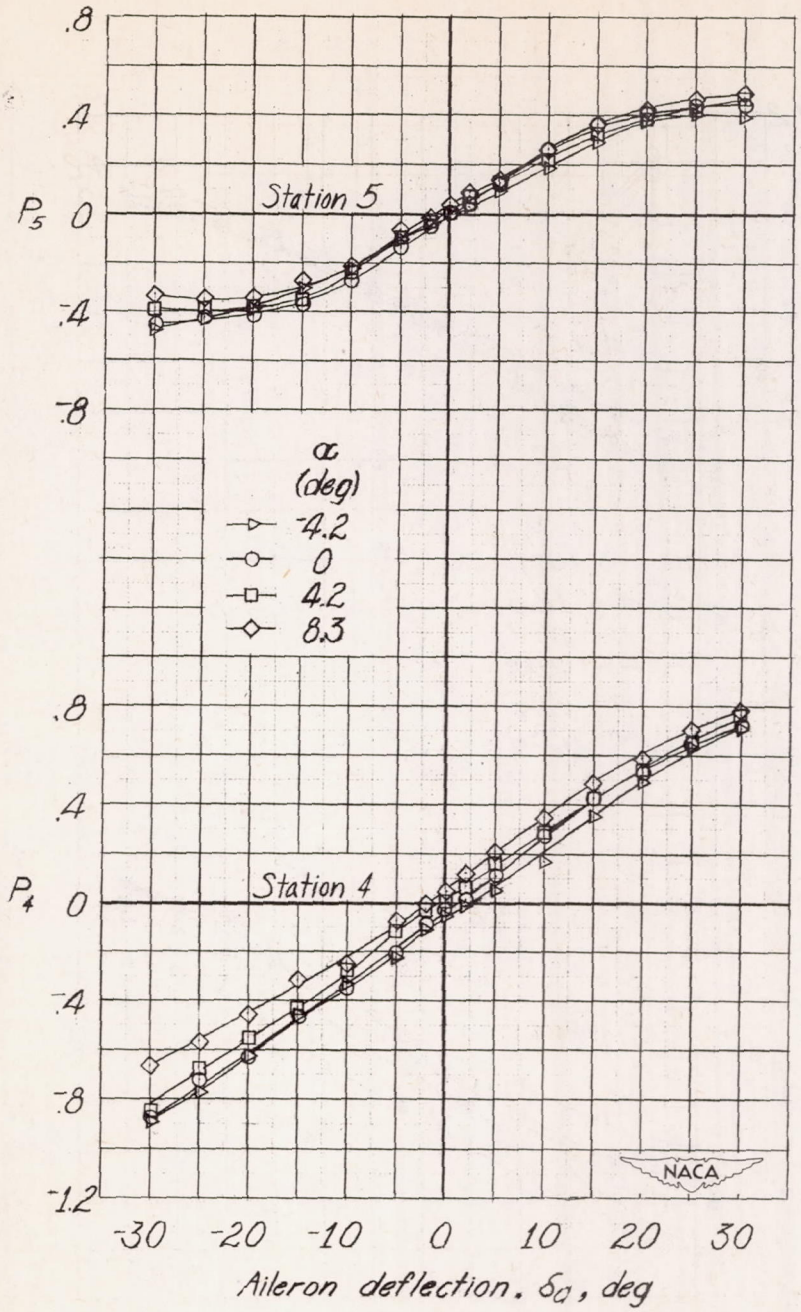


Figure 20.- Continued.

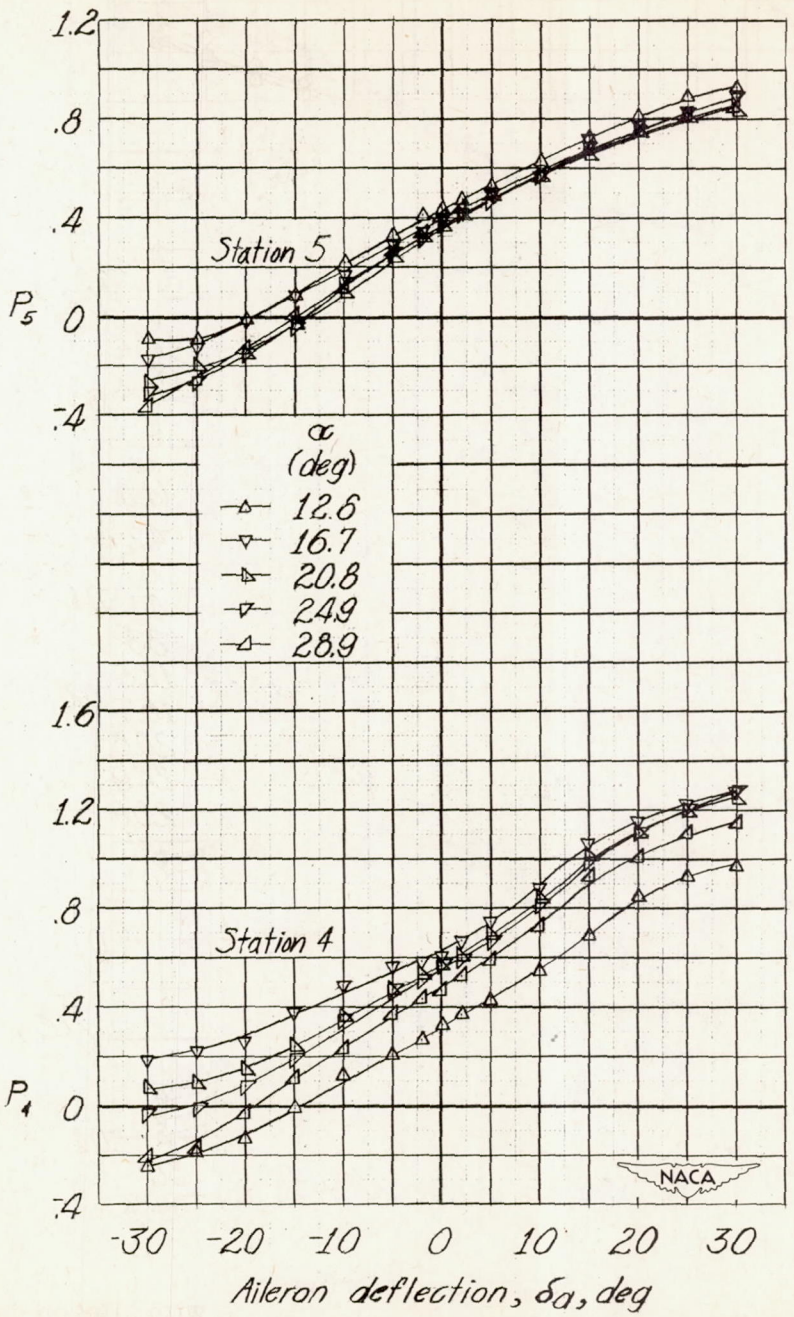


Figure 20.- Concluded.

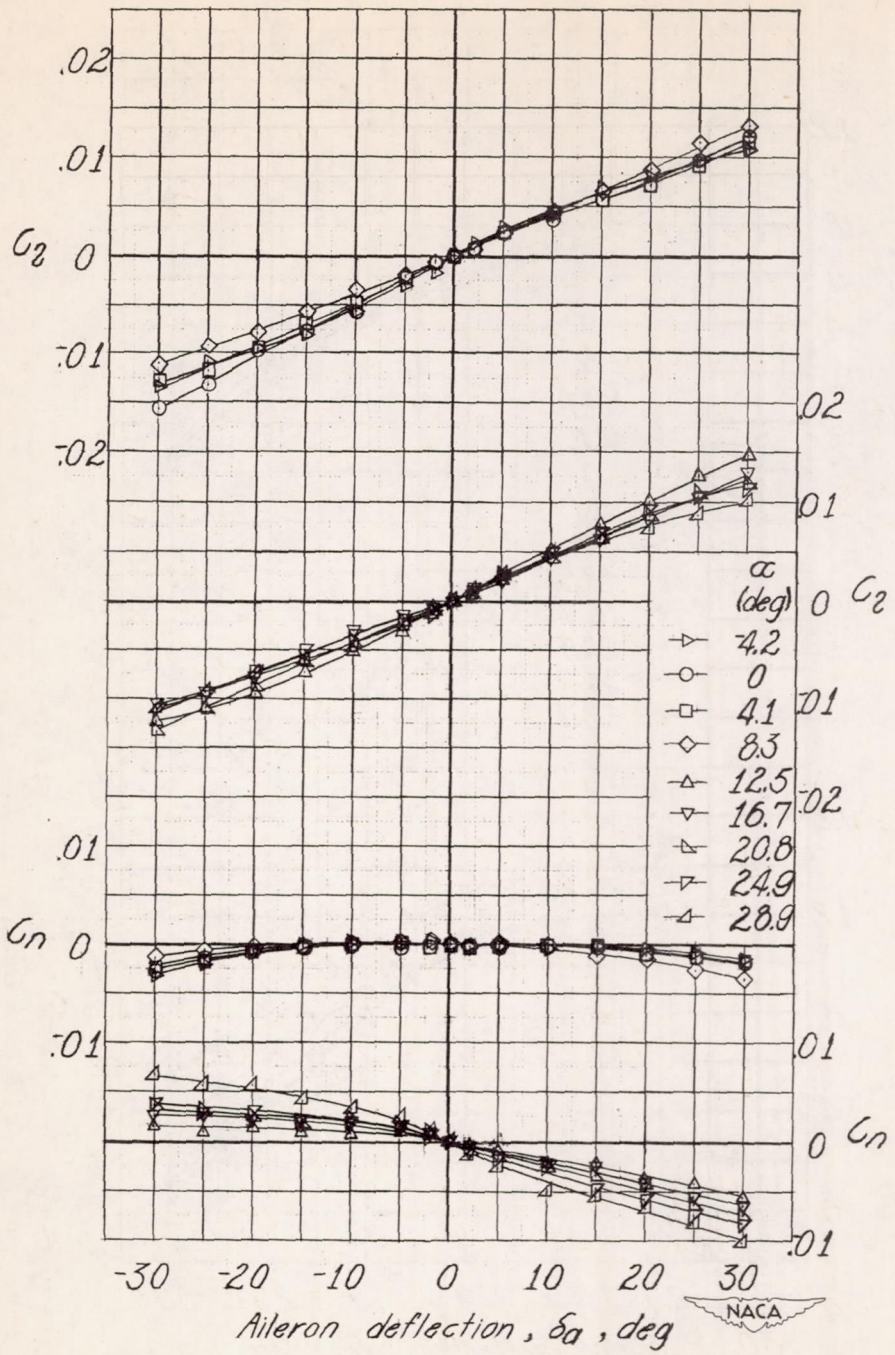


Figure 21.- Variation of lateral control characteristics with aileron deflection on the 51.3° sweptback wing. $b_a = 0.404\frac{b}{2}$; $y_{a_o} = 0.990\frac{b}{2}$; $\phi_a = 25°$, $\phi = 6°$ over remainder of wing span.

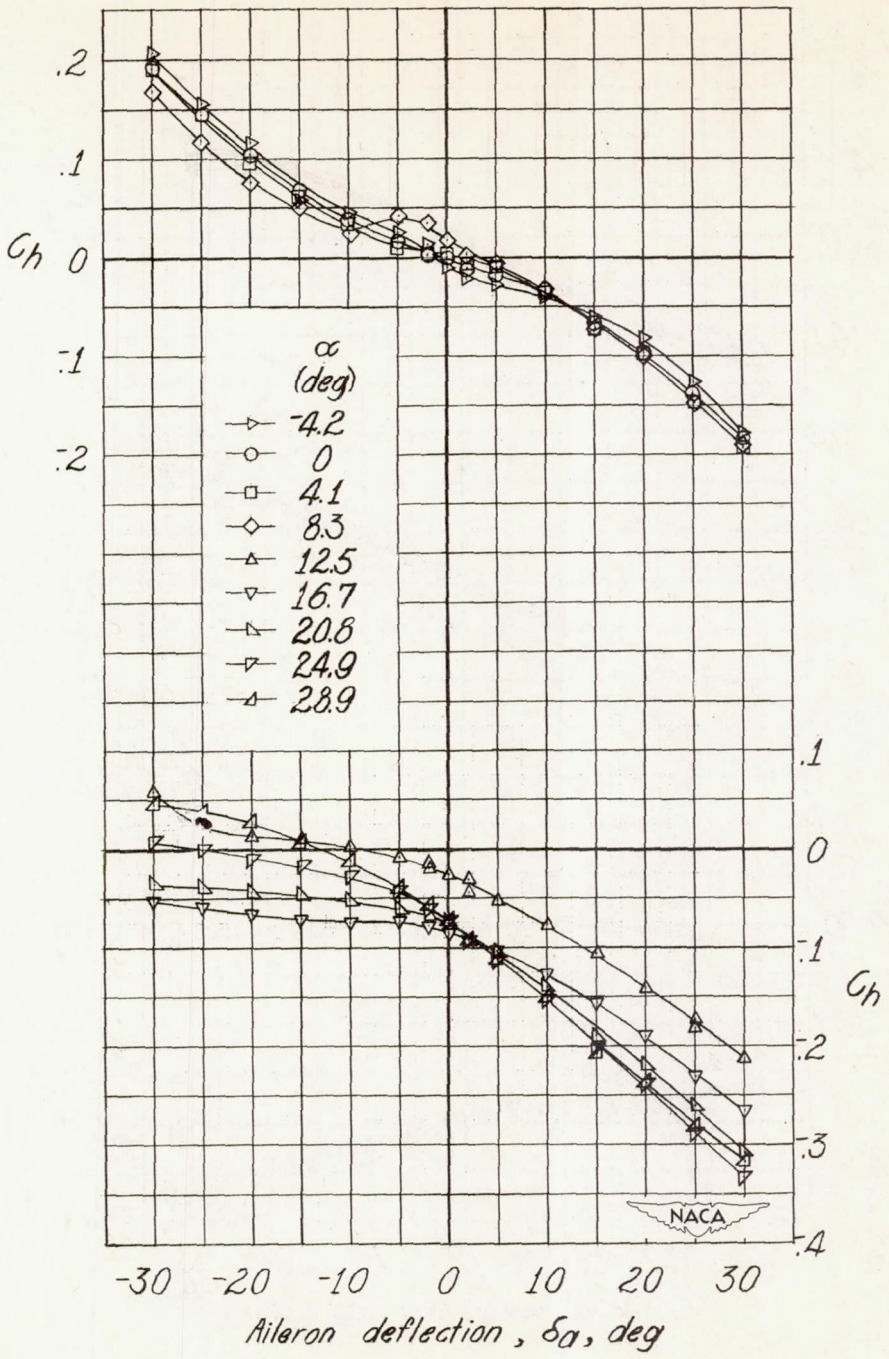


Figure 21.- Continued.

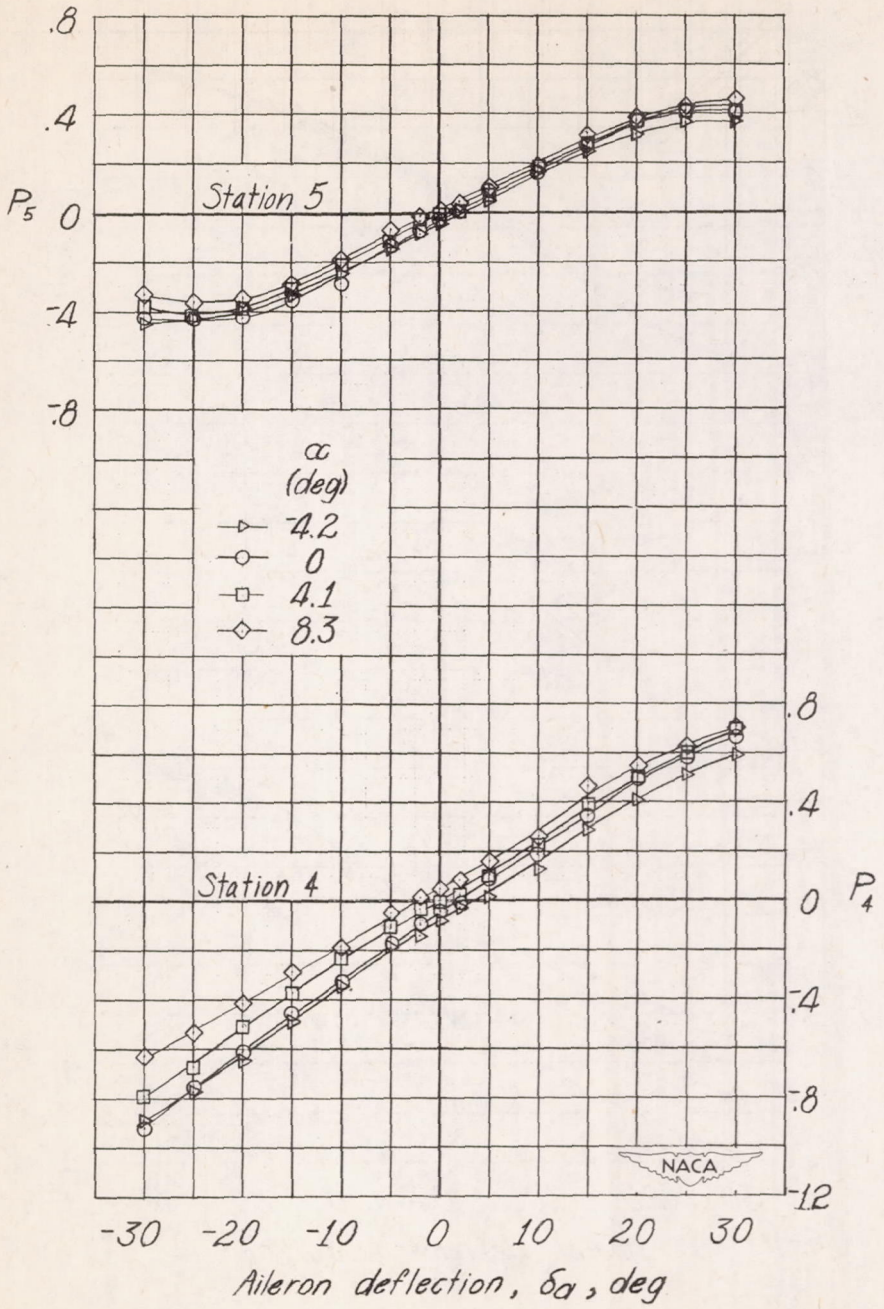


Figure 21.- Continued.

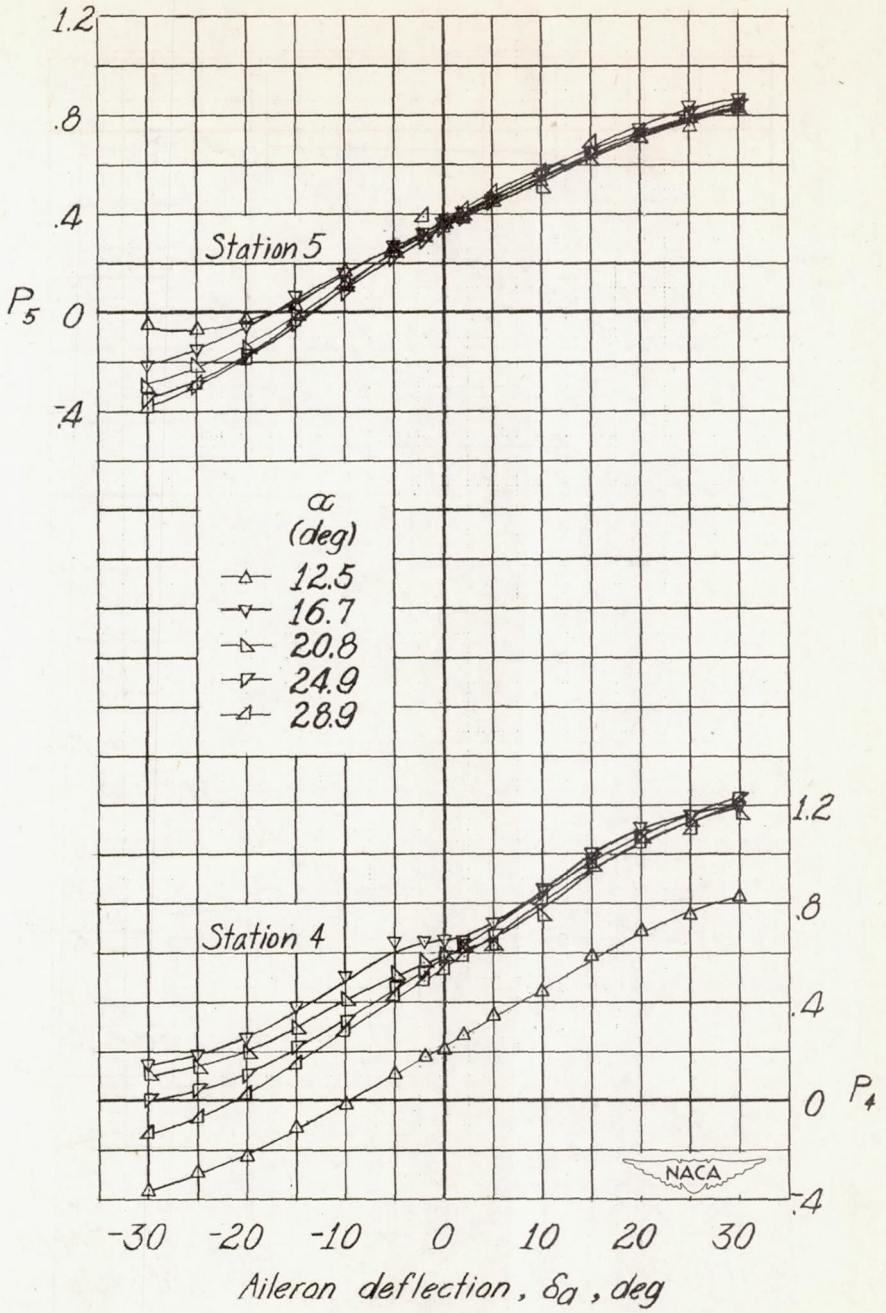


Figure 21.- Concluded.

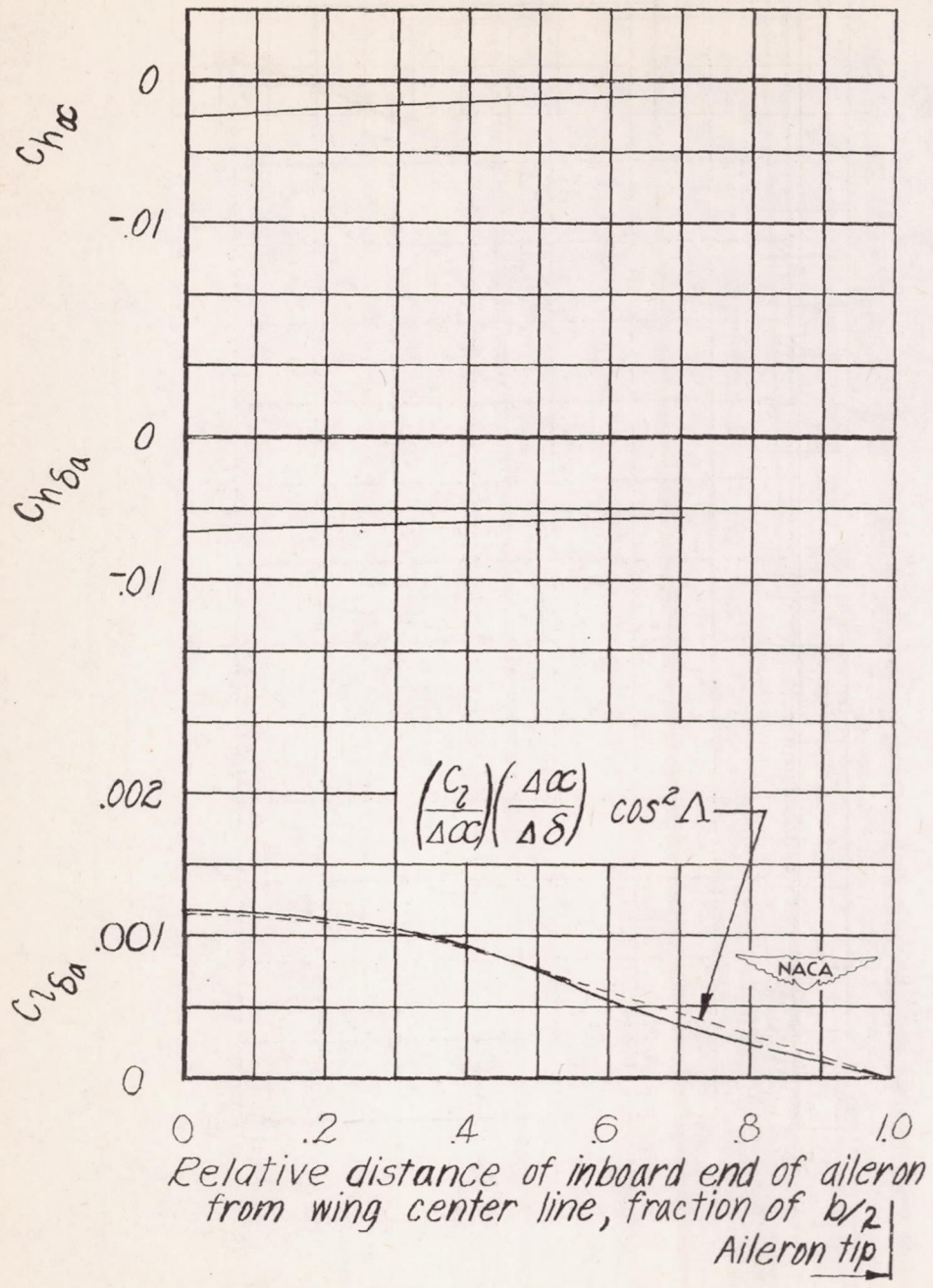


Figure 22.- Variation of aileron parameters $C_{l_{\delta_a}}$, $C_{h_{\delta_a}}$, and C_{h_α} with relative position of inboard end of aileron on the 51.3° sweptback wing $\phi_a = 14^\circ$, $\phi = 6^\circ$ over remainder of wing span; $y_{a_o} = 0.990\frac{b}{2}$.

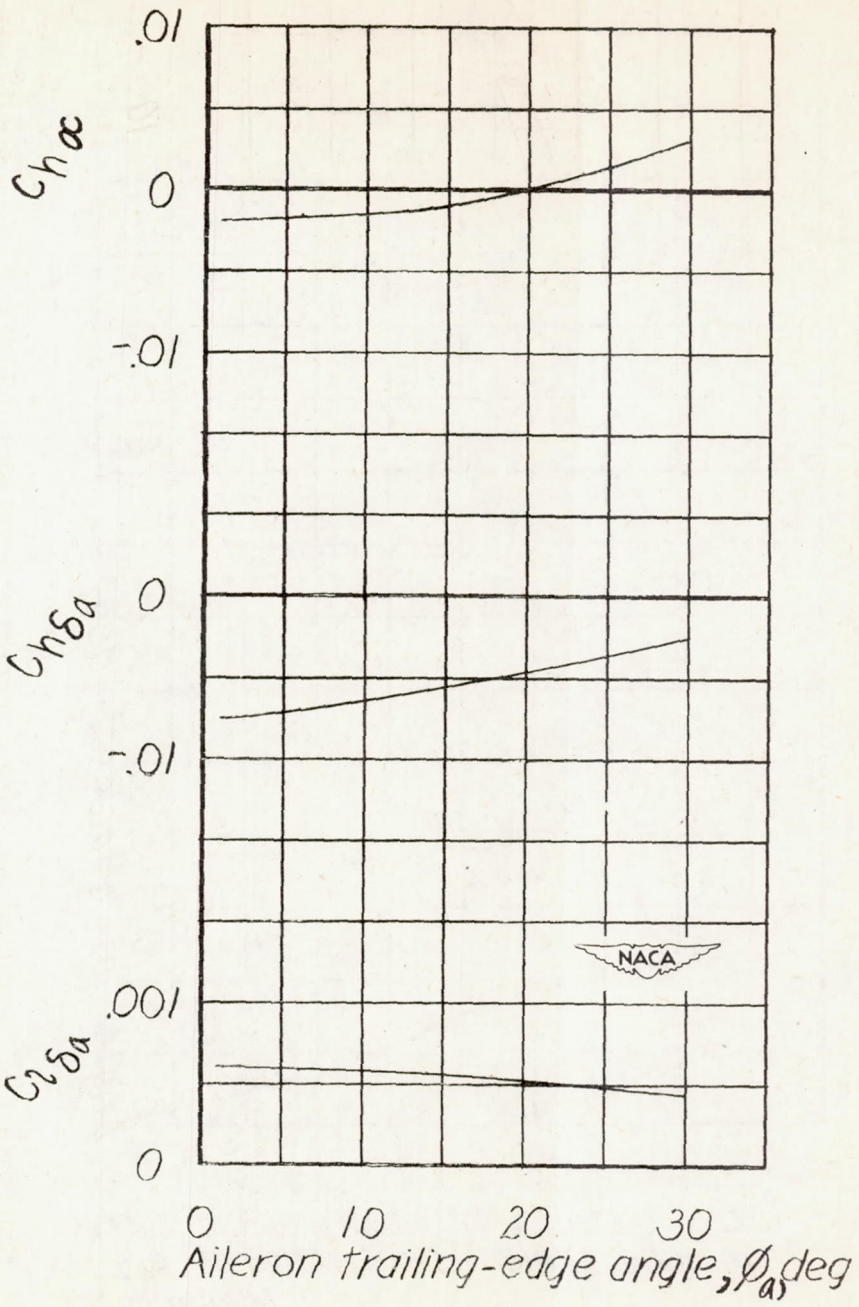


Figure 23.- Variation of aileron parameters $C_{l_{\delta_a}}$, $C_{h_{\delta_a}}$, and C_{h_α} with aileron trailing-edge angle on the 51.3° sweptback wing. $b_a = 0.404\frac{b}{2}$; $y_{a_o} = 0.990\frac{b}{2}$; $\phi = 6^\circ$ on wing inboard of aileron.

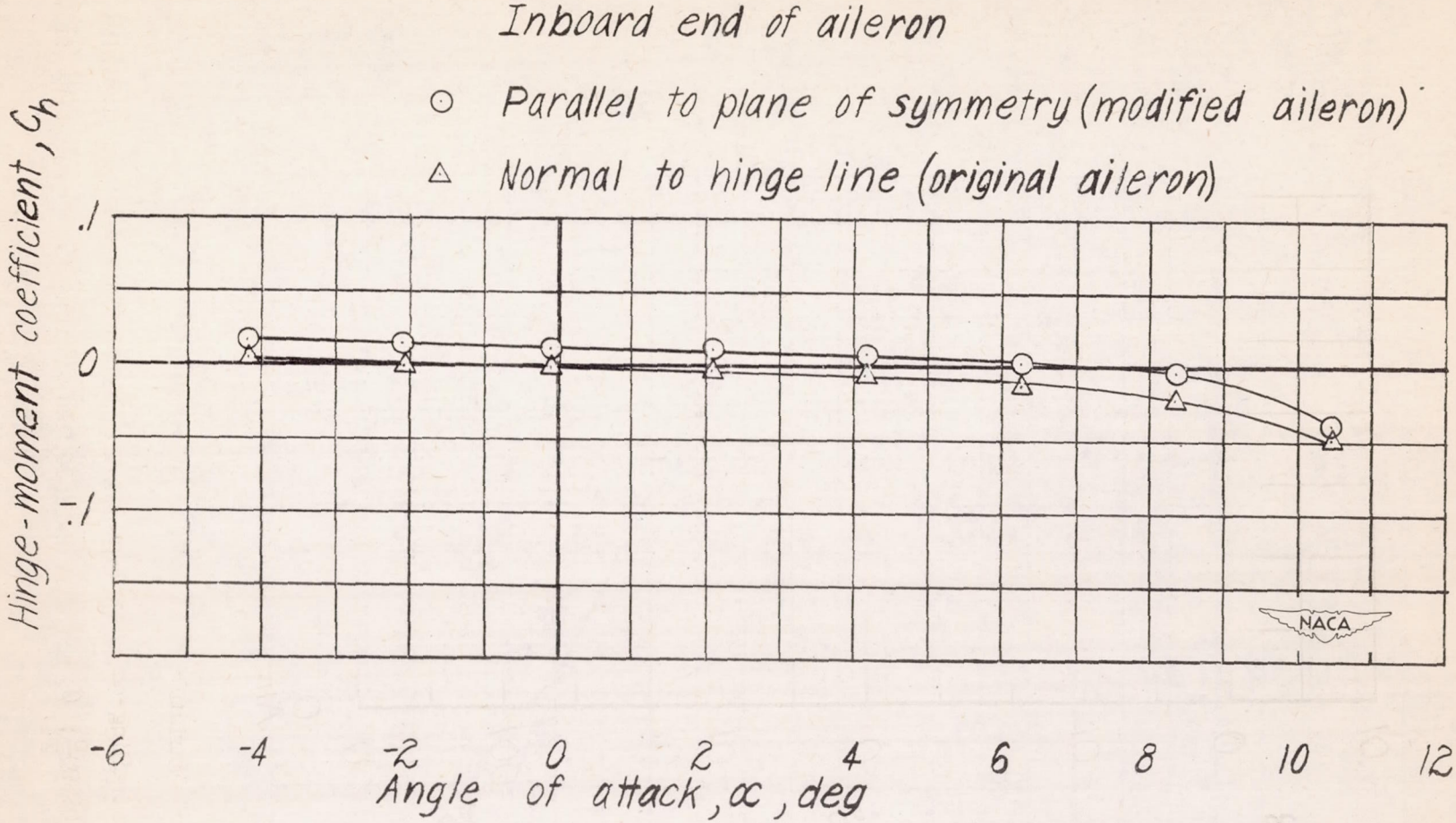


Figure 24.- Comparison of the variation of hinge-moment coefficient with angle of attack for the original and modified ailerons of $b_a = 0.404\frac{b}{2}$ on the 51.3° sweptback wing. $\delta_a = 0°$; $\phi_a = 6°$; $y_{a_o} = 0.990\frac{b}{2}$.

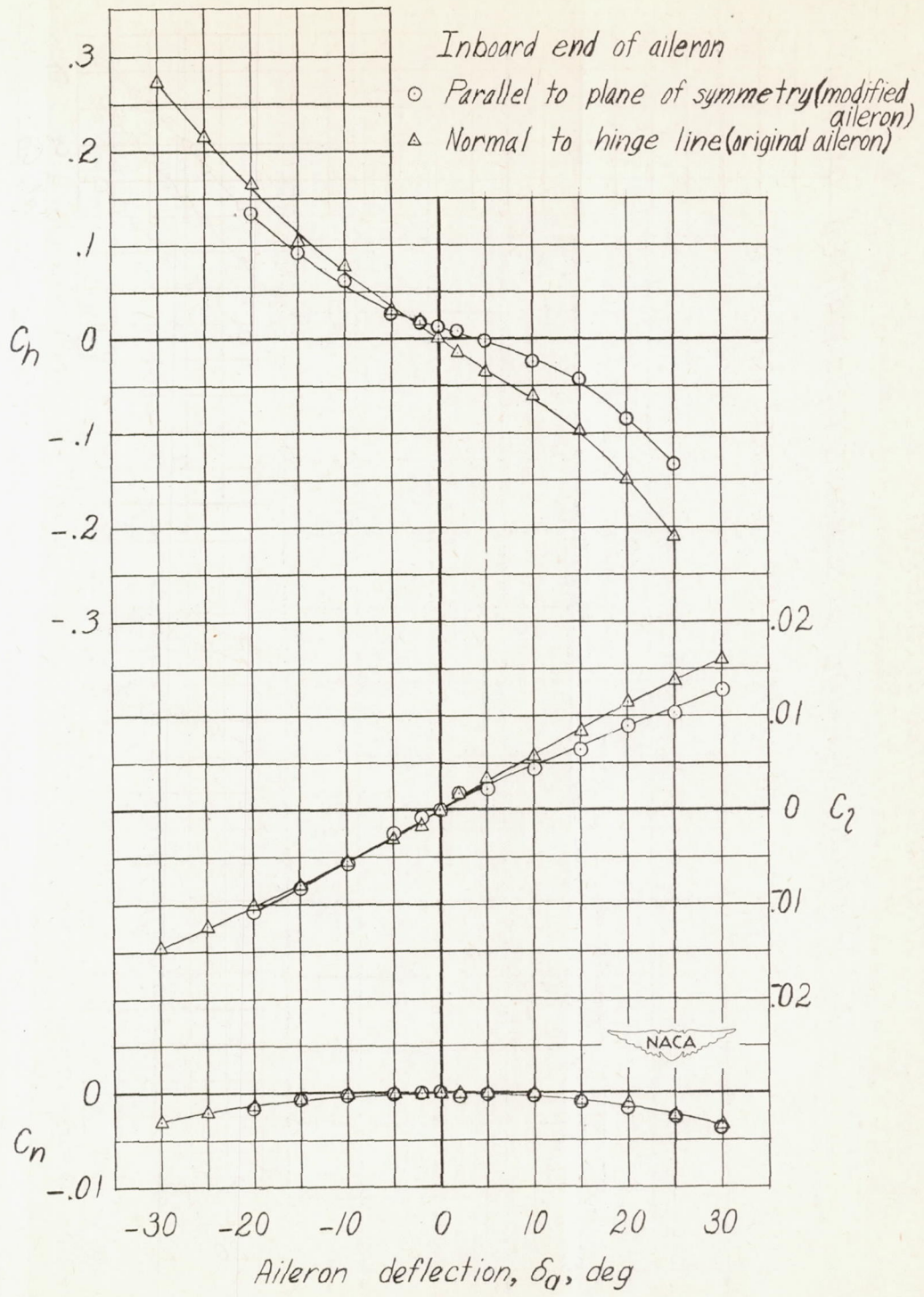


Figure 25.- Comparison of the variation of lateral control characteristics with aileron deflection for the original and modified ailerons of $b_a = 0.404\frac{b}{2}$ on the 51.3° sweptback wing. $\alpha = 0^\circ$; $\phi_a = 6^\circ$; $y_{a_o} = 0.990\frac{b}{2}$.

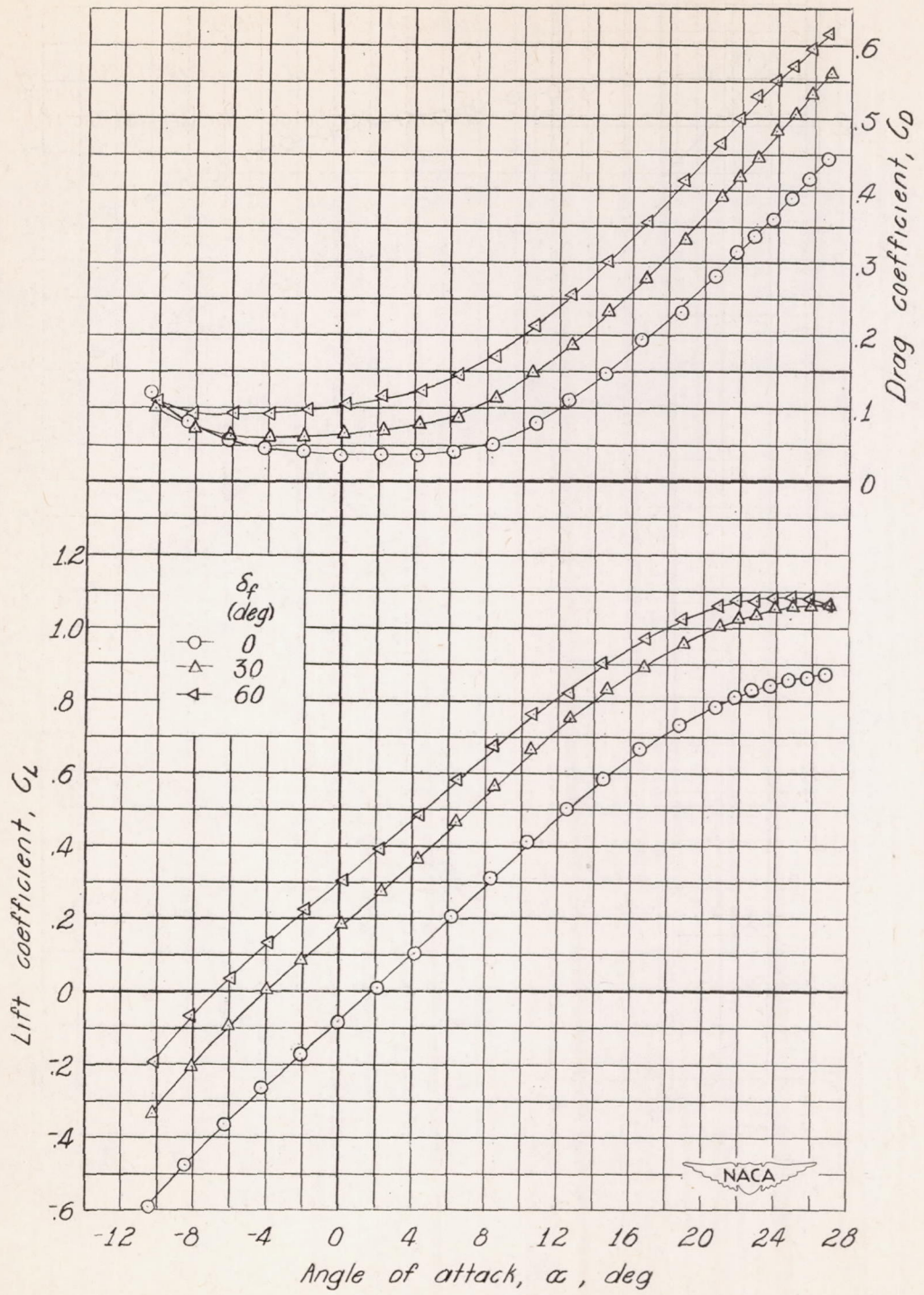


Figure 26.- Variation of aerodynamic characteristics with angle of attack of the 51.3° sweptback wing equipped with $0.600\frac{b}{2}$ spoiler ailerons and a $0.925\frac{b}{2}$ unsealed flap. $\emptyset_f = 14°$; $y_{f_o} = 0.990\frac{b}{2}$.

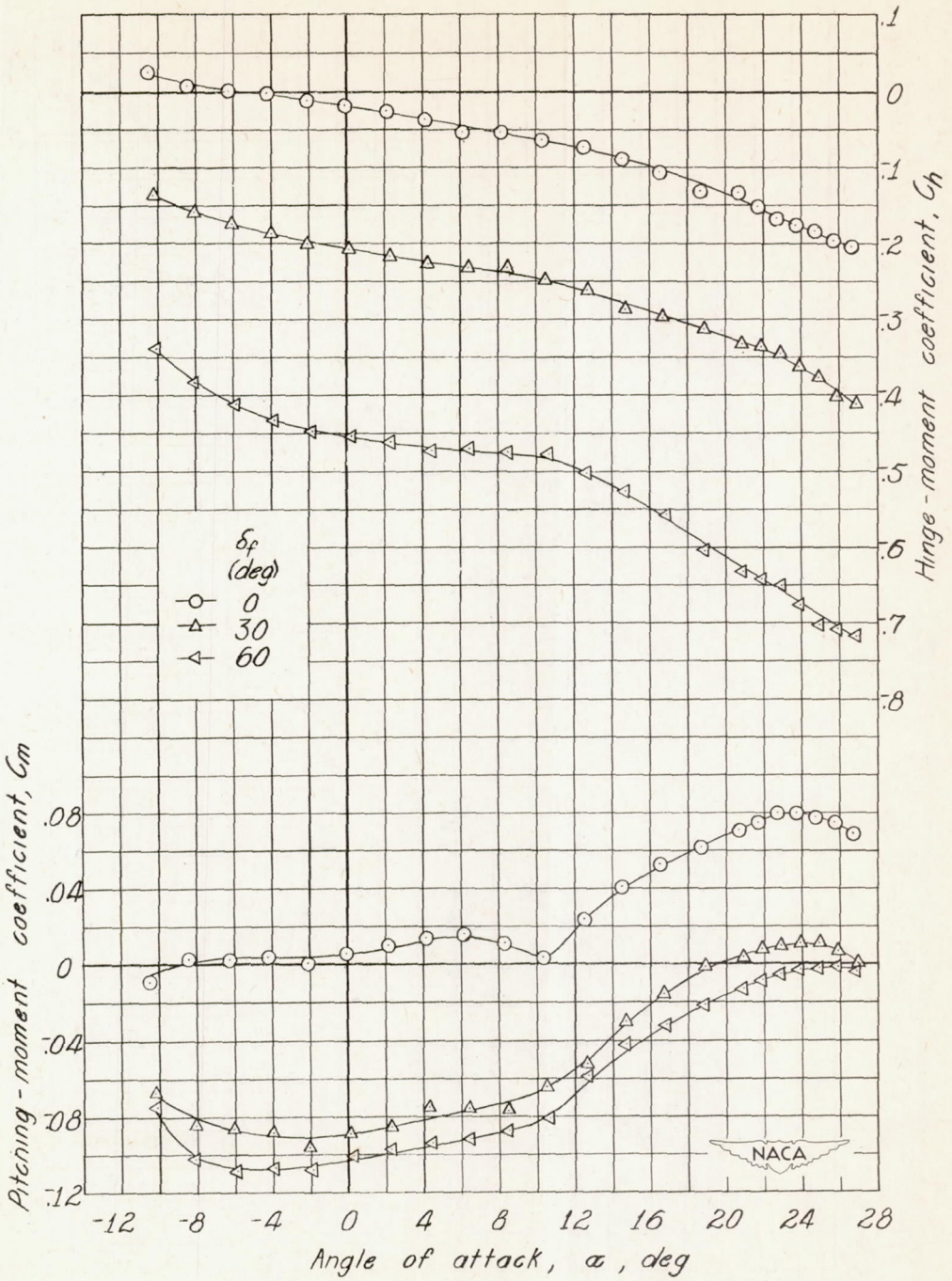


Figure 26.- Continued.

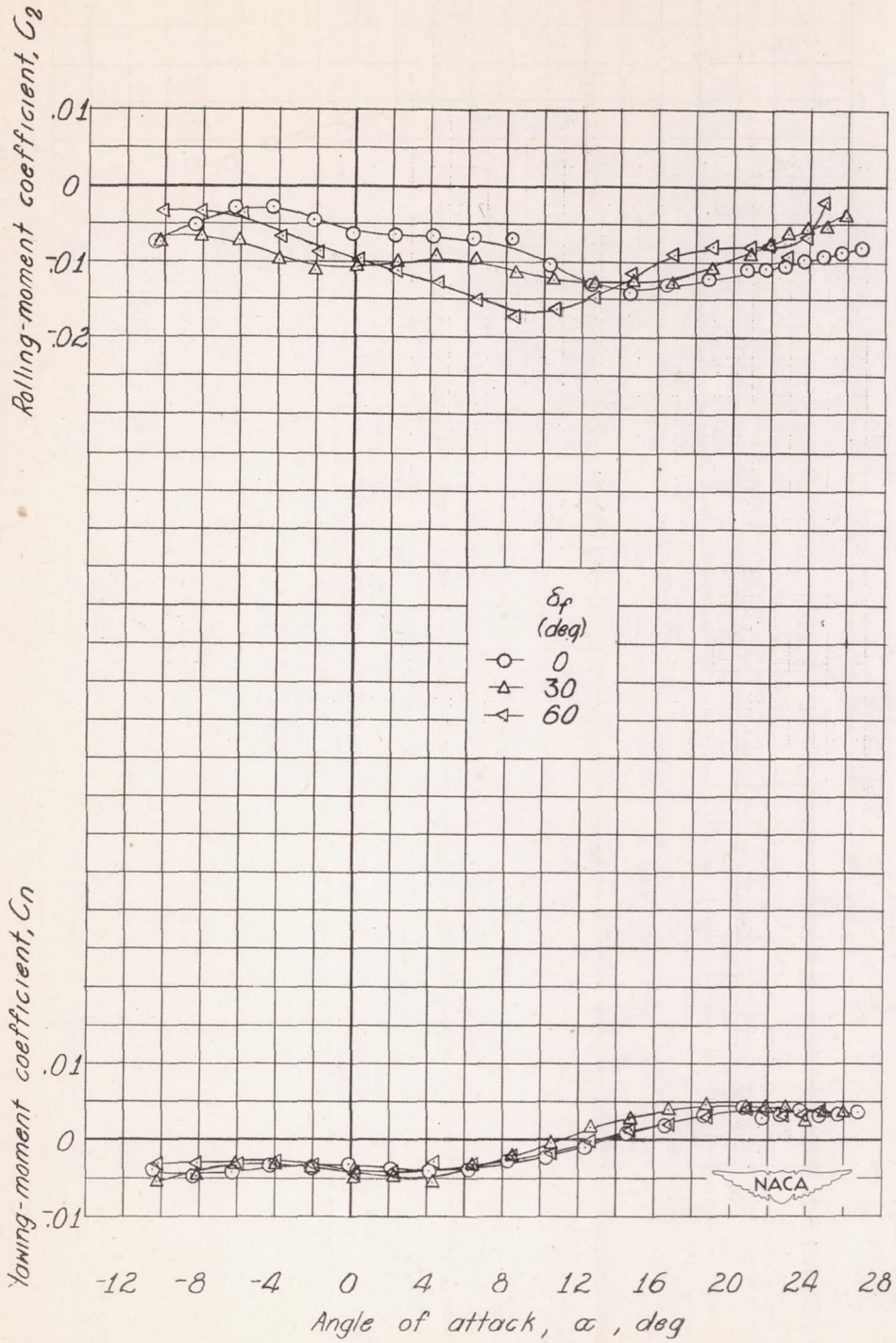


Figure 26.- Concluded.